THE CHEMOKINE REGULATION OF BRUTON'S TYROSINE KINASE IN ACUTE MYELOID LEUKAEMIA

Thesis submitted in accordance with the requirements of the University of Liverpool for the degree of Doctor in Philosophy

By

Sujitra Keadsanti

March 2018

Abstract

Acute myeloid leukaemia (AML) and chronic lymphocytic leukaemia (CLL) are common in the elderly. Bruton's tyrosine kinase (BTK) is an important protein that plays a vital role in several signalling pathways including the B cell receptor (BCR) and SDF-1α/CXCR4 chemokine signalling pathways. Although BTK is a cytoplasmic tyrosine kinase the protein can also found in the nucleus. Thus, the nuclear-cytoplasmic shuttling mechanism of BTK and BTK-binding protein are proposed in other studies, but BTK's actual role in the nucleus is still unclear. Therefore, the first aspect of this study examined BTK and p-BTK in the cytoplasm and nucleus of AML and CLL cells. AML and CLL cellular fractionation showed that BTK and p-BTK were detected in both cytoplasm and nuclear fractions. Thus, BTK may perform important functional roles in their nuclei. The second aspect of this study focused on the SDF-1α/CXCR4 signalling pathway which is important for AML survival and may control cellular responses through BTK. We identified which $G\alpha_{12}$ subclasses can couple with CXCR4 receptor to convey the signalling of BTK, in addition to Gαi–linked signalling seen in AML. Results showed CXCR4 was expressed in AML and CLL, and that BTK is activated after SDF-1α stimulation. Therefore, our AML and CLL models express functional CXCR4. A gene silencing technique was used to identify the roles for $G\alpha_{12}$ subclasses of G-proteins by knocking down $G\alpha_{12}$ or $G\alpha_{13}$ via short hairpin RNAs. The $G\alpha_{12}/G\alpha_{13}$ knockdown cells showed defective SDF-1α-induced migration responses. These results suggest that $G\alpha_{12}$ and $G\alpha_{13}$ can transduce signalling from SDF-1α and may be responsible of the activation of BTK in these leukaemia cells. In summary, these data reveal important new information about the role of BTK in different aspects of leukaemia cell functions and provide useful insight into the role of BTK in AML leukaemia.

Some of the work in this thesis has been previously published in the following publication:

MacEwan DJ, Barrera LN, Keadsanti S, Rushworth SA, Shah NM, Yuan T, Zaitseva L. “Understanding life and death decisions in human leukaemias” Biochem Soc Trans 2014 Aug 1;42(4):747-751.

Acknowledgements

I would like to acknowledge my supervisor team, Prof David MacEwan, Dr Joseph Slupsky, and Prof Andrew Pettitt for supporting me throughout my PhD study. I really appreciative of the kind help from my primary supervisor, Prof David MacEwan (Dave) who give me both scientific support and the mental encouragement to cope with all the difficulties during my study.

I thank all of lab members for their support. Dr Nicholas Harper for lentiviral plasmids construct that I used in this study. Dr John Allen who helped me for FACS analysis and gave me lots of advice. Dr Andrea O'Donnell for the migration assay fluorescence detection experiment. Dr Vanessa Marensi for her help throughout my thesis and giving me useful advice. I also would like to thank other lab members especially Melanie and Niraj, and I also thank people from other research groups in the Cancer Pharmacology labs for their kind help.

I would especially like to thank my loving parents and family for their unending help and encouragement, and to my Thai friends for their backing.

Finally, I deeply acknowledge Mahidol University and the University of Liverpool for choosing me as a recipient of a Mahidol-Liverpool Chamlong Harinasuta PhD scholarship and giving me this opportunity to do my PhD at the University of Liverpool.

Table of Contents

Abbreviations

µg	:	Microgram
µM	:	Micromolar
µL	:	Microlitre
M	:	Molar
mA	:	Milliamperes
mL	:	Millilitre
mM	:	Millimolar
mg/mL	:	Milligram per millilitre
nm	:	Nanometre
ng/mL	:	Nanogram per millilitre
h	:	Hour
ºC	:	Centigrade
Ab	:	Antibody
AML	:	Acute myeloid leukaemia
ANKRD53	:	Ankyrin repeat domain 53
APS	:	Ammonium persulfate
ATCC	:	American type culture correction
BAM11	:	BTK associated molecule 11
BCR	:	B-cell receptor
Bright	:	B cell regulator of Ig heavy chain transcription
BSA	:	Bovine serum albumin
bp	:	Base pair
BTK	:	Bruton’s tyrosine kinase
cDNA	:	Complementary deoxyribonucleic acid
CLL	:	Chronic lymphocytic leukaemia
CMFDA dye	:	5-chloromethylfluorescein diacetate

CO_2	:	Carbon dioxide
CXCR 4	:	C-X-C chemokine receptor 4
DC	:	detergent compatible
DDB1	:	DNA damage-binding protein 1
DMEM	:	Dulbecco's Modified Eagle's medium
DMSO	:	Dimethyl sulfoxide
ECL	:	Enhanced Chemiluminescence
EDTA	:	Ethylenediamine tetra-acetic acid
ERK1/2	:	Extracellular signal regulated kinase
FAB	:	France-American-British
FACS	:	Fluorescence-activated cell sorting
FBS	:	Foetal bovine serum
FLT3-ITD	:	FMS-like tyrosine kinase 3- internal tandem duplications
GAPDH	:	Glyceraldehyde 3-phosphate dehydrogenase
GDP	:	Guanosine diphosphate
GFP	:	Green fluorescence protein
GPCR	:	G-protein-coupled receptor
GTP	:	Guanosine triphosphate
H3	:	Histone 3
HEK293T	:	Human embryonic kidney 293T
HRP	:	Horseradish peroxidase
h.p.t.	:	Hour post transfection
IFNA1	:	Interferon alpha 1
IgG	:	Immunoglobulin G
IgM	:	Immunoglobulin M
IgVH	:	Immunoglobulin variable region heavy chain
IL	:	Interleukin

ITAM	:	Immunoreceptor tyrosine-based activation motif
kDa	:	Kilo Dalton
LB agar	:	Luria-Bertani agar
LPS	:	Lipopolysaccharide
mAb	:	monoclonal antibody
min	:	minute
MM	:	Multiple myeloma
mRNA	:	Messenger RNA
MW	:	Molecular weight
NES	:	Nuclear exported signal
NF-κB	:	Nuclear factor-kB
NLC	:	Nurse-like cells
NLS	:	Nuclear localisation signal
PAGE	:	Polyacrylamide gel electrophoresis
PBS	:	Phosphate buffer saline
p-BTK	:	Phosphorylated Bruton’s tyrosine kinase
PE	:	Phycoerythrin
PH	:	Pleckstrin homology
PI	:	Propidium iodide
PI3K	:	Phosphatidylinositol-3-phosphate
PLCγ2	:	Phospholipase-C gamma 2
PVDF	:	Polyvinylidine difluoride
qPCR	:	Quantitative polymerase chain reaction
RPMI-1640	:	Roswell Park Memorial Institute
RNA	:	Ribonucleic acid
SD	:	Standard deviation
SDF-1α	:	Stromal cell derived factor-1 alpha

SDS	:	Sodium dodecyl sulphate
SEM	:	Standard error of mean
SH	:	Src homology
shRNA	:	Short hairpin ribonucleic acid
SOB	:	Super optimal broth
SOC	:	Super optimal broth with catabolite repression
SYK	:	Spleen tyrosine kinase
TBS	:	Tris buffer saline
TBS-T	:	Tris buffered saline with Tween 20
TEMED	:	Tetramethylethylenediamine
TFII-I	:	Transcription factor II-I
TH	:	Tec homology
TLR4	:	Toll-like receptor 4
TP53	:	Tumour protein 53
Tm	:	Melting temperature
TNF-α	:	Tumour necrosis factor-alpha
UT	:	Untreated
WT	:	Wild-type

Chapter I

Introduction

1.1 Leukaemia

Leukaemia is a disease that defects in proliferation and cell death of immature blood cells. They proliferate rapidly and resist to undergo apoptosis. According to hematopoiesis, blood cells develop into two lineages which are the myeloid lineage and lymphoid lineage as shown in figure 1.1. The myeloid cells comprise of macrophage, erythrocyte, neutrophil, eosinophil, and dendritic cells while B cells T cells, and natural killer (NK) cells derive from the lymphoid linage. Depending on cell type and disease progress, leukaemia can be divided into four major group which are acute myeloid leukaemia (AML), acute lymphocytic leukaemia (ALL), chronic myeloid leukaemia (CML), and chronic lymphocytic leukaemia (CLL). In this study, we concentrate on only AML and CLL subtype.

According to Cancer Research UK, around 350,000 cases of cancer were diagnosed in 2015, with over 160,000 deaths in the same annual period. That equates to an overall 50% 10-year survival rate which is improving, but far from clinically acceptable. Breast cancer and prostate cancer hold the first common incidence cancer in females and males, respectively while leukaemia is around the twelfth most common by incidence in both genders. Considering leukaemia incidence, there are 3% of leukaemia diagnosed from total cancer incidence in 2015. Among all cancer cases, less than 1% is acute myeloid leukaemia (AML) diagnosed in 2015. The incidence of this leukaemia subtype is increased in older people which usually over 75 year old and peaked around 85 to 89 years old. In case of chronic lymphocytic leukaemia (CLL), this leukaemia subtype is also

common in older people which the highest incidence is in older than 90 years old. For acute lymphocytic leukaemia (ALL), there are less than 1% of total cancer cases are ALL diagnosed which this subtype common in childhood around 0-4 years old. The incidence of another leukaemia subtype, chronic myeloid leukaemia (CML), is also less than 1% of total cancer cases and CML is also common in older patient which age around 85-89 years old. All of this information is taken from cancer research UK (WWW.cancerresearchuk.org).

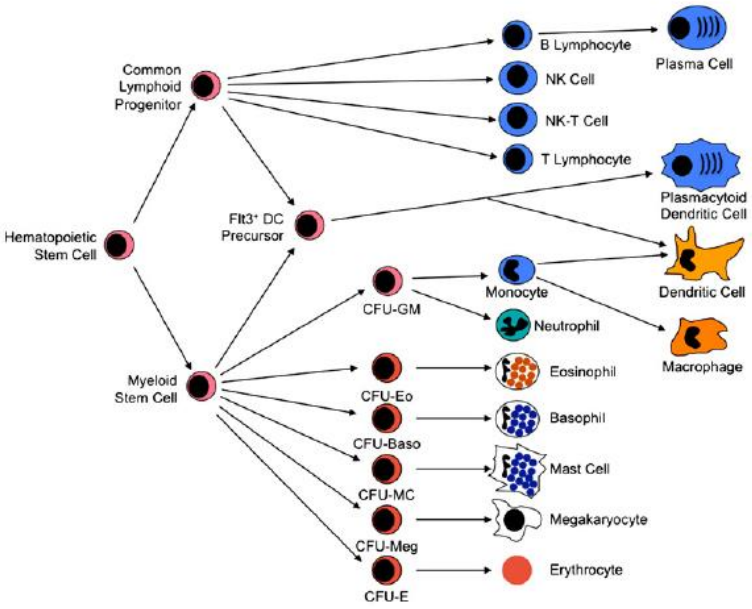

Figure 1.1 Haematopoietic cell lineage development(Chaplin, 2010).

The development of lymphoid and myeloid blood cells is originated develop from haematopoietic stem cells that generate the common progenitor for each cell lineages. The myeloid cell lineage comprises of monocyte, neutrophil, eosinophil, basophil, mast cells, megakaryocyte, and erythrocyte which derived from common myeloid progenitor. Whereas the lymphoid common progenitor cells are developed into B cells, T cells, and natural killer (NK) cells which derive from common lymphoid progenitor. This figure is adapted from Chaplin, 2010, J Allergy Clin Immunol.

1.1.1 Acute myeloid leukaemia

Acute myeloid leukemia is a leukaemia subtype characterized by abnormal proliferation of immature myeloid blasts in bone marrow and peripheral blood and this type of leukaemia is common in the elderly aged over 65 years old. Patient diagnosis for AML is confirmed if more than 20% of immature myeloid cells are detected in bone marrow and peripheral blood (Saultz and Garzon, 2016, Dohner et al., 2010). AML is the most common type of leukaemia among subgroups in United States, 2017 (Siegel et al., 2017). The population of AML cells is heterogeneous which contains variable genetic background including chromosome abnormality, several gene mutations that lead to aberration of gene expression, and abnormality of miRNA expression (Kumar, 2011).

Chromosomal inversion, translocation, and deletion can be found in AML cells, however there are common abnormalities in cytogenetic alteration where the abnormality leads to oncofusion proteins, including PML-RARα from t(15;17), AML1-ETO from t(8;21), CBFβ-MYH11 from inv(16), and MLLs rearrangement from 11q23 (Martens and Stunnenberg, 2010). Gene mutations can be found in AML patients with normal cytogenetics which the gene mutation of AML blast can be categorized into three classes. The disease progression needs more than one class of mutation to develop into leukaemia according to two hit model (De Kouchkovsky and Abdul-Hay, 2016). Class I involves signalling pathways that enhance proliferation and survival of blasts and FLT3-ITD, K/NRAS, TP53, and c-KIT are classified into this class (Kumar, 2011, Estey, 2016, De Kouchkovsky and Abdul-Hay, 2016). The mutation of differentiation regulated gene, NPM1 and CABPA, are classified into class II mutations. Epigenetic regulation

gene mutation including DNMT3A, TET2, IDH1, and IDH2 are classified into class III (De Kouchkovsky and Abdul-Hay, 2016, Dombret, 2011). The different mutations show distinct outcomes for prognostic treatment. Thus the classification of AML blasts at diagnosis is important for treatment.

There are several criteria for AML classification including blast morphology, genomic abnormality, or outcome of treatment. The French American British (FAB) classification is based on morphology and development which can be divided into 9 stages from M0-M7 as shown in Table 1.1 (Bennett et al., 1976). In addition, AML is also classified by genetic alteration background according to World Health Organization classification shown in Table 1.2. AML morphology and chromosome alteration are not the only criteria for AML classification, the prognostic risk is also used as a criteria for classification into favourable, intermediate I and II, and adverse (Saultz and Garzon, 2016).

Since, AML harbours mutations that effect aberrant signalling pathways and epigenetics, signalling protein targeted therapy in these pathways is an interesting candidate for AML treatment after several studies have shown interfering with these pathways affects AML survival. As FLT3-ITD mutation is found in AML blast, FLT3 inhibitors are considered to be potential targeted drugs where the first and the second generation of FLT3 inhibitors have already been applied in clinical trials (De Kouchkovsky and Abdul-Hay, 2016). The BTK inhibitor, ibrutinib, reduces viability of patient AML blasts, in addition, ibrutinib also inhibits pro-survival signal-induced proliferation and adhesion to BMSCs (Rushworth et al., 2014).

Furthermore, there are epigenetic-targeted drugs which are also undergoing clinical trials (Chen et al., 2010, Sun et al., 2018).

AML subtypes	**Morphology**
AML-M0	Undifferentiated acute myeloblastic leukaemia
AML-M1	Acute myeloblastic leukaemia with minimal maturation
AML-M2	Acute myeloblastic leukaemia with maturation
AML-M3	Acute promyelocytic leukaemia
AML-M4	Acute myelomonocytic leukaemia
AML-M4	Acute myelomonocytic leukaemia eosinophilia
AML-M5	Acute monocytic leukaemia
AML-M6	Acute erythroid leukaemia
AML-M7	Acute megakaryoblastic leukaemia

Table 1.1 Acute myeloid leukaemia classification according to French-British-America (FAB) (Kumar, 2011).

The FAB classification is based on AML morphology. AML cells are divided into 9 subgroups. This table is adapted from Kumar, C. C. Genes Cancer (2011) doi: 10.1177/1947601911408076.

Classification	Genetic Abnormalities
AML with recurrent genetic abnormalities	**AML** with t(8;21)(q22;q22.1);RUNX1T1 inv(16)(p13.1q22) or t(16;16)(p13.1;q22);CBFB-MYH11 t(6;9)(p21.3;q23.3);MLLT3-KMT2A t(6;9)(p23;q34.1);DEK-NUP214 inv(3)(q21.3q26.2) or t(3;3)(q21.3;q26.2);GATA2, MECOM BCR-ABL1 provisional entity Mutated NPM1 Biallelic mutation of CEBPA Mutated RUNX1 provisional entity **APL** with PML-RARA **AML (megakaryoblastic)** with t(1;22)(p13.3;q13.3);RBM15-MKL1
AML with myelodysplasia-related changes	
Therapy-related myeloid neoplasm	
AML, not otherwise specific	AML with minimal differentiation AML without maturation/AML with maturation Acute myelomonocytic leukaemia Acute monoblastic/monocytic leukaemia Pure erythroid leukaemia Acute megakaryoblastic leukaemia Acute basophilic leukaemia Acute panmyelosis with myelofibrosis
Myeloid sarcoma	
Myeloid proliferations related to Down syndrome	Transient abnormal myelopoiesis Myeloid leuakemia associated with Down syndrome

Table 1.2 AML classifications according to World health Organization (Arber et al., 2016).

The WHO classification of AML is based on chromosomal abnormality. This table is modified from Arber, D.A., Orazi, A. et al, Blood (2016) doi: 10.1182/blood-2016-03-643544

1.1.2 Chronic lymphocytic leukaemia

Chronic lymphocytic leukaemia is a non-Hodgkin lymphoma which shows high incidence in elderly with median age at 75 years old (Hallek et al., 2018). CLL is diagnosed by accumulation of CD5 positive cells in blood, bone marrow, and lymphoid organs and presence of lymphocytosis and lymphadenopathy (Hallek et al., 2018). CLL cells are more mature than AML subtypes but the problem of this subtype of leukaemia is apoptosis resistance that leads to accumulation of immature lymphoid cells. This leukaemia subtype can be developed from many risk factors including family genetic background and external stimuli exposure such as smoking, farming experience, and infection (Slager et al., 2014). CLL is also a heterogeneous disease that several chromosomal aberrations and genetic abnormalities are involved. The abnormalities of chromosome structure are reported including trisomy12, and deletion at chromosome 6q, 11q, 13q, or 17p (Shahjahani et al., 2015). Moreover, mutations involving signalling pathways, epigenetics, and micro-RNA processing are also found in CLL patients such as *TP53*, *NOTCH1*, and *MYD88*. The gene mutation, prognostic markers, and mutation status of Ig heavy chain variable region (IGHV) are also related to disease outcome as well as disease progression and survival rate of CLL patients (Hallek et al., 2018). The expression of surface markers are characterized and compared the expression with normal B cells which BCR receptor (IgM and IgD) and Igα are lower express while CD5, CD19, CD20, and CD23 are vice versa. (Herman et al., 2010, Matutes et al., 1994a, Matutes et al., 1994b). In order to apply appropriate treatment for patients, the Rai and Binet CLL systems are used for stage characterization. These two systems were published in 1975 and 1981 and are based on patient examination and

laboratory testing (Rai et al., 1975, Binet et al., 1981, Rai and Jain, 2016, Hallek et al., 2018). According to the Rai system, CLL is divided into 3 groups which are low risk (stage 0), intermediate risk (stage I-II), and high risk (stage III-IV) while CLL is classified into 3 groups according to Binet system (Rai and Jain, 2016, Gribben, 2010).

Chemotherapy has been developed as a standard treatment for many years which starts with monotherapy using alkylating agents, to combination chemotherapy, but many chemotherapeutic drugs are not suitable for the treatment of some patients considering their high toxicity (Rai and Jain, 2016). Thus, targeted therapy is an interesting candidate especially drugs targeting the B cell receptor (BCR) signalling pathway and microenvironment because these pathways provide survival supporting signals beneficial to CLL and the aberrant activation of these signalling pathways is reported in CLL progression.

Stage	Clinical features
0 (low risk)	Lymphocytosis in blood and marrow only
I-II (intermediate risk)	Lymphadenopathy, splenomegaly +/- hepatomegaly
III-IV (high risk)	Anemia, thrombocytopenia

Table 1.3 Rai classification system of chronic lymphocytic leukaemia (CLL) (Gribben, 2010).

This table is adapted from Gribben, J. G. Blood (2010) doi: 10.1182/blood-2009-08-207126

Group	Clinical features
A	Fewer than 3 areas of lymphadenopathy; no anemia or thrombocytopenia
B	More than 3 involved node areas; no anemia or thrombocytopenia
C	Hemoglobin < 100 g/L Platelets < 100x10 g/L

Table 1.4 Binet classification of chronic lymphocytic leukaemia (CLL) (Gribben, 2010).

This table is adapted from Gribben, J. G. Blood (2010) doi: 10.1182/blood-2009-08-207126

1.2 Chemotherapeutic treatment for haematological malignancies

Chemotherapy is the first choice treatment for blood cancer. Some of chemotherapeutic drugs have already approved by FDA while lots of them are undergoing clinical trials. The new drugs have been developed for the better outcome. Chemotherapeutic drugs can be prescribed as monotherapy or in combination. The treatment strategy depends on patient's health and genetic background. Below is a table 1.5 that outlines the different chemotherapies used among different blood cancers, and the year they were introduced and added to the clinician's drug arsenal.

Hodgkin's Lymphoma	**Non-Hodgkin's Lymphoma**	**Myelomas**
Carmustine – 1947+	Methotrexate – 1947	Carmustine – 1947+
Prednisone – 1950	Carmustine – 1947+	Prednisone – 1950
Doxorubicin – 1950s	Prednisone – 1950	Doxorubicin – 1950s
Cyclophosphamide – 1954	Doxorubicin – 1950s	Cyclophosphamide – 1954
Lomustine – 1954+	Cyclophosphamide –1954	Thalidomide – 1957
Vincristine – 1963	Lenalidomide – 1957+	Lenalidomide – 1957+
Bleomycin – 1966	Cytarabine – 1959	Pomalidomide– 1957+
Dacarbazine – 1975	Bendamustine – 1963	Pamidronate – 1976 (Bisphosphonate)
Chlorambucil – 1977	Vincristine – 1963	Zoledronate – 1976+ (Bisphosphonate)
Brentuximab – 2011 (CD30/TNFRSF8 mAb)	Bleomycin – 1966	Plerixafor – 1987 (CXCR4 inhibitor)
	Chlorambucil – 1977	Bortezomib – 1995 (26S proteasome inhibitor)
	Plerixafor – 1987 (CXCR4i)	Carfilzomib – 1995+ (26S proteasome inhibitor)
	Romidepsin, Vorinostat, Belinostat – 1994 (HDACi)	
	Bortezomib – 1995 (26Si)	
	Denileukin Diftitox – 1996 (IL-2R mAb diphtheria tox)	
	Rituximab – 1998 (CD20 mAb)	
	Ibrutinib – 2007 (BTK TKI)	

		Idelalisib – 2008 (PI-3-Kδi) Brentuximab – 2011 (CD30/TNFRSF8 mAb)	
ALL	**AML**	**CLL**	**CML**
Methotrexate – 1947 Sydney Farber Prednisone – 1950 Daunorubicin – 1950s Doxorubicin – 1950s Cyclophosphamide – 1954 Clofarabine – 1957 Cytarabine – 1959 Vincristine – 1963 Mercaptopurine – 1967 Imatinib (Gleevec) – 1992 Dasatinib – 1992+ Ponatinib – 1992+ Blinatumomab – 2014 (CD3/CD19 mAb)	Arsenic Trioxide – 1920 Daunorubicin – 1950s Idarubicin – 1950+ Doxorubicin – 1950s Mitoxantrone – 1950s Cyclophosphamide – 1954 Cytarabine – 1959 Vincristine – 1963	Mustargen – 1947+ Prednisone – 1950 Cyclophosphamide – 1954 Chlorambucil – 1977 Bendamustine – 1963 Fludarabine – 1968 Alemtuzumab – 1983 (CD52) Rituximab – 1998 (CD20 mAb) Ofatumumab – 1998+ (CD20 mAb) Obinutuzumab – 1998+ (CD20 mAb) Ibrutinib – 2007 (BTK TKI) Idelalisib – 2008 (PI-3-Kδ inhibitor)	Mustargen – 1947+ Cyclophosphamide – 1954 Busulfan – 1959 Cytarabine – 1959 Imatinib (Gleevec) – 1992 Dasatinib – 1992+ Ponatinib – 1992+ Omacetaxine – 2011 (translation inhibitor)

Table 1.5 Chemotherapeutic drugs for haematological malignancies.

This table shows variety of drugs that use for blood cancer treatment.

1.2.1 Chemotherapy treatment for acute myeloid leukaemia (AML)

The chemotherapeutic treatment for AML is divided into two stages which are induction and consolidation. The induction is the first treatment after patient is diagnosed as AML which aims for the clearance the circulating leukaemic cells from the blood and the bone marrow. The standard treatment composes of high dosage treatment with 60 mg/m^2 of daunorubicin for 3 days and 100-200 mg/m^2 of cytarabine for another 7 days (Dohner et al., 2015). Once induction treatment has finished, consolidation starts in order to prevent relapse which due to the presence of resisted AML clone from induction therapy. In consolidation treatment, patient is treated with intermediate dose of cytarabine or transplantation (Dohner et al., 2015). However, these two main chemotherapy regiments cause unpleasant side effects for unfit or elderly patients. Therefore, the targeted therapies are considered as an alternative treatment for unfit patients (Short and Ravandi, 2016). FLT3 inhibitors, epigenetics regulator inhibitors, nuclear exporter inhibitor, and cell cycle regulator inhibitors are undergoing clinical trials and be considered as novel drugs for AML treatment (Saultz and Garzon, 2016, Dohner et al., 2015).

1.2.2 Chemotherapy for chronic lymphocytic leukaemia (CLL)

In the beginning, the alkylating agents (Chlorambucil) and purine analogs (Fludarabine, Pentostatin, and Cladribine) have been used as monotherapy drug for CLL diagnosed patients. Then the combination of fludarabine, cyclophosphamide, and rituximab (FCR) is developed as a

frontline chemotherapy treatment for the fit group of patient which the combination of bendamustine and rituximab is more preferable in elderly patient. Beside rituximab, the others anti-CD20 antibodies have been developed which are ofatumumab and obinutuzuman (Jamroziak et al., 2017, Hallek, 2017). Overall, the choice of drugs and treatment strategies are selected based on genetic background, patient's health condition, and outcome of the first treatment. As CLL is common in old patient and chemotherapeutic drugs have non-suitable side effects, the alternative drugs that have high efficiency with lesser side effects have been developed. The inhibitors of proteins that play an important role in signalling pathway and protein that involved in apoptosis mechanism are considered as alternative drugs for unfit patient.

1.2.3 Chemotherapy in acute lymphocytic leukaemia (ALL)

Acute lymphocytic leukaemia (ALL) is leukaemia subtype that common in childhood which this subtype is also diagnosed in adult. The treatment in adult ALL shows lower successful rate than the rate in children (Jabbour et al., 2010). The treatment comprises of three steps which are remission, consolidation, and maintainance in ALL diagnosed patients. The induction treatment schedule starts with cyclophosohamide then follow by other drugs including daunorubicin, vincristine, L-asparaginase, and prednisone (Terwilliger and Abdul-Hay, 2017). The modified regiment is considered for elderly and unfit patient (Wolach et al., 2017). In addition to the main regimen, CNS prophylaxis by using radiation, systemic chemotherapy, or

intrathecal chemotherapy, is applied in ALL diagnosed patient since CNS recurrence has been reported (Jabbour et al., 2010). However the better drug and treatment strategy are undergoing development.

1.2.4 Chemotherapy in chronic myeloid leukaemia (CML)

CML diagnosed patients were treated with Busalfan and Hydroxyurea then these chemotherapeutic drugs were replaced with imatinib which is tyrosine kinase inhibitor. Imatinib shows favourable outcome for Philadelphia positive mutation (Baccarani et al., 2014, Cortes et al., 1996). Interferon-alpha is also used as an option for CML diagnosed patient in combination with imatinib (Jabbour and Kantarjian, 2016). There are four front line tyrosine kinase inhibitors are approved by FDA to apply in CML-chronic phase which are imatinib, dasatinib, nilotinib, and bosutinib (Jabbour and Kantarjian, 2018). The stem cells transplantation shows good treatment outcome after chemotherapeutic relapse with limited age of patient (Baccarani et al., 2014).

In summary, chemotherapeutic drugs show several side effects and some of drugs are only suitable to the specific group of patients which depends on age and genetic background of patient in common with all subtype of leukaemia. Therefore, the drugs are still developing in order to improve specificity and minimize side effects. Most of the new drugs are designed based on the better understanding of molecular pathogenesis to inhibit the

specific protein in aberrant signalling pathway or reverse some mutations in each type of leukaemia.

1.3 Bruton's tyrosine kinase

1.3.1 Bruton's tyrosine kinase biology

Bruton's tyrosine kinase is non-receptor tyrosine kinase which belongs to the Tec family of tyrosine kinases and share the same family with TEC, ITK/EMT/Tsk, BMX, and TXK/RLK (Mano, 1999). BTK structure is composed of five domains: which are the Pleckstrin homology (PH), Tec homology (TH), SRC homology domain 3 (SH3), SRC homology domain 2 (SH2), and SRC homology domain 1 (SH1) also known as the kinase domain, as arranged from the N-terminus to C-terminus as shown in Figure 1.1 (Hendriks et al., 2014, Lindvall et al., 2005).

This protein was originally identified in B cells as a signalling molecule in the B cell signalling pathway (BCR), nevertheless BTK is not only expressed in B cells, but this protein is also found in other hematopoietic cells, including spleen, bone marrow, lung, and pancreas but not T cells and plasma cells (Vihinen et al., 2000). In the 1980s, BTK was reportedly mutated to cause severe X-linked agammaglobulinemia (XLA) in humans and less severely in xid mice. BTK is conserved throughout evolution. Since BTK plays an important role in B cells, BTK mutation may cause the defect in B-cell development which leads to X-Linked agammaglobulinemia (XLA) in humans and X-linked immunodeficiency (XID) in mice. In humans, B cell development is arrested at the transition stage from pre B cell to mature B cell. In human, XLA patients are susceptible to recurring infection since BTK in human causes almost

complete absence of mature B cells which leads to a lack of circulating antibody and defect in T cell dependent immune response (Khan et al., 1995). Since mutation BTK is not important in the early stage of B cell development and mutation is found in later stage, therefore circulating B cells in XID are more mature than in XLA and this deficiency is less severe than XLA in humans, even if BTK is deleted in mice. Although BTK mutation causes milder effect in mice, xid mice shows low amount of IgM/IgD B cells, circulated IgM and IgG3, and defect in response to TI-II antigen and other activation signals (Khan et al., 1995).

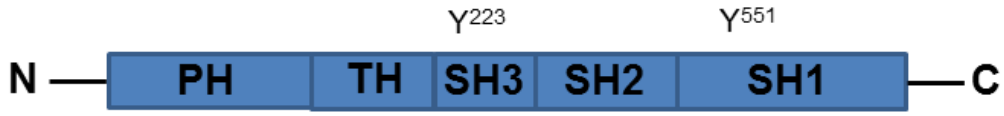

Figure 1.2 Bruton's tyrosine kinase structure.

Bruton's tyrosine kinase (BTK) composes of five domains and the auto- and trans-phosphorylation site are embedded in SH3 and SH1 (kinase domain), respectively. This figure is adapted from (Hendriks et al., 2014).

1.3.2 Subcellular distribution of Bruton's tyrosine kinase

BTK expression is mainly in the cytoplasm, but can also be found in other cellular compartments under specific circumstances. BTK translocates to the plasma membrane and binds to PIP3 after receptors stimulation (Nore et al., 2000). The fully phosphorylated BTK regulates cell response by transducing the signal information through a downstream cascade. There is a small amount of BTK found in nucleus and BTK contains the nuclear localization signal (NLS) which is a transport signal for Exportin 1 (Mohamed et al., 2000). The SH3 domain is important for nuclear export since BTK is retained in nucleus of SH3 mutant cells, and the SH3 domain is proposed to be a binding site of Liar. The BTK-Liar complex is transported to the cytoplasm using the carrier protein, Expotin 1 (Mohamed et al., 2000, Gustafsson et al., 2012). Other studies also propose the nucleocytoplasmic shuttle mechanism of BTK and its binding protein partner which prove nucleus-cytoplasm shuttle and possibility that BTK plays an important role in nucleus. BAM11 and Liar are identified as BTK binding protein and may involve in nucleus-cytoplasm travelling of BTK (Kikuchi et al., 2000, Hirano et al., 2004, Gustafsson et al., 2012, Gustafsson et al., 2017).

The B cell regulator of Ig heavy chain transcription (Bright) is proposed as a putative BTK binding partner and BTK is needed to form a DNA binding complex (Webb et al., 2000, Rajaiya et al., 2005). Although, the role of BTK itself in the nucleus still remains to be discovered, however there are several studies showing that BTK regulates nuclear proteins such as NF-κB, transcription factor II-I (TFII-I), and Bright. So, this data may imply the

possibility that BTK has a role in nucleus. Nevertheless, we need more evidence to prove this hypothesis.

1.3.3 Bruton's tyrosine kinase and relevant signalling pathways

As BTK is a player in several signalling pathways, it can act as a linker protein activated by various receptors to control diverse cellular responses. We explore only two of these signalling pathways here that relate to this study.

1.3.3.1 B cell receptor (BCR) signalling pathway

The BCR signalling pathway controls B cell survival and proliferation, where the B cell receptor comprises a surface immune receptor associated with Igα/Igβ or CD79A/CD79B heterodimer with immunoreceptor tyrosine based activation motifs (ITAMs), and co-receptor (CD19). As BTK was firstly identified in XLA and XID where BTK mutation affects B cell development, the participation of BTK in BCR is well characterized in normal B cells and B cell malignancies.

Once BCR is activated by IgM binding, there are two situations which may occur at the same time. The Src family protein tyrosine kinase, LYN phosphorylates ITAMs and CD19 which recruits SYK and PI3K binding at ITAMs of the Igα/Igβ heterodimer and CD19, respectively (Hibbs and Dunn, 1997, O'Rourke et al., 1998). BTK is recruited to plasma membrane and anchored to the membrane via the PH domain and the second messenger, PIP3 which is generated from PI3K (Saito et al., 2001). The membrane bound BTK is fully activated by both SYK phosphorylation at Y^{551} and auto-phosphorylation at Y^{223}. The activated p-BTK transduces

signals to control cellular responses via several downstream signalling proteins by phosphorylates phospholipase C-γ2 (PLCγ2), which is a direct substrate of BTK (Kurosaki, 2002). The PLCγ2 is a Ca^{2+} regulator via PIP3 generated from PIP2 and this pathway lead to activation of nuclear factor of activated T cells (NFAT) (Pal Singh et al., 2018). In parallel, another secondary messenger which also generated from PIP3, diacylglycerol (DAG) activates protein kinase C beta (PKCβ). The p-PKCβ can control two important downstream effector molecules which are ERK1/2 via Ras-dependent phosphorylation and NF-κB (Pal Singh et al., 2018). The BCR signalling pathway is shown in Figure 1.2.

1.3.3.2 SDF-1α/CXCR4 chemokine signalling pathway

SDF-1α/CXCR4 is involved in leukaemia pathogenesis by providing the survival support signal and protecting leukaemia cells from drug-induced apoptosis by induced CXCR4 receptor expressed, stimulating cells to migrate towards SDF-1α and retain inside bone marrow microenvironment. BTK is reported to be involved in this pathway and BTK inhibition shows effects from SDF-1α/CXCR4 interference. As shown in Figure 1.4, CXCR4 transduces signalling to BTK via G protein subunit and links BCR signalling pathway and SDF-1α/CXCR4 by using BTK as a linker molecule.

There are studies showing that BTK can receive signalling from CXCR4 receptor and transduce signalling to regulate migration and adhesion in response to SDF-1α in mouse and human B cells. In addition, BTK deficient B cells also show defects in homing to lymphoid organs (de Gorter et al., 2007, Ortolano et al., 2006). In CLL, BTK inhibition using

ibrutinib blocks pro-survival signal from NLCs and diminishes cell survival and migration induced by CXCL12 (SDF-1α) and CXCL13 (Ponader et al., 2012). Even though the role of BTK in AML is not well understood, there are a few studies that show involvement between BTK and CXCR4 receptor in this leukaemia subtype. BTK inhibition reduces SDF-1α induced cell migration in AML patient samples (Zaitseva et al., 2014).

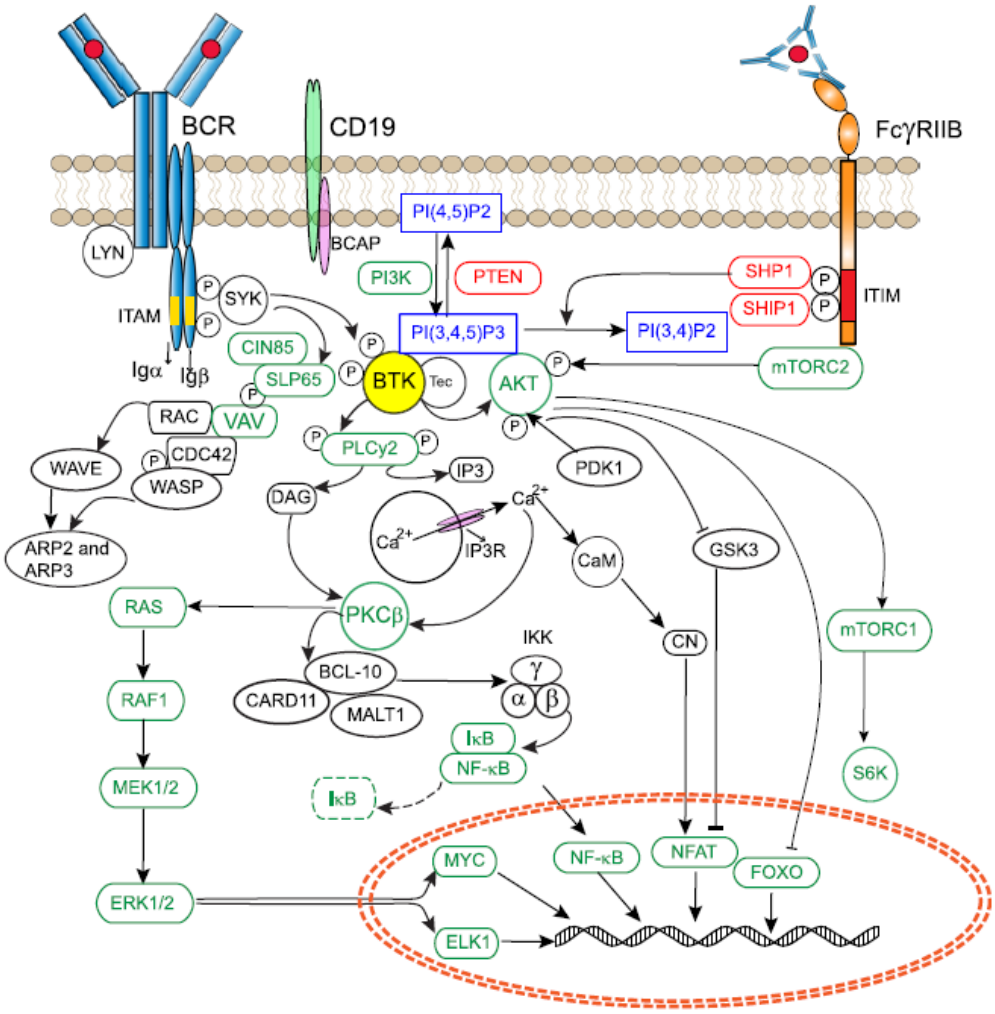

Figure 1.3 B cell receptor (BCR) signalling pathway (Pal Singh et al., 2018).

This figure shows BTK is one of several participants in B cell receptor signalling pathway. BTK is recruited to plasma membrane and activated by SYK. The phosphorylated BTK activates downstream signalling molecule which transduce the signalling in order to response to stimuli. This figure is adapted from Pal Singh et al. Molecular Cancer (2018) doi: 10.1186/s12943-018-0779-z.

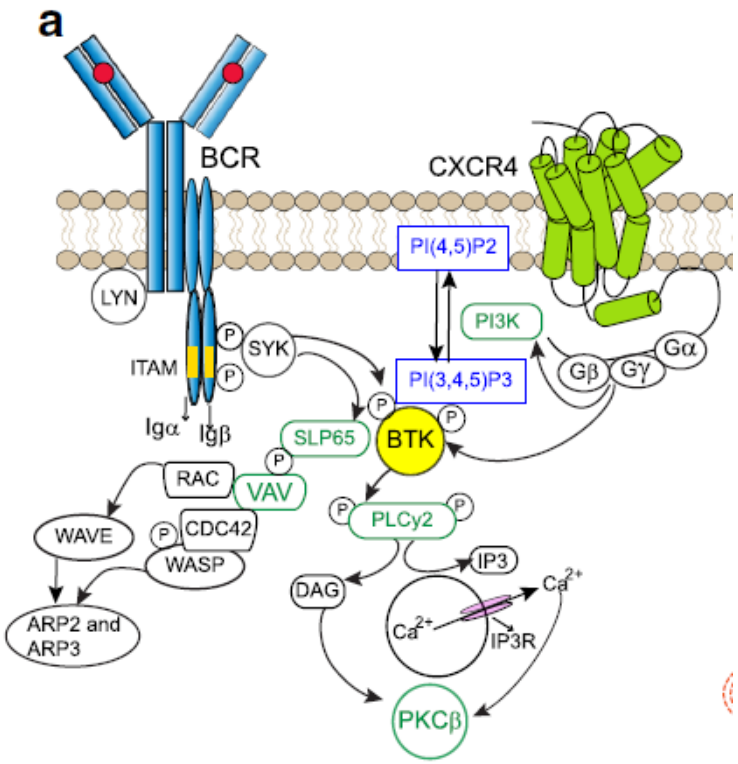

Figure 1.4 Role of Bruton's tyrosine kinase in B cell receptor and SDF-1α/CXCR4 signalling pathway (Pal Singh et al., 2018).

BTK participates in SDF-1α/CXCR4 signalling pathway in addition to BCR signalling pathway and act as a linker molecule to link each signaling pathway into the signalling network as shown in this figure. This figure is adapted from Pal Singh et al. Molecular Cancer (2018) doi: 10.1186/s12943-018-0779-z. The Creative Commons License (http://creativecommons.org/licenses/by/4.0/)

1.3.4 Role of BTK in chronic lymphocytic leukaemia

As BTK controls cell survival and proliferation, aberrant p-BTK may lead to an imbalance of cell proliferation related diseases, especially cancers. In CLL, the participation of BTK is well characterized compared to its role in AML. The difference in BCR signalling responses has been reported in normal B cells and CLL including BCR and co-receptor density and variety in downstream signalling protein activation (Woyach et al., 2012). In CLL, BTK mRNA expression is elevated compared to normal B cells and BTK expression at protein level is varied among CLL patients without correlation to with other disease-related factors (Herman et al., 2011). The important roles for BTK were proven by investigation into the effect of BTK inhibition on the downstream cellular responses in several studies. Other proteins proposed as downstream molecules were also investigated after BTK inhibition. The phosphorylation of ERK1/2 decreased compared to untreated, and DNA-binding activity of NF-κB was reduced after CLL patient samples were treated with PCI-32765 (Herman et al., 2011). Since BTK is involved in BCR signalling pathways that control cell survival and proliferation, several studies showed BTK inhibition diminished these two cellular responses (Ponader et al., 2012, Herman et al., 2011).

Since, BTK can transduce signals from several receptors and the role of BTK is not restricted to BCR signalling, the effects of BTK inhibition on CLL survival and other effector responses was investigated in other pathways including microenvironment-involved signalling pathways. PCI-32765 reduced the effect of cytokine supporting survival signals that provided from TNF-α, IL-6, IL-4, CD40L, BAFF, and co-culture with stromal cells and induced apoptosis in co-treatment. (Herman et al.,

2011). There is evidence to show BTK is also critical in the SDF-1α/CXCR4 axis which Ibrutinib treatment interferes in CLL. Ibrutinib treatment effects CXCR4 receptor density and downstream effectors which cause CLL cells egress from secondary lymphoid organs into the blood circulation (lymphocytosis)(Chen et al., 2016).

1.3.5 Role of BTK in acute myeloid leukaemia

Although participation of BTK is reported in B cells and B cell malignancies, the supporting evidence that BTK may be important in AML is expanded in AML leukaemia subtype research even though roles of BTK in AML are not well understood. The proposed role of BTK in this leukaemia subtype is emphasized in survival signals that are provided from bone marrow microenvironment. BTK and p-BTK is also detected in AML patients with variation among patients as shown in CLL. Moreover, BTK itself and other downstream proteins of BTK are activated after SDF-1α treatment, moreover, genetically BTK inhibition affects AML cell migration toward SDF-1α (Rushworth et al., 2014, Zaitseva et al., 2014). Since BTK is a linker molecule, the aberrant mode of BTK and p-BTK also affects other pathways. As BTK may be important in AML as well as in CLL, BTK inhibitors are interesting therapeutic treatments. We need more information to understand the roles of BTK in AML.

1.4 SDF-1α/CXCR4 signalling pathway

CXCR4 is a seven transmembrane G-protein-coupled receptor firstly identified as a co-receptor for HIV-1 T-tropic virus infection (Feng et al., 1996). The stromal cell-derived factor (SDF-1α) also known as CXCL12 is a chemotactic cytokine (chemokine) belonging to the CXC group. SDF-1α

was firstly identified in murine bone marrow stromal cells (Teicher and Fricker, 2010, Tashiro et al., 1993). The SDF-1α is encoded from the same gene as another isoform, SDF-1β, by splicing (Shirozu et al., 1995). SDF-1α induces directional migration of CXCR4 expressing cells towards SDF-1α. In normal circumstances, SDF-1α/CXCR4 is responsible for several processes including haematopoiesis, germ cell development, neurogenesis, cardiogenesis and vascular formation (Nagasawa, 2014). SDF-1α/CXCR4 induced cell mobilization is important for cancer cells because the signalling pathway is necessary for processes in normal cells and those dysregulated in cancer development such as preventing apoptosis and promoting migration.

In general, SDF-1α/CXCR4 signalling pathways play a vital role in normal cells, however cancer cells can take advantage of this pathway to support survival, proliferation, and other effects. The SDF-1α/CXCR4 signalling pathway is one of the pathways controlling chemotactic cell migration, adhesion, and cell survival. This pathway is crucial in the microenvironment that provides supportive sustenance for cell survival and to prevent drug-induced apoptosis. As such, CXCR4 can be used as a prognostic marker in leukaemia.

1.5 G-protein-coupled receptor and Heterotrimeric G proteins

The G-protein-coupled receptor (GPCR) is the largest class of human membrane receptors with each possessing seven transmembrane-loops in their structure (Kobilka, 2007). Once a GPCR is activated with a specific ligand, signalling conveys to downstream proteins via a heterotrimeric G protein linked to the cytoplasmic tail of the receptor (Simon et al., 1991).

The heterotrimeric comprises of Gα, Gβ, and Gγ subunits. The Gα subunit can be classified into $G\alpha_i$, $G\alpha_s$, $G\alpha_q$, and $G\alpha_{12}$ based on amino acid similarity with each subclass linked with different surface receptors and transduce signalling to diverse effector proteins as shown in Figure 1.4 (Simon et al., 1991). The activation of heterotrimeric G proteins is regulated by guanine nucleotide triphosphate (GTP) binding with the Gα subunit. In its resting state, Gα, Gβ, and Gγ are together in a heterotrimeric form with Gα bound to GDP. In activation, ligand binding induces receptor conformational change and GDP is replaced with GTP and the heterotrimeric G protein becomes active. The G protein complex dissociates into Gα-GTP and Gβγ which lead to downstream pathway activation. Once GTP-bound Gα protein is hydrolysed to GDP, the heterotrimeric structure reforms and returning to an inactive state (Kamp et al., 2016). The occupancy of Gα with GTP or GDP is controlled by guanine nucleotide exchange factors (GEFs), GTPase-activating protein (GAPs), and guanine nucleotide dissociation inhibitor (GDIs) as shown in Figure 1.5 (Siderovski and Willard, 2005).

GPCRs can transduce information from ligand to more than one class of Gα subunit which increases the variety of cellular responses as different classes of Gα regulate distinct effector responses. The $G\alpha_s$ subclass activates adenylyl cyclase and cAMP while $G\alpha_i$ or pertussis toxin sensitive G protein inhibits adenylyl cyclase and regulates ion channel. The $G\alpha_q$ subunit controls Ca_2^+ mobilization via PLCβ, IP3 and DAG generation which in turn controls Ca_2^+ efflux and activates PKC, respectively (Neves et al., 2002). Although the $G\alpha_{12}$ subclass is not fully understood, the study of this subclass is still growing and $G\alpha_{12}$ has been reported to bind BTK,

Ras-GAP, ERK5 and JNK (Jiang et al., 1998, Neves et al., 2002). Another member of this subclass, $G\alpha_{13}$ is reported to transduce signals to GTPase Rho and PI3K pathways (Neves et al., 2002, Shi and Kehrl, 2001). In addition, studies show GPCRs can couple with more than one Gα subclass and the same receptor can be linked with different Gα subunit in different cell line. The chemokine signalling pathway SDF-1α/CXCR4 can transduce signalling from SDF-1α to downstream proteins through both $G\alpha_i$ and $G\alpha_{12}$ in hematopoietic cells and breast cancer respectively (Tan et al., 2006, Zaitseva et al., 2014, Yagi et al., 2011). This information demonstrates the complexity of GPCRs and cellular responses through G protein regulation which need to be investigated in different cell lines.

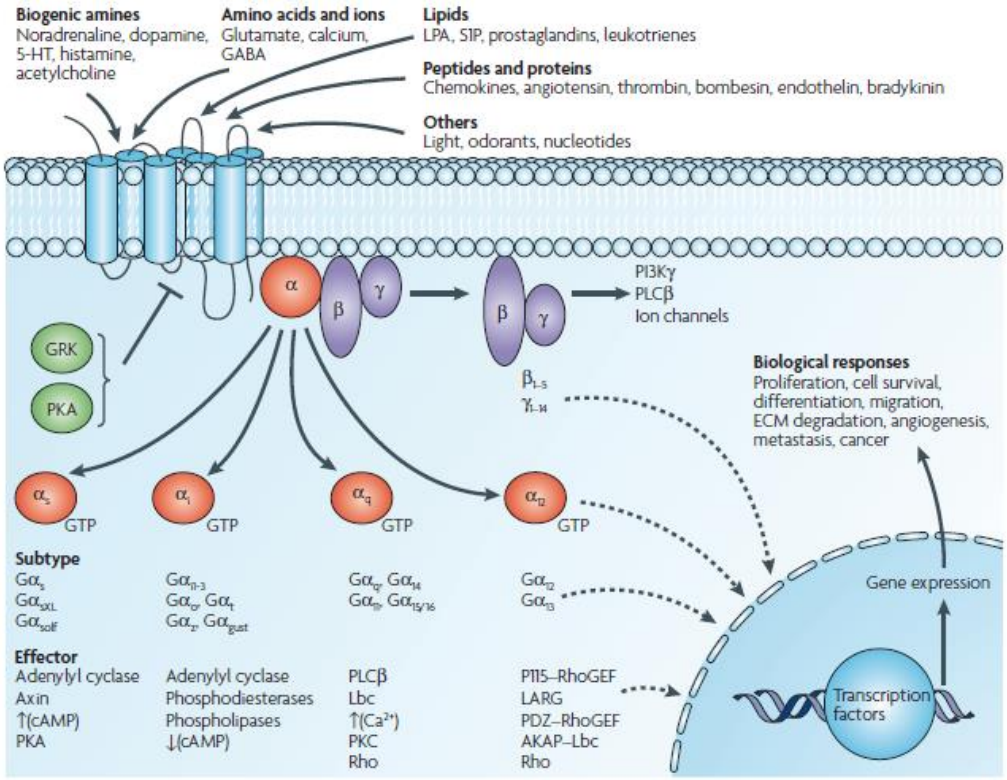

Figure 1.5 Diversity of G protein signal transduction.

GPCR signalling is initiated from external stimuli and signalling information is transduced downstream via G protein coupled receptor containing an α subunit and βγ heterodimer. The diversity of GPCR signal transduction is associated to the differenced in the seven-transmembrane receptor. G protein coupled receptor can be activated with various types of stimuli. Gα subunit is divided into four subclasses resulting in the activation of different signaling molecules. This figure is adapted from (Dorsam and Gutkind, 2007)

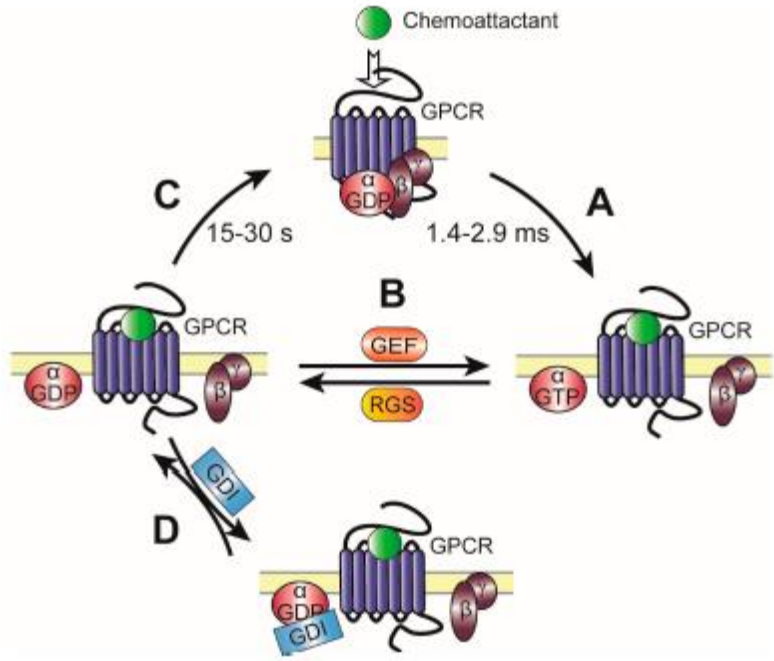

Figure 1.6 The regulation of Gα subunit (Kamp et al., 2016).

The active and inactive state of G proteins is controlled by GTP/GDP binding with Gα protein. This figure is adapted from (Kamp et al., 2016) doi: 10.3390/ijms17010090.

1.6 Lentiviral vector and short hairpin RNA-based gene silencing technology

Lentiviruses are single stranded positive RNA viruses which are classified into *Retroviridae* family, *Retrovirus* genus (Sakuma et al., 2012). The lentiviral vectors are constructed based on HIV-1. Lentiviral technology takes advantage of the retrovirus life cycle as the viral genome is integrated into host chromosomes which is beneficial for long term expression of the transgene. Lentiviruses are capable of infecting a wide variety of cell types including dividing and non-dividing cells including cells of a hematopoietic lineage (Wiznerowicz and Trono, 2005).

Lentiviral vectors have been modified to increase biosafety and enhance transfection performance. As a safety consideration, only the necessary viral genes for viral capsid (*gag*), transcriptional enzyme (*pol*), and viral envelope (*env*) are embedded in the lentiviral vector while the virulence involved accessary genes are removed (Blesch, 2004, Kim et al., 1998).

In order to increase biosafety and transfection efficiency, the viral genes are separated into different vectors and the lentiviral *env* gene is changed to another viral *env* gene. The lentiviral vectors are developed into several generations of vector (Figure 1.7). In the first and second generation lentiviral vector, structure and packaging encoded genes are separated into 2 plasmids and the transgene is placed on another plasmid along with 5' LTR, 3' LTR region and viral accessory genes (*vif*, *vipu*, *vpr*, and *nef*) are deleted in the second generation. In the third generation, there are three main modifications. The rev is placed solely on another plasmid, separated from the packaging plasmid. The 5' and 3' LTR are modified in the transgene plasmid in to minimize the opportunity of creating replication-competent lentivirus. The promotor of the transgene vector is changed to a CMV promotor (Sakuma et al., 2012).

Gene silencing is a useful application to study the importance of an interesting protein or to dissect signalling pathways. Short hairpin RNA (shRNA) mediated gene silencing provides long term gene suppression. The structure of shRNA comprises an siRNA sequence, loop region, complementary siRNA sequence, and terminator (Manjunath et al., 2009). As shown in Figure 1.7, the process of shRNA mediated gene silencing starts from lentivirus production of shRNA containing lentiviral particles in

packaging cells. HEK293T cells are usually used as a factory for lentiviral production (Manjunath et al., 2009). Once targeted cells are transfected with shRNA containing viruses, the transgene vector is integrated into the host genome and the shRNA is produced and processed by Drosha in the nucleus. The shRNA that serves as siRNA precursor is transported to the cytoplasm and the loop part is cut by Dicer to create siRNA. The anti-sense strand is loaded into RISC and binds to complementary regions in the target mRNA. Gene suppression may result from mRNA degradation or translation suppression. Since shRNA integrates into the host genome, the siRNA is constitutively expressed and target mRNA is stably suppressed (Torrecilla et al., 2014).

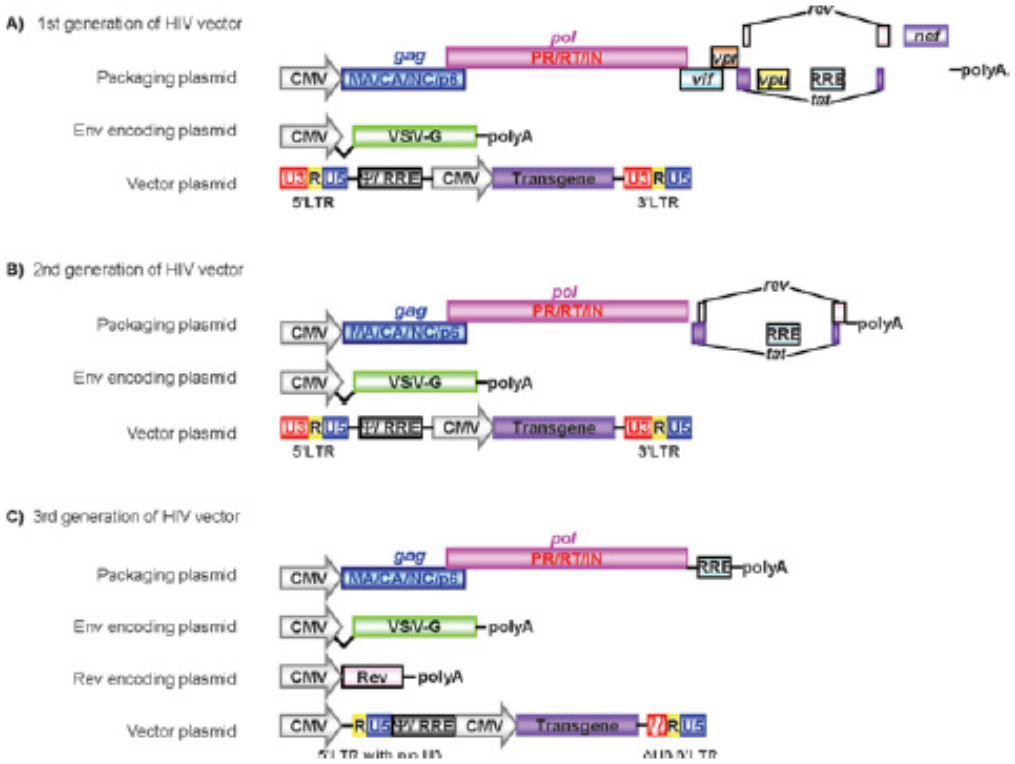

Figure 1.7 The development of the lentiviral vector system. Figure adapted from (Sakuma et al., 2012). As a safety consideration, the lentiviral genes are separated to different plasmids. The first generation, the necessary viral genes are separated into two plasmids (A). The accessory genes (vif, vpu, vpr, and nef) are removed from plasmids in the second generation (B). The third generation plasmid, rev is separated into its own plasmid therefore this generation contain four plasmids.

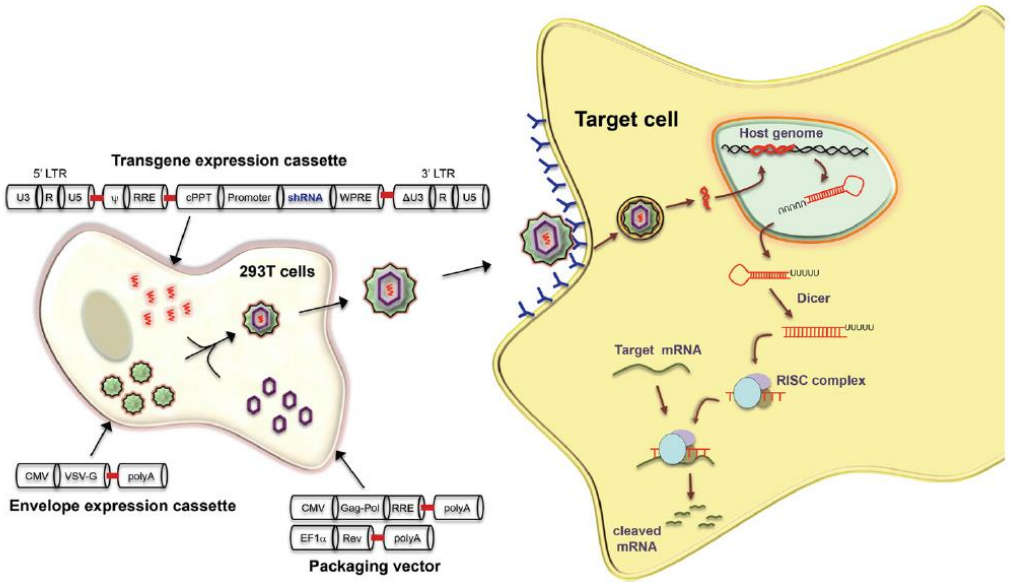

Figure 1.8 Short hairpin RNA containing lentivirus production. Figure adapted from (Manjunath et al., 2009). Shown are the structural lentivirus plasmids and transgene plasmid co-transfected into HEK293T cells to produce shRNA containing lentivirus particles. The lentiviruses are transduced into target cells and the shRNA integrated into host genome after successful transfection. Short hairpin RNA is transcribed and processed to produce siRNA which suppresses target mRNA.

1.7 Objectives

This study is composed of three main objectives in order to understand the importance of the role of BTK in acute myeloid leukaemia subtypes.

1. To determine the BTK and p-BTK distribution in the cytoplasm and nucleus and the role for BTK in the nucleus.
2. To identify whether $G\alpha_{12}$ or $G\alpha_{13}$ G-protein subclasses transduce signalling information from the CXCR4 chemokine receptor.
3. To determine whether BTK can transduce the chemokine signal through $G\alpha_{12}$ or $G\alpha_{13}$.

Chapter II

Materials and Methods

2.1 Materials

2.1.1 Reagents and Materials

Most of the chemical reagents were purchased from Fisher Scientific or otherwise stated if those chemicals were purchased from other companies.

2.1.2 Cell lines

U937, THP-1, HL-60, and OCI-AML3 were obtained from American Type Culture Collection (ATCC). U937 and THP-1 are acute monocytic leukaemia cells classified as AML M5 according to FAB classification system. THP-1 harbour t(9;11) and MLL-AF9 translocation while U937 carries t(10;11)(p13;q14) translocation (Tsuchiya et al., 1980, Sundstrom and Nilsson, 1976). HL-60 is an acute promyelocytic leukaemia line which classified into M2/M3 and bears c-myc mutation and several chromosomal abnormalities (Birnie, 1988). Kasumi-1 is a t(8;21) translocation caused AML1-ETO gene fusion with a c-kit mutation in the tyrosine kinase domain and is classified into AML M2 subtype (Asou et al., 1991). OCI-AML3 is AML M4 carrying a nucleoplasmin mutation in exon 12 (Quentmeier et al., 2005). JEKO-1 (Mantle Cell Lymphoma), OCI-LY19 (B cell lymphoma), and Kasumi-1, are kindly gifted from Dr. Joseph Slupsky's laboratory. Human embryonic kidney cells (HEK293T) was kindly given from other laboratories (John Quinn).

Cell lines	Leukaemia Subtype
OCI-AML3	AML M4
HL-60	AML M2/M3
U937	AML M5
THP-1	AML M5
Kasumi-1	AML M2
Jeko-1	Mantle Cell Lymphoma
OCI-LY19	B cell lymphoma

Table 2.1 AML and CLL cell lines.

This table shows the detail of AML and CLL cell lines that we used as models in this study. AML cell lines were classified according to France-American-British Classification (FAB) where AML was classified into 7 subclasses from M0-M7 according to their genetic abnormality.

2.1.3 Antibodies

Antibodies were purchased from Cell Signalling Technology. The anti-mouse and anti-rabbit secondary antibodies conjugated to horseradish peroxidase (HRP) were obtained from Santa Cruz Biotechnology. The specific company will be stated if antibodies were purchased from other sources. Details of each antibody are shown in Tables 2.2 and 2.3.

Primary Abs	Type	Host	Dilution	MW (kDa)	Company
p-BTK (Y^{223})	Polyclonal	Rabbit	1:1000	76	Cell signalling technology®
p-BTK (Y^{223}) (D9T6H)	Monoclonal	Rabbit	1:1000	76	Cell signalling technology®
BTK (D3H5)	Monoclonal	Rabbit	1:1000	76	Cell signalling technology®
p-Erk1/2	Polyclonal	Rabbit	1:2000	42 and 44	Cell signalling technology®
p44/42 MAPK (Erk1/2)	Polyclonal	Rabbit	1:2000	42 and 44	Cell signalling technology®
p-PLCϒ2	Polyclonal	Rabbit	1:2000	150	Cell signalling technology®
PLCϒ2 (B-10)	Monoclonal	Rabbit	1:2000	150	Santa Cruz Biotechnology
$G\alpha_{12}$ (S-20)	Polyclonal	Rabbit	1:500	42	Santa Cruz Biotechnology
$G\alpha_{13}$ (A-20)	Polyclonal	mouse	1:200	42	Santa Cruz Biotechnology
Anti-β-actin	Monoclonal	Mouse	1:10000	42	Sigma
GAPDH	Monoclonal	Rabbit	1:2000	30	Cell signalling technology®

Table 2.2 List of primary antibodies.

Primary antibodies used are described in this table.

Secondary Abs	Conjugated Substrate	Host	Dilution	MW (kDa)	Company
Anti-rabbit IgG	Horseradish peroxidase conjugate	Goat	1:5000	-	Santa Cruz Biotechnology
Anti-mouse IgG	Horseradish peroxidase conjugate	Goat	1:5000	-	Santa Cruz Biotechnology
Anti-rabbit IgG	Horseradish peroxidase conjugate	Goat	1:3000	-	Cell signalling technology®
Anti-mouse IgG	Horseradish peroxidase conjugate	Horse	1:3000	-	Cell signalling technology®

Table 2.3 List of secondary antibodies.

Secondary antibodies used are described in this table.

2.2 Methods

2.2.1 Sterile cell culture maintenance

Cell culture medium and supplements were purchased from Gibco Life Technologies. The AML cell lines which were U937, HL-60, MV4-11, OCI-AML3, and Kasumi-1 were cultured in Rosewell Park Memorial Institute (RPMI) 1640 supplemented with 10% foetal bovine serum (FBS) and 1000 unit/mL of penicillin/streptomycin (Pen/Strep). The OCI-LY19 cell line was grown in RPMI 1640 media supplemented with 20% FBS and 1000

units/mL of Pen/Strep. The Human Embryonic Kidney 293T (HEK293T) cells were cultured in Dulbecco's Modified Eagle Medium (DMEM) supplemented with 10% FBS and 1000 unit/mL of Pen/Strep. Cells were incubated under 37ºC, 5% CO_2 environment. Cell sub-culturing was performed regularly.

2.2.2 Cryopreservation and cell recovery

To store cells, they were maintained in culture conditions until they reached exponential growth phase. Cells were harvested by centrifugation at 200 x g for 5 min, culture medium was removed, the pellet was resuspended in freezing medium (10% DMSO (Sigma Aldrich, UK) + 90% FBS) and transferred to cryovials (Corning, UK). Cells were placed in a 'Mr Frosty' freezing container and kept at -80ºC for 24 h to allow temperature to be gradually reduced before transferring to liquid nitrogen for long-term storage.

To recover cells from liquid nitrogen, cryovials containing cells were rapidly thawed in water bath at 37ºC. The complete medium was added directly to the cryovial tube then transferred to 15 mL tube 10 volumes of complete medium. Then cells were spun at 200 x g for 5 min removing dead cells and DMSO because DMSO has cytotoxic effects on the cells. Cell pellets were re-suspended in an appropriate volume of complete medium then transferred to appropriate cell culture vessel and incubated at 37^{o}C, 5% CO_2.

2.2.3 Molecular Biology Techniques

2.2.3.1 RNA extraction and complementary DNA synthesis

RNA extraction was performed following the protocol from Qiagen's RNeasy Mini Kit (Qiagen, UK). Cells at 5 x 10^5 cells per sample density were pelleted at 300 x g for 5 min at 4ºC. Cells were lysed with Buffer RLT and vortexed for 1 min. The homogenized sample was stored at -80ºC or used for mRNA extraction immediately. Then 1 volume of 70% ethanol was added to cell lysate with repeat pipetting until homogenized. Next, this was applied onto an mRNA binding column before spinning at 1,200 x g for 20 s. The column was washed with 700 µL of RW buffer and spun at 1,200 x g for 20 s then 500 µL of RPE buffer was added onto the column which was spun as above. Another 500µL of RPE buffer was then added and spun at the same speed for 2 min. The empty column was spun at 1,400 x g for 2 min to remove the remaining RPE buffer. Warm DNase/RNase free water was added to column to elute RNA then the column was left on the bench for 5 min before spinning at 1,200 x g for 1 min. The elution step was performed twice and RNA concentration was measured by NanoDrop Spectrophotometer.

The complementary DNA (cDNA) was synthesized with iScript cDNA synthesis kit (BIO-RAD, UK) as per manufacturer's protocol. The protocol comprises three main steps which are priming at 25ºC for 5 min, reverse transcription at 46ºC for 20 min, reverse transcriptase inactivation at 95^{o}C for 1 min, and an optional step to hold the reaction at 4ºC.

2.2.3.2 Protein extraction and quantification

In order to examine the expression of interested proteins, cells were centrifuged at 800 x g, 4ºC for 1 min and supernatant was removed. The cell pellet was washed once with 1 x ice-cold PBS and pelleted again at 800 x g, 4ºC for 1 min. PBS was prepared by dissolving 1 PBS tablet (Sigma Aldrich, UK) with 200 mL of MilliQ and sterilising in an autoclave at 121ºC for 15 min. The harvested cells were lysed with SDS clear sample buffer (1% SDS, 50 mM Tris-HCl pH6.8, 5 mM EDTA, and 10% glycerol) 100 µL per 3 x 10^6 cells. Then DNA was removed by sonication and protein was boiled at 95ºC for 5 min. Cell debris and unbroken cells were cleared by spinning at 1,400 x g for 10 min. The supernatant containing protein was transferred to pre-chilled Eppendorf tubes and stored at -20ºC for further experimentation.

Bovine serum albumin (BSA) (Sigma Aldrich, UK) was used as a protein standard for the detergent-compatible assay (DC Assay) by 2-fold serial diluting in SDS clear lysis buffer from 2 mg/mL to 0 mg/mL Protein quantification is a critical step for investigation of the expression level of targeted proteins. The DC assay kit was composed of Reagent A, Reagent S, and Reagent B. Five microliters of blank, standards ranging from 0.125 mg/mL to 2 mg/mL, and protein samples were added into separate wells of a 96-well plate. Then 25 µL of AS solution mixture (50:1 ratio) was added to each well before 200 µL of Reagent B was added on top of the AS mixture. The plate was incubated for 10 min (room temperature) before reading absorbance at 750 nm on plate reader. DC Assays were performed in duplicate.

2.2.3.3 Western Blotting

Protein was separated by electrophoresis according to molecular weight. The sodium dodecyl sulphate-polyacrylamide (SDS-PAGE) was prepared by using gel setting apparatus (BIO-RAD, UK). Different percentages of polyacrylamide gels were used according to size of the targeted protein. The resolving gel and stacking gel were prepared as shown in Table 2.4. The resolving gel was poured between glass plates on the casting frame, 70% ethanol was overlain on top of the gel which was allowed to polymerize for 30 min. Then the stacking gel was poured on top of the resolving gel after 70% ethanol was removed and rinsed with water before a comb was inserted between glass plates and the gel was left to polymerize for another 30 min. The required protein concentration was mixed with lysis buffer and loading dye (5 x loading dye to give a final 1 x concentration of 10% glycerol, 5% β-mercaptoethanol, 3% SDS, and 62.5 mM Tris, pH 6.8) then loaded onto stacking gel. The SDS-PAGE was resolved at constant 30 mA per gel. The SDS-PAGE was performed until the loading dye reached the bottom of the gel (around 1 h). The transfer sandwich was prepared following the order, cassette, sponge, two pieces of filter paper, gel, membrane, two pieces of filter paper, and sponge. The sandwich was placed into a tank containing cold transfer buffer (25 mM Tris Base and 0.2 M glycine). Protein transferring was performed with constant 400 mA for 1 h. After that, the membrane was blocked with blocking buffer (5% skimmed milk in TBS-T, (10 x TBS; 10 mM Tris, 150 mM NaCl, pH 8 with 0.1% Tween-20 added after diluted 10 x TBS to 1 x TBS) for 1 h, then the membrane was incubated overnight at 4ºC with primary antibody. Next day, the membrane was washed with TBS-T twice x 15 seconds, twice x 5 min, and a last wash step of 15 min. Membrane

was incubated for a further 1 h with the desired primary antibody at the required concentration (typically 1:1000). Primary antibody was then washed 3 times with 1 x TBST (5 min each) before incubation for 1 h with the necessary species-matched secondary antibody conjugated with horseradish peroxidase (HRP), being diluted (typically 1:10,000) in blocking buffer (5% skimmed milk in TBS-T). After secondary antibody incubation, the membrane was washed with the same protocol for primary antibody. In order to detect the interested protein, the membrane was incubated with enhanced chemiluminescence (ECL) (Millipore) which contains luminol (the substrate of HRP). The light emitted from the oxidation reaction between HRP and luminol was detected by X-ray film or the ChemiDoc Imaging System from BIO-RAD. A list of primary antibodies and secondary antibodies are shown in Tables 2.2 and 2.3.

Reagent	8%Resolving gel	10%Resolving gel
Acrylamide (Geneflow)	4mL	5.7mL
Resolving Buffer	4.25mL	4.25mL
MilliQ	8mL	7.05mL
APS (Thermo Scientific)	50µL	50µL
TEMED (Sigma-Aldrich)	15µL	15µL

Reagent	5%Stacking gel
Acrylamide (Geneflow)	4.36mL
Stacking Buffer	1.9mL
MilliQ	1.24mL
APS (Thermo Scientific)	50µL
TEMED (Sigma-Aldrich)	15µL

Table 2.4 Sodium dodecyl sulphate polyacrylamide gel (SDS-PAGE) electrophoresis.

Protein was separated according to molecular weight on different percentages of acrylamide.

2.2.4 Cell Fractionation

This protocol was adapted from Trentin L et al, blood, 2008 (Trentin et al., 2008) . In order to examine the phosphorylation pattern and expression of BTK in different cellular compartments, 5 x 10^7 cells were harvested, centrifuged for 5 min at 200 x g and washed once with ice-cold PBS. The pellet was lysed with isotonic buffer (50 mM Tris-HCl pH 7.5, 0.25 M saccharose), transferred to pre-chilled 1.5 mL Eppendorf tubes and subjected to 3 times sonication on ice with 25% amplitude for 5 seconds, with 15 second intervals between each 5 second burst. After sonication, the lysate was pelleted at 10,000 x g for 10 min with nuclear protein present in this pellet. The supernatant which contains cytoplasmic protein, light membrane protein, and heavy membrane protein, was transferred to a new pre-chilled 1.5 mL Eppendorf tube and were separated further as described below.

To isolate nuclear protein, the pellet from above sample was washed once with ice-cold PBS and spun at 10,000 x g for 10 min to remove contaminants before being lysed with clear SDS-PAGE sample buffer (1% SDS, 50 mM Tris-HCl pH 6.8, 5 mM EDTA, and 10% glycerol). The nuclear lysate was further sonicated at 40% amplitude for 10 seconds. This fraction was analysed later as a ***nuclear protein fraction***.

In order to separate other cellular fractions, the previous supernatant from the first step, was spun at 16,000 x g for 30 min. The supernatant was transferred to a new pre-chilled tube which contained light membrane and cytoplasmic protein mixture. At the same time, the pellet was washed once with ice-cold PBS and centrifuged again at the same speed and time.

Then protein was sonicated with 40% amplitude for 10 sec. This fraction was referred as a ***heavy membrane protein fraction***.

The last fraction which is the mixture of light membrane protein and cytoplasmic protein was ultra-centrifuged at 105,000 x g for 1 hour. Then the supernatant was transferred to a new pre-chilled 1.5 mL tube. This fraction was analysed as ***cytoplasmic protein fraction***. The pellet from this fraction was washed once with ice-cold 1 x PBS and lysed with clear SDS-PAGE sample buffer. This fraction was sonicated with 40% amplitude for 10 sec in order to get ***light membrane protein fraction***.

2.2.5 CXCR4 staining on AML and CLL cell lines

AML and CLL cell lines were cultured in serum-free RPMI overnight at 5 x 10^5 cells density in 24-well plate. On the day of the experiment, cells were pelleted at 500 x g for 5 min then resuspended in 100 µL of PBS. In order to stain surface CXCR4 receptor, cells were incubated with 25 µg/mL of CD184-PE antibody or 25 µg/mL of mouse IgG2a-PE for CXCR4 receptor and isotype control, respectively. Cells were incubated in darkness for 20 min before washing once with 1 x PBS at 2000 x g for 2 min. Then pellets were resuspended with PBS and the stained cells were analysed for the expression of the CXCR4 receptor by FACS analysis.

2.2.6 SDF-1α treatment in AML and CLL cell lines

AML and CLL cell lines were seeded on 6-well plates at 1 x 10^6 – 3 x 10^6 cell/mL in serum-free RPMI overnight. Cells were treated with 100 ng/mL of SDF-1α in time-course from 0, 1, 5, 10, 20, and 30 min and incubated at 37ºC. Cells were pelleted at 500 x g for 1 min at 4ºC and whole cell protein extraction performed as described in section 2.2.3.2 and SDS-PAGE and Western blot according to the section 2.2.3.3. Phosphorylated BTK (Y223) and BTK were probed for in order to investigate down-steam signalling molecules of the SDF-1α/CXCR4 signalling pathway.

2.2.7 $G\alpha_{12}$/$G\alpha_{13}$ knockdown by lentivirus technology and functional assay

2.2.7.1 Bacteria Transformation

Escherichia coli strain C3040 was used as a bacterial host for plasmid transformation. Bacteria and plasmids were mixed and incubated on ice for 30 min. The heat shock transformation was performed by incubating bacteria-plasmid mixture at 42ºC for 1 min with the mixture replaced directly on ice for 2 min afterward. The 350 µL of super optimum broth with catalytic suppression medium (SOC) (SOB with 1 mL of 2 M glucose) was added and bacteria culture was agitated at 37ºC for 1 h to recovery. 100 µL of transformed bacteria were plated on LB agar containing selective antibiotic according to plasmid backbone and the rest of the bacterial culture was spun at 500 x g for 5 min and approximately 200 µL of the supernatant was removed and the bacterial pellet was resuspended with the remained culture and plated on another LB agar plate. Bacteria were grown at 37ºC for 16 h. Short hairpin RNA plasmids were obtained from the RNAi consortium shRNA library (Broad Institute, MIT) by Dr. Mark

Glenn. The short hairpin RNA plasmids pLKO.1 vector contained shRNA sequences for $G\alpha_{12}$ or $G\alpha_{13}$ and puromycin resistance gene as a selectable marker with gene expression driven by human U6 promoter.

2.2.7.2 HEK293T transfection by using JetPEI

In order to investigate the knockdown ability of each shRNA plasmid, HEK293T was used as a screening system to select the efficient shRNA plasmid able to knockdown the gene of interest in hematopoietic cells transfection. At day one, HEK293T cells were seeded at 2 x 10^5 cells per well on 6-well plates and cultured until cells reached confluence. Five hundred of each shRNA plasmid were mixed with 150 mM NaCl in a final volume of 100 µL. Four microliters of JetPei were mixed with 96 µL of 150 mM NaCl, then JetPei mixture was added into DNA mixture, vigorously vortexed and incubated at room temperature for 20 min before dropwise addition onto seeded HEK293T cells. The transfected cells were incubated in cell culture conditions for 3 days before knockdown efficiency was examined by Western blotting.

2.2.7.3 Lentivirus production

The third generation lentivirus plasmid was used in this thesis in which the necessary genes for viral production were separated into three different plasmids. HEK293T cells were plated at 3 x 10^5 cells/ mL of 10% FCS DMEM without antibiotics in 10 cm petri-dish for 18 to 20 h. On the next day, the transfer plasmid which is pLKO.1 containing $G\alpha_{12}$- or $G\alpha_{13}$-targeted shRNA and the three lentivirus plasmids (pCMV-VSV-G, pRSV REV, and pMDLg/pRRE) were mixed in ratio 4:2:2:2 by using JetPei as a carrier to deliver plasmid into host cells. Culture medium was changed

after 24 h post transfection (h.p.t.) and further incubated for 3 days. The virus particles produced were collected from supernatant at 48 h and 72 h post transfection (h.p.t.). The viral particles were concentrated by ultracentrifugation at 25,000 x g, 4ºC for 2 h then the supernatant was removed and tubes were put upside down in order to dry the remaining liquid. The viral particles were resuspended with sterile PBS in 1:1000 dilution and left at 4ºC for complete resuspension. Finally, viruses were aliquoted and stored at -80ºC until needed for experimentation.

2.2.7.4 Lentivirus transduction in AML and CLL cells

OCI-AML3 and OCI-LY19 cells were seeded at 4 x 10^5 cell/mL (0.5 mL volume/well) in 24-well plates with complete medium in the presence of 8 µg/mL polybrene on the day of the experiment. Then shRNA containing viruses were transfected into the cells by spinoculum method, in which 16 µL of the virus was added onto cells and the plate spun at 120 x g, 37ºC for 1 h. 0.5 mL of medium was added to the transduced cells after 4 h to dilute polybrene final concentration to 4 µg/mL and transduced cells were incubated for 24 h. On the next day, transduced cells were pelleted at 150 x g for 5 min and the supernatant was replaced by new complete medium. Cells were incubated for further 3 days before the transduced cells were selected using 2-4 µg/mL puromycin.

2.2.7.5 Puromycin selection

The transduced cells were pelleted at 100 x g for 5 min then cultured with complete media containing 2-4 µg/mL puromycin in order to select the $G\alpha_{12}$-, $G\alpha_{13}$-targeted shRNA, or scramble control integrated cell population. The puromycin containing medium was replaced every 2 days

and the puromycin selection was performed for 6 days. The surviving cells were harvested and transduction efficiency was checked by Western blotting with $G\alpha_{12}$ or $G\alpha_{13}$ antibody as previously described in section 2.2.3.3. Transduced cells were reselected with puromycin and transduction efficiency checked by Western blotting regularly. OCI-AML3 wild-type (WT) and OCI-LY19 wild-type (WT) were treated with puromycin for control.

Short hairpin RNA $G\alpha_{12}$			
Clone ID	**Hairpin sequence**	**Vector**	**Selectable marker**
TRCN0000036757 (E6)	5'-CCGG-**CGTCAACAACAAGCTCTTCT T**-CTCGAG-AAGAAGAGCTTGTTGTTGAC G-TTTTTG-3'	pLKO.1	Puromycin resistance
TRCN0000036754 (E7)	5'-CCGG-**CGAGTGATGATGTTGTGAAT A**-CTCGAG-TATTCACAACATCATCACTCG -TTTTTG-3'	pLKO.1	Puromycin resistance
TRCN0000036755 (G10)	5’-CCGG-**GCTGAATTACTTTCCTAGTAA** -CTCGAG-TTACTAGGAAAGTAATTCAGC -TTTTTG-3’	pLKO.1	Puromycin resistance

TRCN0000036756 (G11)	5'-CCGG-**GCACGAGATAAGCTTGGCATT**-CTCGAG-AATGCCAAGCTTATCTCGTGC-TTTTTG-3'	pLKO.1	Puromycin resistance
TRCN0000036758 (H1)	5'-CCGG-**CCATGCTGTGAAAGACACCAT**-CTCGAG-ATGGTGTCTTTCACAGCATGG-TTTTTG-3'	pLKO.1	Puromycin resistance
Short Hairpin RNA $G\alpha_{13}$			
Clone ID	**Hairpin sequence**	**Vector**	**Selectable marker**
TRCN0000036884 (C7)	5'-CCGG-**CCGTGACGTGAAGGATACTAT**-CTCGAG-ATAGTATCCTTCACGTCACGG-TTTTTG-3'	pLKO.1	Puromycin resistance
TRCN0000036885 (C8)	5'-CCGG-**GCTCGAGAGAAGCTTCATATT**-CTCGAG-AATATGAAGCTTCTCTCGAGC-TTTTTG-3'	pLKO.1	Puromycin resistance
TRCN0000036886 (C9)	5'-CCGG-**GTCTCCATAATTCTGTTCTTA**-CTCGAG-TAAGAACAGAATTATGGAGAC	pLKO.1	Puromycin resistance

	-TTTTTG-3'		
TRCN0000036887 (C10)	5'-CCGG-**GATAAGATGATGTCGTTTGAT**-CTCGAG-ATCAAACGACATCATCTTATC-TTTTTG-3'	pLKO.1	Puromycin resistance
TRCN0000036888 (C11)	5'-CCGG-**CAATCGTCAATAACCGGGTTT**-CTCGAG-AAACCCGGTTATTGACGATTG-TTTTTG-3'	pLKO.1	Puromycin resistance

Table 2.5 List of short hairpin RNA plasmids.

This table shows the detail of each shRNA clone used in this study. The siRNA specific sequenced is emphasized in bold letter within the hairpin sequence. This table was adapted from siRNA library consortium, Broad Institute.

2.2.7.6 Chemotaxis transwell migration assay

In order to investigate the effect of $G\alpha_{12}/G\alpha_{13}$ knockdown upon migration in response to SDF-1α/CXCL12, the 8 μm pore size transwell insert was used in this experiment. 2 x 10^5 cells of OCI-AML3 wild-type (WT) and $G\alpha_{12}/G\alpha_{13}$ knockdown cells were pelleted and washed once with RPMI supplemented with 1% FBS. These cells were resuspended in 100 μL of the same medium then plated onto a transwell insert. 200 ng/mL SDF-1α was also prepared in 1%FBS RPMI. Then 600 μL of 1% FBS RPMI, 200 ng/mL SDF-1α, or 10% FBS RPMI were added to the bottom chamber.

The transwell plate was incubated at cell culture conditions for 4 h to allow cells to migrate toward SDF-1α. Then the migrated cells were harvested from lower chamber and counted using trypan blue exclusion staining in which cells were counted in triplicate and results were analysed by GraphPad Prism6 program. Results were reported as a fold-change compared with the untreated control.

2.2.7.7 The effect on survival of Gα protein subunit knockdown cells after ibrutinib treatment

The wild-type (WT), $G\alpha_{12}$ or $G\alpha_{13}$ knockdown, and scramble control OCI-AML3 and OCI-LY19 cells were seeded at 1 x 10^6 cell/ mL in 12-well plates. AML and CLL cells were treated with different conditions of ibrutinib ranging from 0, 0.1, 0.5, 1, 5, and 10 µM. The control and treated cells were incubated for 3 days and cells were treated with 2.5% DMSO for 24h as a positive control. The annexin-V/PI was used to stain ibrutinib treated cells in order to assess the effect of ibrutinib treatment on cell survival. Ibrutinib treated and DMSO treated cells were harvested at 150 x g for 5 min and washed once with 1 x binding buffer. Pellets were resuspended with diluted annexin-V (1:1000 with 1 x binding buffer) and cells were incubated in darkness for 20 min and unbound annexin-V was removed by washing cells with 1 x binding buffer once before resuspended with 1 x binding buffer. PI was added to the tube before annexin-V/PI measurement by FACS analysis.

2.2.7.8 Effect of migration on $G\alpha_{12}/G\alpha_{13}$ knockdown cells after Ibrutinib treatment

OCI-AML3 wild-type (WT), $G\alpha_{12}$ or $G\alpha_{13}$ knockdown, and scramble control cells were seeded at 5 x 10^6 cell/mL in RPMI supplemented with 10% FBS and Pen/Strep in 24-well plates. Cells were treated with different concentrations of ibrutinib for 2 h. After ibrutinib treatment, cells were washed twice with RPMI containing 1% FBS and resuspended with 100 µL of 1% FBS RPMI and seeded on transwell insert. Then 600 µL of 1% FBS RPMI, 200 ng/mL SDF-1α, or 10% FBS RPMI were added to the bottom chamber. Cells were allowed to migrate for 4 h and the migrated cells were counted by using trypan blue exclusion staining. The migration assay illustration is shown in Figure 2.1.

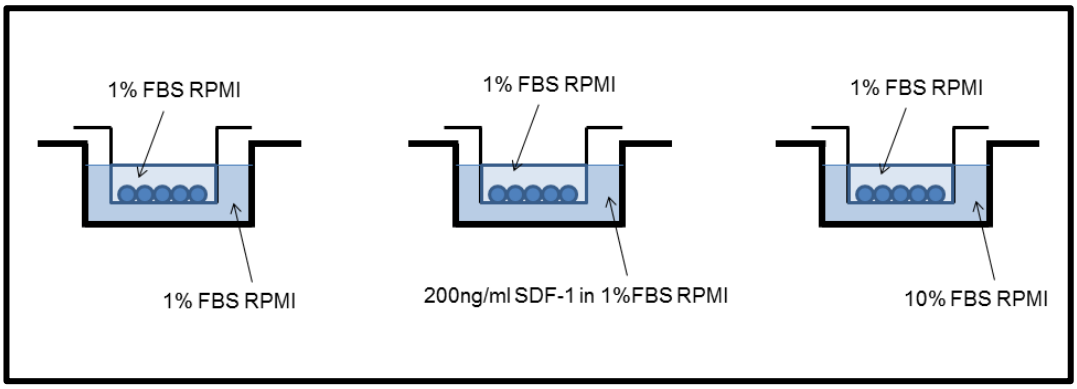

Figure 2.1 Migration Assay.

This illustration shows migration assay experiment. Migration assay was performed on 8 independent repeats and Student's T-test was used as a statistical test which P-value < 0.05 is considered as a significant difference.

2.2.7.9 Effect on cytokine production on $G\alpha_{12}/G\alpha_{13}$ knockdown cells after ibrutinib treatment

OCI-AML3 wild-type (WT) and $G\alpha_{12}$ subclass knockdown (KD) cells were seeded at 2.5 x 10^5 cell/0.5 mL on 24-well plate. Cells were treated with ibrutinib for 2 h then treated continuously with 200 ng/mL SDF-1α for 4 h. Tumour necrosis factor-α (TNF-α) was used as a positive control at 20 ng/mL concentration. After treatment, cells were harvested and subjected to RNA extraction followed by cDNA synthesis as described in section 2.2.3.1. The cytokines expression was analysed by qPCR using the SybrGreen detection system. The qPCR primers were designed and purchased from Integrated DNA Technologies which shown in Table 2.6 below. The SybrGreen qPCR reaction was prepared according to table 2.7. Besides cDNA, each component was prepared in master mix then added to the cDNA contained 96-well plate. The 96-well plate was spun briefly and loaded into qPCR machine.

The qPCR reaction was performed with 50 amplification cycle. Gene expression was calculated from ΔΔCt and fold change of gene expression after treatment was compared to untreated condition. GAPDH was used as a housekeeping gene expression control which GAPDH primer was purchased from Qiagen.

Gene	Forward	Reverse	Product size (bp)	Tm
IFNA1	CCTCGCCCTTTGCTTTACT	GCATCAAGGTCCTCCTGTTATC	114	58
IL-10	TTTCCCTGACCTCCCTCTAA	CGAGACACTGGAAGGTGAATTA	123	58
IL-12A	CCCGGGAGTTAATCCGAAAG	TCTCCTTCTGTGTCTCTCTCTAC	95	58
IL-4	GTTCTACAGCCACCATGAGAA	CCGTTTCAGGAATCGGATCA	94	58
IL-6	GGAGACTTGCCTGGTGAAA	CTGGCTTGTTCCTCACTACTC	99	58
IL-8	CTTGGCAGCCTTCCTGATTT	GGGTGGAAAGGTTTGGAGTATG	111	58
TNFA	CAGGTTCTCTTCCTCTCACATAC	GTCCCGGATCATGCTTTCA	90	58

Table 2.6 Primer list for qPCR.

This table shows list of primers used for qPCR. GAPDH was used as a housekeeping gene control.

Component	Volume (µL)
2XSybrGreen	5
Forward and Reverse Primers Mixture	0.5
RNase free H_2O	2
cDNA (up to 1µg)	2.5
Total Volume	10

Table 2.7 The SybrGreen qPCR reaction component.

This table shows the component of qPCR reaction. Apart from cDNA template, the other components were prepared as master mix.

Chapter III

BTK Expression and its Subcellular Distribution

3.1 Introduction

Bruton's tyrosine kinase (BTK) is a protein kinase which is predominantly expressed in the cytoplasm of cells, however, several reports have supported the concept of functional BTK travelling to the nucleus of cells as well as its association with the plasma membrane. BTK is crucial for B cell development and impairment of normal BTK function in those cells can cause defects in B cell development, as well as such defective BTK function being linked to the generation and propagation of several types of blood cancers.

Upon specific ligand stimulation (for example, B cell receptor linkage to antibodies or chemokine ligand interaction with its receptors), BTK can translocate to different subcellular compartments within the target cells (Hendriks et al., 2014). A GFP-tagged BTK variant was shown to associate with the plasma membrane upon PI3K activation, via the stimulation of several cell surface receptors, including G-protein-coupled receptors, growth factor receptors, and the B cell receptor (Varnai et al., 2005). In addition, translocation of BTK to the plasma membrane can be dependent upon the stimulation of Src protein kinase, with the amount of BTK at the plasma membrane increasing in relation to the levels of Src and BTK-GFP co-transfection (Nore et al., 2000). Another study from this group also showed the domains of BTK that appear important for the process of translocation to the plasma membrane and proposed a shuttling mechanism between cytoplasm and nucleus, using leukaemic and non-leukaemic cells as model systems. Their results showed BTK translocates to the nucleus in both exogenously transfected cells systems and endogenously BTK-expressing cells. Moreover, the PH and SH3

domains of BTK were reported to be involved in the BTK translocation process. BTK which harbours mutations within its pleckstrin homology (PH) domain were redistributed in a manner showing equal distribution in both cytoplasm and nucleus regions within cells. BTK was also found to be predominantly found in nuclear compartments when SH3 domain mutations were present (Mohamed et al., 2000). Thus, subcellular distribution of BTK between cytoplasmic, membrane and nuclear areas is achievable in cells and involves its PH and SH3 domains.

BTK distributes to several cellular compartments upon its activation including the nucleus, although its role at the nucleus is speculative at present. Clearly, BTK can readily shuttle to the nucleus, hence, this information implies that BTK may have significant functional role in each of these cellular compartments. Here, we focus on BTK translocation to nucleus, as most of studies were performed in non-leukaemic cells and normal B cells. Moreover, the role of BTK in the nucleus of leukaemia cells, especially AML and CLL subtypes, is still elusive. Therefore, this experimental chapter aims to investigate the distribution of BTK in the cytoplasm and nucleus on AML and CLL cell lines, to enlighten our understanding of any role for BTK in the nucleus in human leukaemic cells.

3.2 Results

As this chapter aims to investigate BTK expression in different subcellular compartments, protein extraction protocols and p-BTK antibody Western analyses were optimised. Due to the poor nature of the p-BTK antibodies commercially available, extensive optimisation was performed. The data presented within this chapter represents the optimal protocols that were exhaustively undertaken.

3.2.1 Protein extraction optimisation

In order to extract cytoplasmic protein and nuclear protein from human leukaemic cells, two protein extraction protocols were performed. The first protein extraction protocol was not described fully in the Method section, thus the protocol is briefly described here. Cells were harvested at 5 x 10^6 cells density collected by centrifugation at 1,000 x g for 5 min, then the cell pellet was washed once with 1 x ice-cold PBS (4ºC). The cell pellet was lysed with isotonic lysis buffer. In these experiments, the cell pellet was sonicated for 5 min in a sonic bath, then placed on ice for 1 min – this sonication cycle was repeated three times (15 min bath sonication in total). The lysate was then spun at 1,000 x g for 10 min (4ºC). The supernatant was regarded as the cytoplasmic protein. The remaining pellet was washed once with 1 x ice-cold PBS. In order to extract nuclear protein, clear SDS sample buffer was used to lyse the cell pellet, before sonication for a further 5 min (repeated three times) using the sonic bath method. Cell debris was removed by centrifugation at 1,200 x g for 20 min then the supernatant was collected and analysed as nuclear protein.

The results showed protein contamination of cytoplasmic and nuclear protein when the sonic bath method was used, as shown in Figure 3.1. Phosphorylated BTK could not be detected in the Western blot (see Figure 3.1) which we considered as an antibody quality issue. Focusing on the cytoplasmic markers β-actin and GAPDH, these two cytoplasmic proteins were detected in both cytoplasm and nucleus fractions, whereas conventionally, they are believed to be found only in cytoplasm fractions of cells. Therefore, we concluded that this protocol was not sufficient to give good protein extraction and cell fractionation for sub-cellular studies.

The second method tested was sonic probe-fractionation of protein from leukaemic cell lines, as described in the Materials and Methods section. As shown in Figure 3.2, only trace amounts of β-actin were found in the nuclear fraction while GAPDH was detected only in cytoplasmic protein fraction. Therefore, this protocol was more suitable for cell fractionation studies, and was used for the more detailed experiments in this chapter.

3.2.2 Phosphorylated BTK antibody optimisation

As mentioned above, the p-BTK (Y^{223}) antibody was difficult to gain a consistent band for analysis. Thus, we endeavoured to test different protein and antibody concentrations to optimise our consistent detection of the phosphorylated form of BTK in cytoplasmic and nuclear fractions. First, p-BTK (Y^{223}) cannot be detected when 2.5 μg of fraction protein was loaded and probed with the p-BTK at a dilution of 1:300. Therefore the protein level was increased to 20 μg, with the antibody dilution at 1:300. The result showed that p-BTK was slightly detected in both cytoplasmic protein and nuclear protein. The last condition in Figure 3.2C was the best

condition for this antibody to consistently detect p-BTK, where 20 μg protein was subjected to SDS-PAGE and antibody concentration increased to 1:150 to probe for BTK protein phosphorylation by Western blot. This extraction protocol and concentration of protein and antibody dilution was applied in all subsequent experiments.

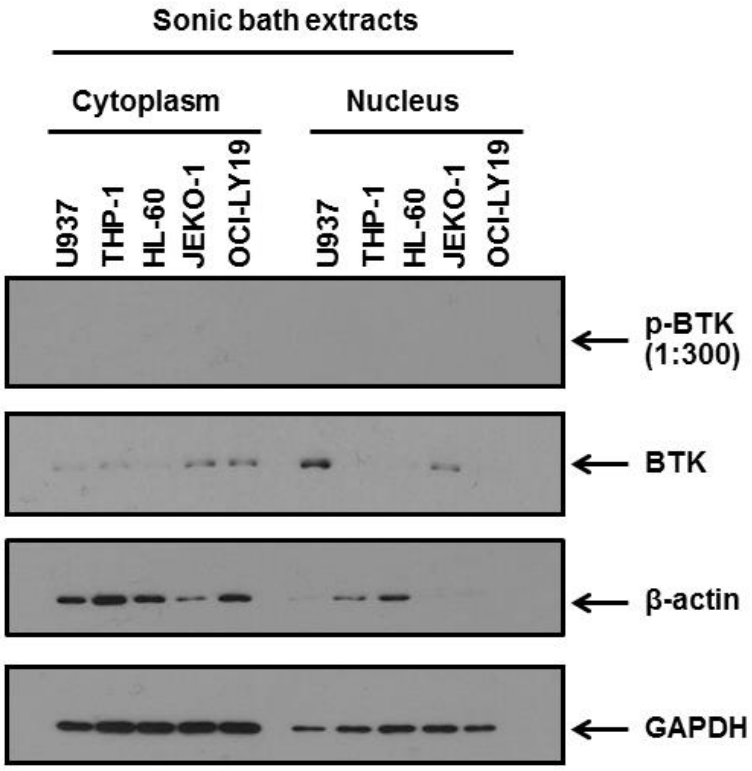

Figure 3.1 Cytoplasmic and Nuclear protein content in human leukaemia cell lines extracted by the sonic bath method.

Human leukaemic cell lines had cytoplasmic and nuclear extracts prepared as described in the text of this chapter. Western blotting analysis of the indicated proteins was performed. The arrows indicate the expected molecular mass of each of the proteins (BTK, 77 kDa; β-actin 45 kDa; GAPDH, 37 kDa).

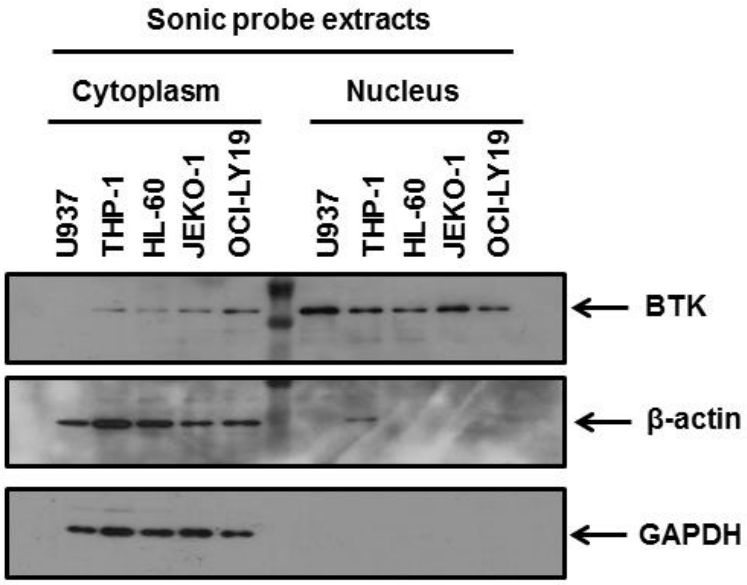

Figure 3.2 Cytoplasmic and Nuclear protein content in human leukaemia cell lines extracted by sonic probe.

Human leukaemic cell lines had cytoplasmic and nuclear extracts prepared as described in the Materials and Methods section. The sonic probe method was used in this protocol. Western blotting analysis of the indicated proteins was performed. The arrows indicate the expected molecular mass of each of the proteins (BTK, 77 kDa; β-actin 45 kDa; GAPDH, 37 kDa).

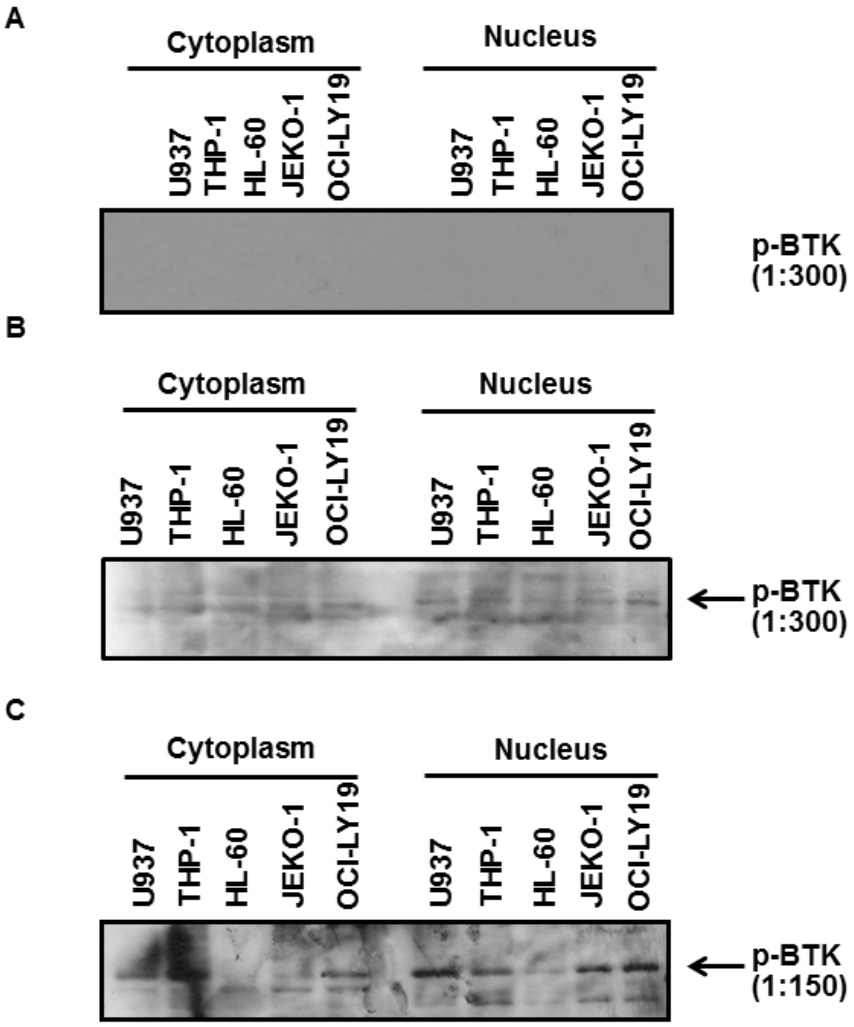

Figure 3.3 Phosphorylated BTK expression in cytoplasm and nucleus on AML and CLL cell lines (antibody optimisation).

Human leukaemic cell lines had cytoplasmic and nuclear extracts prepared as described in the Materials and Methods chapter. Western blotting analysis of the indicated proteins was performed, with arrows indicating the expected molecular mass. Different antibody and protein concentration were optimised which are 2.5 μg protein and 1:300 antibody dilution (A), 20 μg protein and 1:300 antibody dilution (B) and 1:150 antibody dilution (C), respectively.

3.2.3 Phosphorylation pattern of BTK (Y^{223}) in the subcellular compartments of leukaemic cell lines

As we aimed to investigate the phosphorylation of BTK in the two sub-cellular compartments (cytoplasm and nucleus) in AML and CLL lines, we performed optimal fractionation and p-BTK (Y^{223}) expression was analysed by Western blotting. JEKO-1 and OCI-LY19 were used as CLL model cell lines, while U937, HL-60, and THP-1 are AML cell lines. As shown, endogenous BTK levels were substantially different among the cell lines tested as each lane showed different band intensity, compared to GAPDH intensity which was relatively equal among each sample. Phosphorylated BTK was found in both nuclear and cytoplasmic fractions from U937, THP-1, HL-60, JEKO-1, and OCI-AML3. The phosphorylated BTK expression correlated well with the total BTK found in each cell line – thus, cells that expressed BTK also expressed phospho-BTK, whether it be found in their cytoplasmic or nuclear compartments. GAPDH as a cytoplasmic marker, was detected only in the cytoplasmic fractions from each cell line. Therefore, we are confident that nuclear BTK or p-BTK was not merely cytoplasmic protein contamination. As another test of the purity of the fractions, we tested the samples for histone H-3, which is believed to be a purely nuclear-located protein. While the majority of H3 signal was found in the nucleus, some minor protein was detected in the cytoplasmic fractions of these cells. However, in general there was clear distinction between the cytoplasmic and nuclear fractions, and we definitively showed there to be BTK (and p-BTK) present in both sub-cellular fractions.

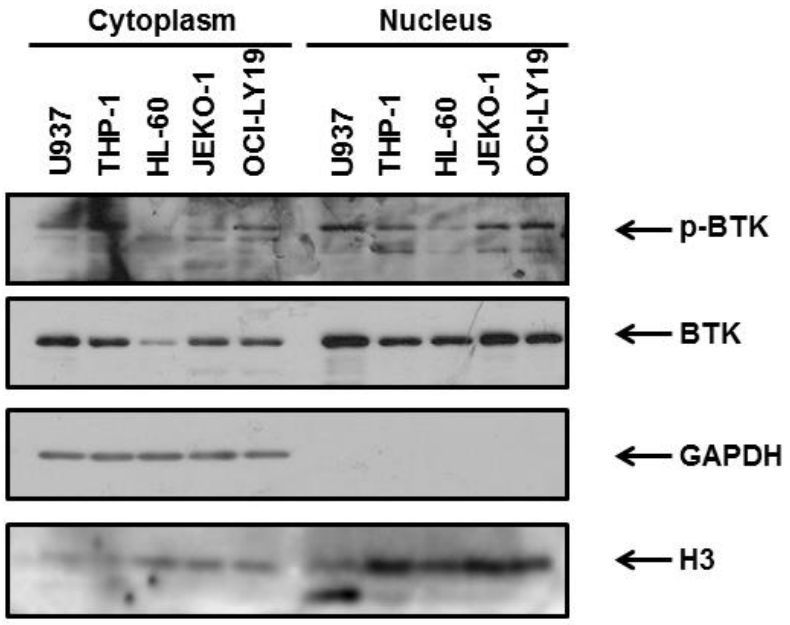

Figure 3.4 Phospho-BTK (Y^{223}) phosphorylation pattern in cytoplasm and nuclear area of human leukaemia cell lines.

U937, THP-1, and HL-60 AML cell lines and JEKO-1 and OCI-LY19 CLL cell lines were fractionated and analysed as described previously. The p-BTK and total BTK expression were investigated in the cytoplasmic and nuclear fractions. The GAPDH and Histone H3 proteins were compared as markers for cytoplasmic and nuclear proteins, respectively. The arrows indicate the expected molecular mass of each of the proteins (BTK, 77 kDa; β-actin 45 kDa; GAPDH, 37 kDa; Histone H3, 17 kDa).

3.3 Discussion

This chapter aimed to investigate the expression of BTK in the nucleus and cytoplasm of human leukaemic cell lines, and to determine the optimal protocol for efficiently measuring cytoplasmic and nuclear protein extraction and p-BTK antibody usage, to obtain a reliable and consistent result.

The result showed different protein extraction efficiency between the two protocols used. The first protocol, using a sonic bath, where the pellet was not washed properly after cytoplasmic protein collection. There was obvious contamination of protein between the two fractions as detected by β-actin, with the contamination being even more pronounced when measuring GAPDH levels. The second protocol, using a higher energy sonic probe to disrupt cells, and the extracts washed more fully to remove the remaining protein from the two fractions, showed less contamination and more precise results when protein expression was compared between the two sub-cellular compartment fractions. Therefore, the second protocol was applied for the remainder of the experiments.

Earlier work from the lab showed that BTK was expressed in AML cell line and AML patient samples (Rushworth et al., 2014). At the time, there was considerable skepticism about the presence of BTK in any myeloid cells, as BTK was seen to be associated with B cell receptor activation mechanisms only. This earlier study also suggested by immunohistochemistry, that BTK was indeed present in AML cells and that some of the BTK may be expressed in or near the nucleus of the cell. Here we have definitively shown for the first time, that BTK is indeed

present in AML cells, and that its total level are comparable to the levels seen in lymphoid cells, such as CLL. Moreover, we have shown conclusively for the first time, that BTK is present in both the expected cytoplasmic regions of AML and CLL cells, but also more surprisingly in the nuclear compartments of all these cells too.

Although, p-BTK (Y^{223}) was not detected initially in our studies, our studies did reveal that BTK was expressed in AML cells. BTK is accepted as an important signalling protein in B cells. Therefore, we hypothesised that our p-BTK (Y^{223}) antibody and protein loading were not used at a suitable concentration, and we persevered with antibody optimisation throughout this chapter, ultimately proving that our hypothesis is correct and that p-BTK is present in both AML and CLL cells.

After protein extraction protocol and adequate amounts of both antibody and protein loading were stablished, we turned our consideration to the main objective of this study in which we aimed to investigate the expression of BTK in cytoplasm and nucleus of AML and CLL cells. Our results show p-BTK (Y^{223}) and its total counterpart is presented in both cytoplasm and nucleus. According to the protein marker for each fraction, it is obvious that the nuclear fraction was relatively pure for cytoplasmic proteins. Therefore, that both p-BTK and BTK being found in nucleus was reliable, even if there were any cytoplasmic protein contamination at low levels. Nevertheless, we cannot definitively compare and quantitate the absolute expression levels of these proteins in both fractions, since a small amount of Histone H3 nuclear protein was found in the cytoplasmic fraction. Nonetheless, we have proven for the first time, that BTK is

present in the nucleus of AML and CLL cells, notwithstanding any possible contamination issues of cytoplasmic protein found in our nuclear extracts.

Several studies showed evidence of BTK in the nucleus of other cells. In terms of how BTK may translocate to the nucleus and any putative role of BTK at the nucleus, there remains much conjecture. A small amount of phospho-BTK was found in the nucleus of transfected COS7 cells and B cells, even though this protein mainly expresses in the cytoplasm. The investigation revealed that BTK travels to the nucleus, and interestingly, that BTK may need other proteins to help in shuttling between the two cellular compartments. A nuclear localisation signal (NLS) was found in the PH domain of BTK in these studies (Mohamed et al., 2000). BAM11 and ANKRD53 (the latter also known as Liar) co-localised with BTK in the nucleus. Both BTK and BAM11 were found in the nucleus and truncated BAM11, amino acid 240-368, inhibited BTK kinase activity and reduced IL-5 stimulation in transfected cells (Kikuchi et al., 2000). Liar or ANKRD53 is an SH3 domain-binding protein with a NLS and nuclear exported signal (NES) embedded within its sequence. Liar interacts with BTK inside the nucleus, which can shuttle and accompany BTK to the cytoplasm as a complex (Gustafsson et al., 2012).

Since a small amount of BTK is able to shift to nucleus, this protein may perform some crucial functions inside this organelle. Considering the phosphorylation state of BTK in the nuclear fraction, this protein may have an important role in the nucleus, whereby it probably regulates other proteins via a partner or directly controls functions by itself. BTK binding partner proteins were revealed by several research groups. BTK

Associated Molecule-11 (BAM11), one of the proposed partner proteins of BTK, was identified by co-immunoprecipitation studies. The interaction of BTK and BAM is a paradoxical relationship because BAM-11 acts as negative regulator of BTK, as BTK kinase activity was found to be decreased in the presence of truncated BAM-11 (amino acid 240-368) while BTK also enhances BAM transcriptional co-activation activity when these two proteins were co-transfected. In addition, TFII-I also enhances the BTK-dependent transcriptional co-activation activity of BAM (Hirano et al., 2004, Kikuchi et al., 2000), with the study showing BAM-11 and BTK co-localisation at the nucleus. The putative role of BTK in the nucleus has been reported where NF-κB and TFII-I were identified as a target for BTK regulation. The TFII-I was identified as a BTK target which required BTK for its phosphorylation and transcriptional activity in COS7 cells and mouse B cells (Novina et al., 1999). Interestingly, B cell regulator of Ig heavy chain transcription called Bright, is a transcription factor that enhances transcription of the Ig gene in B cells, was reported as a direct target of BTK in the nucleus in both B cells and COS7 cells. In the absence of BTK, Bright cannot form DNA binding complexes, therefore Bright requires BTK in order to perform its nuclear functions (Rajaiya et al., 2005).

In summary, p-BTK and BTK were detected in both cytoplasm and nucleus in all AML and CLL cell line models tested. In further work, we attempt to investigate the mechanism of BTK translocation in AML and CLL leukaemia subtypes, as the nuclear shuttling to and the role of BTK at the nucleus, are not well understood. BTK wild-type and different mutated domains BTK could be transfected into AML and CLL to help identify the

different protein binding partner between wild-type and mutant BTKs. The co-localisation of BTK wild-type and mutants together with candidate protein would help us to understand the mechanism of BTK function at the nucleus. Since leukaemia is a heterogeneous disease and the disease mechanisms may vary considerably among patients, we also aim to investigate the role of BTK in the nucleus from patient samples to better fulfil our understanding of BTK in leukaemia.

Chapter IV

Bruton's Tyrosine Kinase is downstream of the SDF-1α/CXCR4 signalling pathway in AML and CLL

4.1 Introduction

The SDF-1α/CXCR4 signalling pathway plays several important cellular roles in both normal and malignant cells. These cellular responses include migration, tissue homing of blood cells, survival and differentiation and development (Nagasawa, 2014). This pathway is well characterized in normal and cancer cells. CXCL12, also known as stromal derived factor-1 alpha (SDF-1α), is a chemokine secreted from stromal cells in bone marrow (Nagasawa et al., 1996). SDF-1α attracts CXCR4 expressing cells which then migrate toward SDF-1α secreted microenvironmental niches and attach beside bone marrow stromal cells to provide them with pro-survival signals. In cancer, this pathway also influences cell migration, survival, and in addition, protects cancer cells from drug-induced apoptosis (Burger and Kipps, 2006).

Despite BTK being critical and participating in many vital signalling pathways in normal B cells or B cell malignancies, this protein is mostly regarded as being involved in lymphocytes with pathways including B cell receptor signalling and SDF-1α/CXCR4 signalling pathways. Here we focus on SDF-1α/CXCR4 axis, BTK has been reported as a part of this pathway when signalling molecules upstream and downstream of BTK and BTK itself are activated upon SDF-1α ligand binding to CXCR4 receptor (Chen et al., 2016). There are several studies that provide evidence to support SDF-1α/CXCR4 being a BTK-dependent signalling pathway in normal B cells and B cell malignancies. Mostly these are based upon the pharmacological inhibition of BTK using ibrutinib and the examination of the resulting downstream inhibitory effect on the cells investigated. BTK inhibition causes lymphocytes to egress from the lymphoid tissue, in vivo –

a process known as lymphocytosis (Chen et al., 2016). There is evidence showing that BTK may be important in AML, and indeed ibrutinib has been considered as a potential therapeutic drug in this leukaemia subtype (clinicaltrials.gov). Studies from our lab have shown ibrutinib increases cytarabine and daunorubicin chemotherapeutic sensitivity when AML was treated with ibrutinib in combination with either drug (Rushworth et al., 2014). The SDF-1α/CXCR4 axis is established in AML as well as other cell types but only a few studies have shown participation of BTK in this pathway. BTK activation has been reported in acute myeloid leukaemia after AML was treated with SDF-1α which increased p-BTK detected via CXCR4 receptor stimulation. The downstream cellular events of SDF-1α/CXCR4 pathway activation are affected by BTK inhibition. AML cells showed reduced migration toward SDF-1α in BTK knockdown AML cells (Zaitseva et al., 2014). Interference of the SDF-1α/CXCR4 pathway by inhibiting CXCR4 receptor with an inhibitor diminished AML cells survival and migration. Therefore, this pathway appears important in AML and may be one of the candidate pathways for therapeutic development to treat this cancer much better than the relatively poor options presently available.

As we proved in the previous chapter that BTK expression is significant in AML, and BTK may be a potential drug target in AML, a better understanding of any role for BTK in the SDF-1α/CXCR4 pathway may be ripe for beneficial therapeutic development. This part of the thesis aims to investigate any participation that BTK may have in SDF-1α/CXCR4 pathway and responses in AML and CLL human leukaemias.

4.2 Results

In this chapter, we aim to identify whether BTK play any role in the SDF-1α/CXCR4 signalling pathway in our AML and CLL model systems.

4.2.1 Optimization of phosphorylated BTK activation after 100 ng/mL SDF-1α treatment

The activation of phosphorylated BTK was examined after CXCR4 receptor engagement by its ligand, SDF-1α/CXCL12, and whether BTK may be a putative pathway to exploit via CXCR4 pathway signalling. Phosphorylation of BTK was investigated after 100 ng/mL SDF-1α treatment. We initially optimized cell treatment with 100 ng/mL SDF-1α for 10 min in some of the cell lines, then examined p-BTK and p-ERK protein levels downstream, measured by Western blotting in order to prove that this signal is transduced through BTK.

Using THP-1 and Jeko-1 cell lines as AML and CLL representative models respectively, treatments were 100 ng/mL SDF-1α for 10 min or BCR cross-linking assay for 15 min, by way of a positive control for p-BTK activation in B cells. In the BCR cross-linking assay, human IgM was used as a BCR receptor stimulus and donkey IgG was used as a control agent. Phosphorylation of BTK and ERK was not elevated by 100 ng/mL SDF-1α after 10 min treatment in both THP-1 and JEKO-1 while activation of p-ERK was obviously detected after BCR cross-linking in Jeko-1 cells, but not THP-1 (Figure 4.1).

Other AML cell lines (HL-60, U937, OCI-AML3, MV4-11 and Kasumi-1) were screened for p-BTK (Y^{223}) and p-ERK activation. Cells were treated

for 10 min with 100 ng/mL SDF-1α and 1 μg/mL LPS acting as a positive control for p-ERK activation. In addition, p-BTK (Y^{551}) was also examined after within the same cell treatments. Although p-BTK (Y^{551}) antibody was not able to show much clear signal (even after much optimisation), the result can be interpreted as activation of both p-BTK (Y^{551}) and p-BTK (Y^{223}) not being obviously increased after SDF-1α treatment or LPS treatment. However, phosphorylation of ERK was more obviously increased in some of the cell lines comparing to untreated cells in both 100 ng/mL SDF-1α and 1 μg/mL LPS treatments. A combination of variable levels of BTK among the AML cell lines, and often high basal p-BTK levels in some cell lines, means that there is no clear activation by SDF-1α or LPS in any of the AML cell lines tested here. Activation of p-ERK by both SDF-1α and LPS was more apparent in U937, OCI-AML3, and less so in THP-1 cells. Thus, the two ligands were successfully stimulating their receptors (CXCR4 and TLR4) but their ability to activate the BTK pathway is still to be determined, due once again to the limitations of the p-BTK antibodies available.

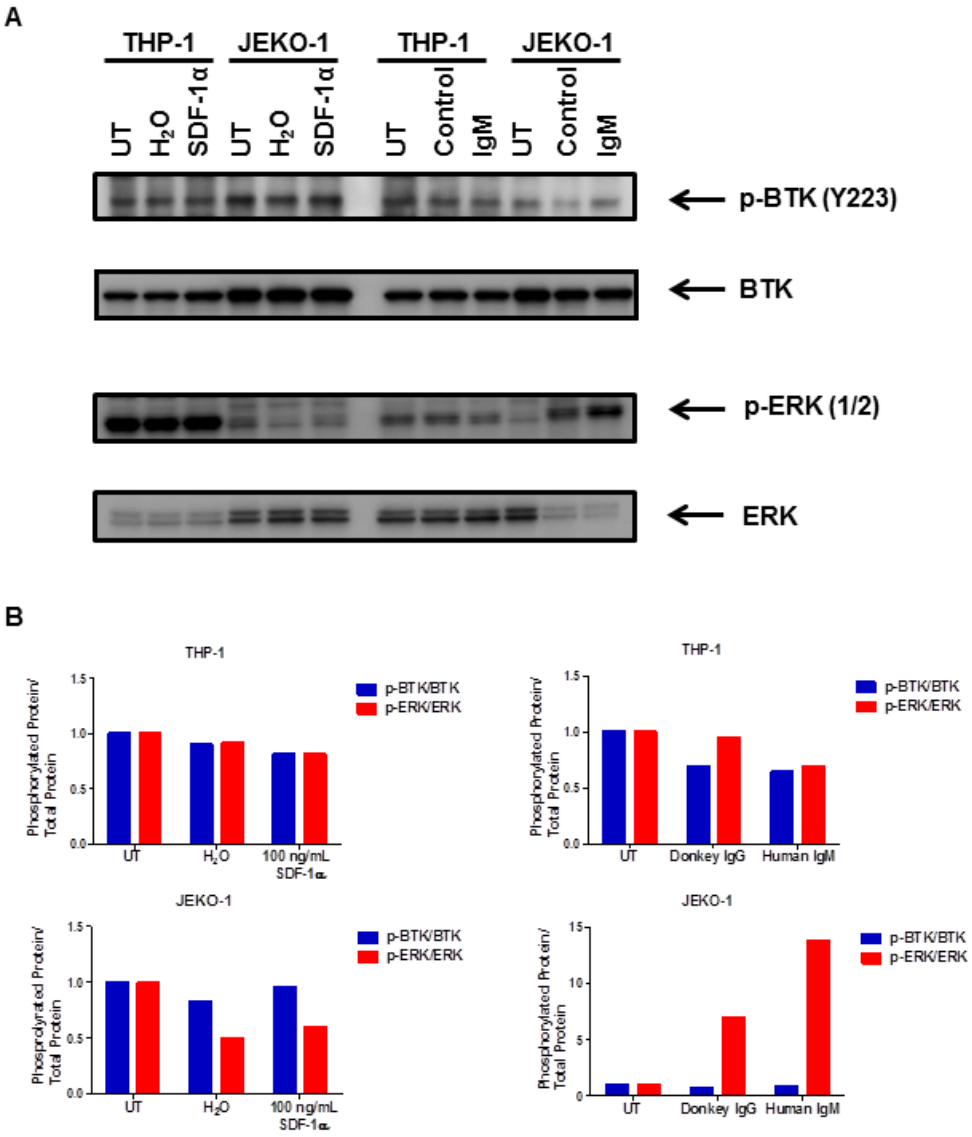

Figure 4.1 SDF-1α and BCR crosslinking stimulation on AML and CLL cell lines.

THP-1 and JEKO-1 were stimulated by SDF-1α or anti-IgM antibody for 10 min at 100 mg/mL and 10 ng/mL, respectively. BTK (anti-pBTK 1:1000) and ERK (anti-pERK 1:1000) phosphorylation were analysed by Western (A). Densitometric levels of phosphorylation were compared to total protein levels using ImageJ and plotted with GraphPad Prism (B).

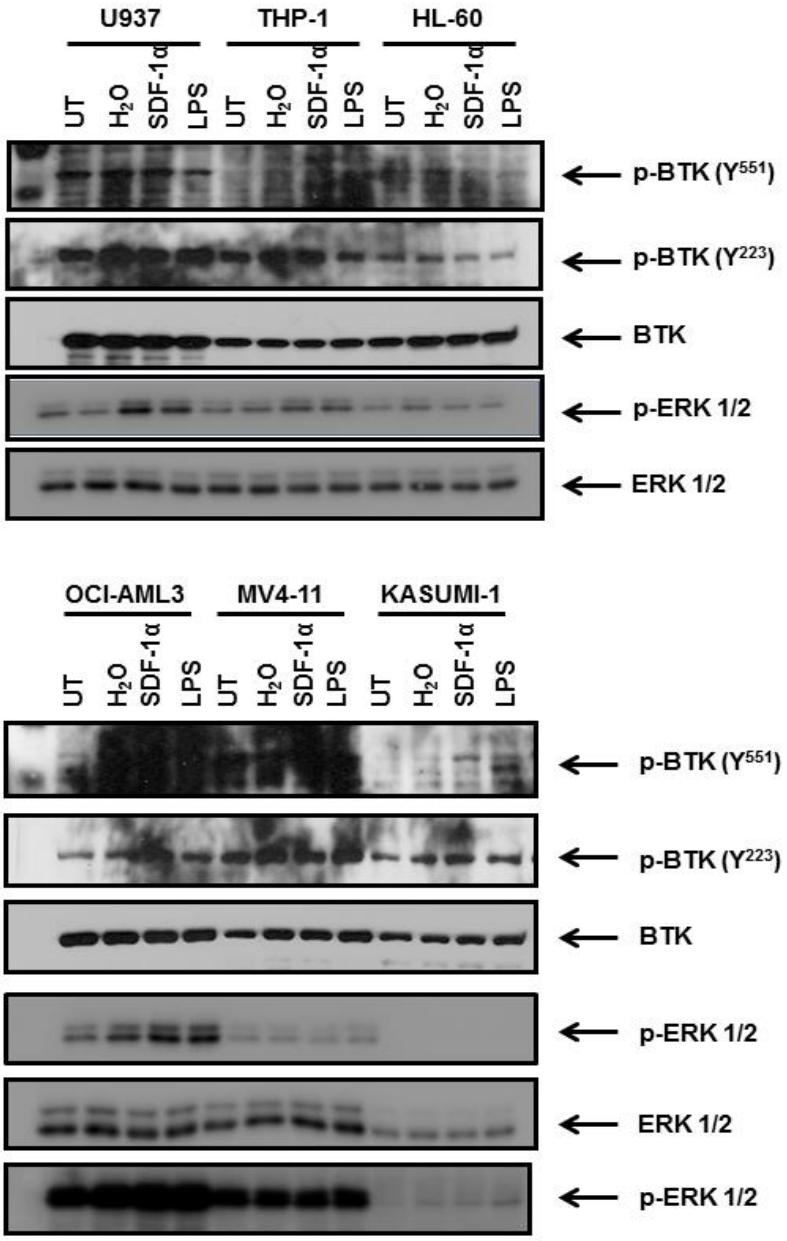

Figure 4.2 Activation of phosphorylated BTK after 100 ng/μL SDF-1α treatment for 10 minutes.

Human leukaemic cell lines were stimulated with 100ng/mL SDF-1α for 10 min, water was used as vehicle control and 1 μg/mL LPS used as positive control for ERK, respectively. Protein was harvested and activation of interested proteins were determined by Western blot.

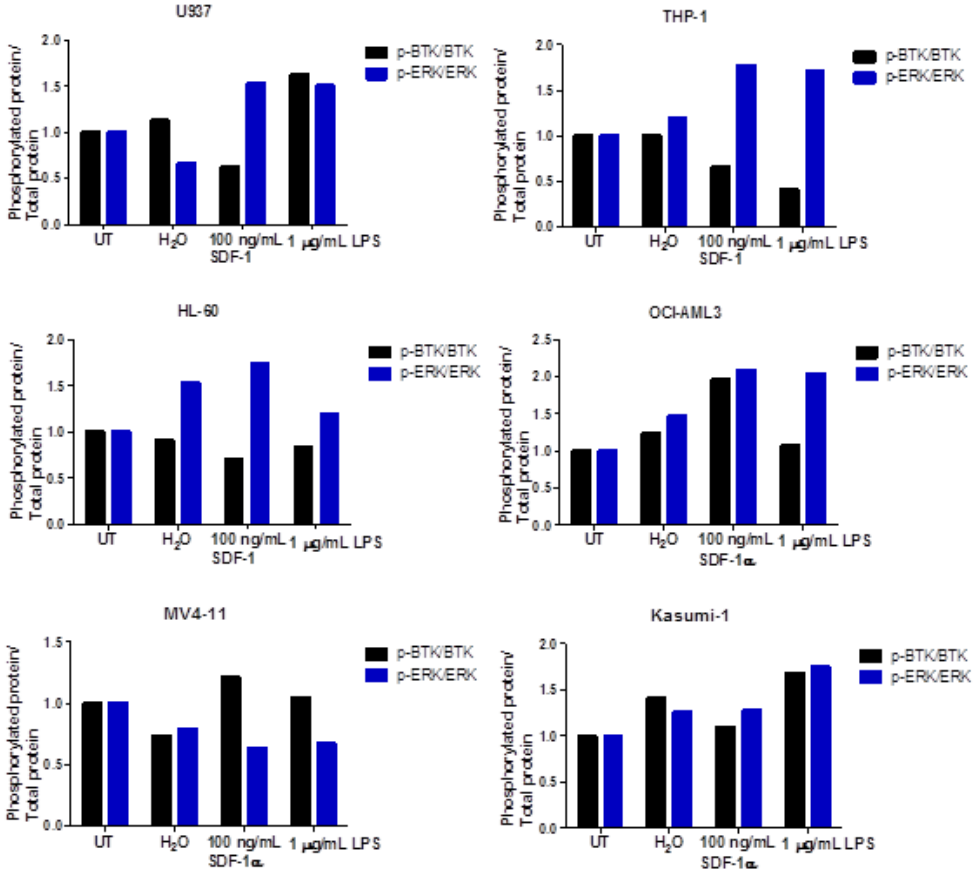

Figure 4.3 Densitometry of phosphorylated BTK Western blots.

Phosphorylated protein band intensity was normalized with its total protein then each value was calculated in relative to untreated cells.

4.2.2 Expression of surface CXCR4 receptor on AML and CLL cell lines

No increase in p-BTK was detected after 100 ng/mL SDF-1α stimulation (Figure 4.1 and 4.2), therefore, we needed to determine that the selected cell lines express CXCR4 receptor. In order to examine whether CXCR4 was expressed on our leukaemia models, human leukaemia cell lines U937, THP-1, HL-60, MV4-11, OCI-AML3, Kasumi-1, and OCI-LY19 were subjected to CXCR4 receptor cell surface examination. Cells were stained with CXCR4-PE and IgG-PE antibodies for receptor staining and isotype controls according to the Materials and Methods chapter, section 2.5. The CXCR4 receptor staining (and isotype control) were examined by FACS analysis. As shown in Figure 4.3A, the expression of CXCR4 varied among cell lines, with OCI-AML3 cells showing the highest CXCR4 expression levels among the AML and CLL cell lines, while CXCR4 expression was the lowest in Kasumi-1 cells. CXCR4 expression levels on OCI-LY19 and THP-1 were the second and third highest respectively. Beside Kasumi-1, the expression of this receptor was similar in the remainder of the cell lines. The mean fluorescence index was plotted as demonstrated in Figure 4.3B. Interestingly, all cell lines expressed high amounts of CXCR4 receptor on their cell surface. Nevertheless, despite this high level of CXCR4 expression, and ability of SDF-1α to activate p-ERK, elevation of BTK phosphorylation could not be detected after 100 ng/mL SDF-1α treatment, as judged by our phospho-antibody Western blotting experiments.

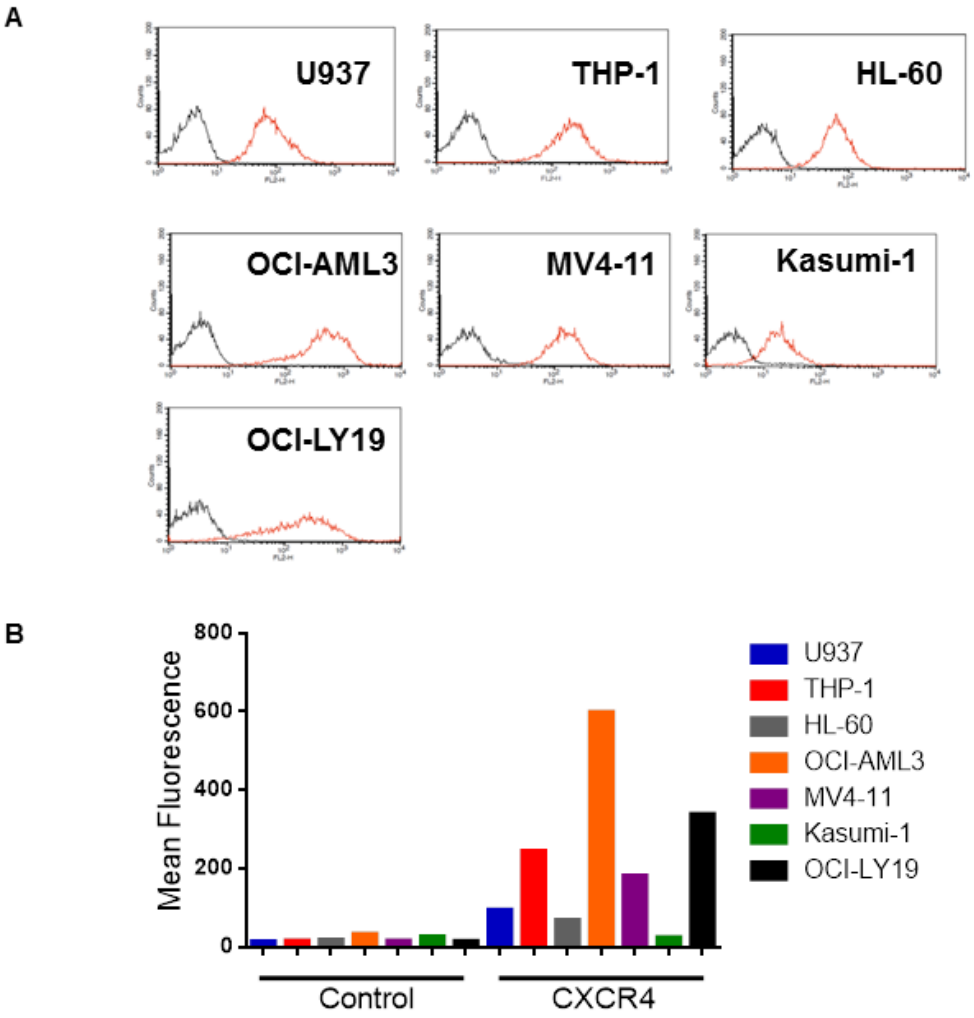

Figure 4.4 Expression of surface CXCR4 receptor on AML and CLL. U937, THP-1, HL-60, OCI-AML3, MV4-11, Kasumi-1, and OCI-LY19 as indicated, were stained with CXCR4-PE according to the protocol outlined in the Materials and Methods chapter. CXCR4-PE and IgG-PE antibodies were used to detect CXCR4 and the isotype control, respectively. Cells were analysed for cell surface CXCR4 expression by FACS analysis (A). The mean fluorescence intensity was plotted (B).

4.2.3 BTK phosphorylation upon CXCR4 stimulation

According to the FACS analyses, surface CXCR4 receptor was highly expressed on human leukaemic cell lines used in this study. Therefore, one possible reason that BTK phosphorylation could not be detected previously is the signalling from CXCR4 receptor occurs very rapidly and transiently, and we may not be able to detect p-BTK at only one specific time point. Therefore, all cell lines were screened for p-BTK activation upon 100 ng/mL SDF-1α treatment at 0, 1, 5, 10, 20, and 30 min time points, according to an improved protocol outlined in chapter II, section 2.6. Expectedly, p-BTK signal was elevated after CXCR4 activation in U937, HL-60, OCI-AML3, MV4-11, and OCI-LY19. Phosphorylated BTK signal gradually increased then peaked at different time point in each of the different cell lines. U937 cells showed p-BTK gradually increased continuously until after 30 min treatment, while stimulation of p-BTK activation by SDF-1α peaked at 20 min, declining thereafter in treated OCI-AML3 and HL-60 cells. Phosphorylated BTK slightly increased from 1 min and reached to maximum at 10 min treatment in OCI-LY19 CLL cells, with the apparent activation more rapid in CLL cells than AML cell lines. There was an unconvincing increase of p-BTK in MV4-11 cells, and little activation could not be seen in either THP-1 and Kasumi-1. Western blotting was performed four dependent experiments and densitometric analyses was shown in Figure 4.5 and 4.6.

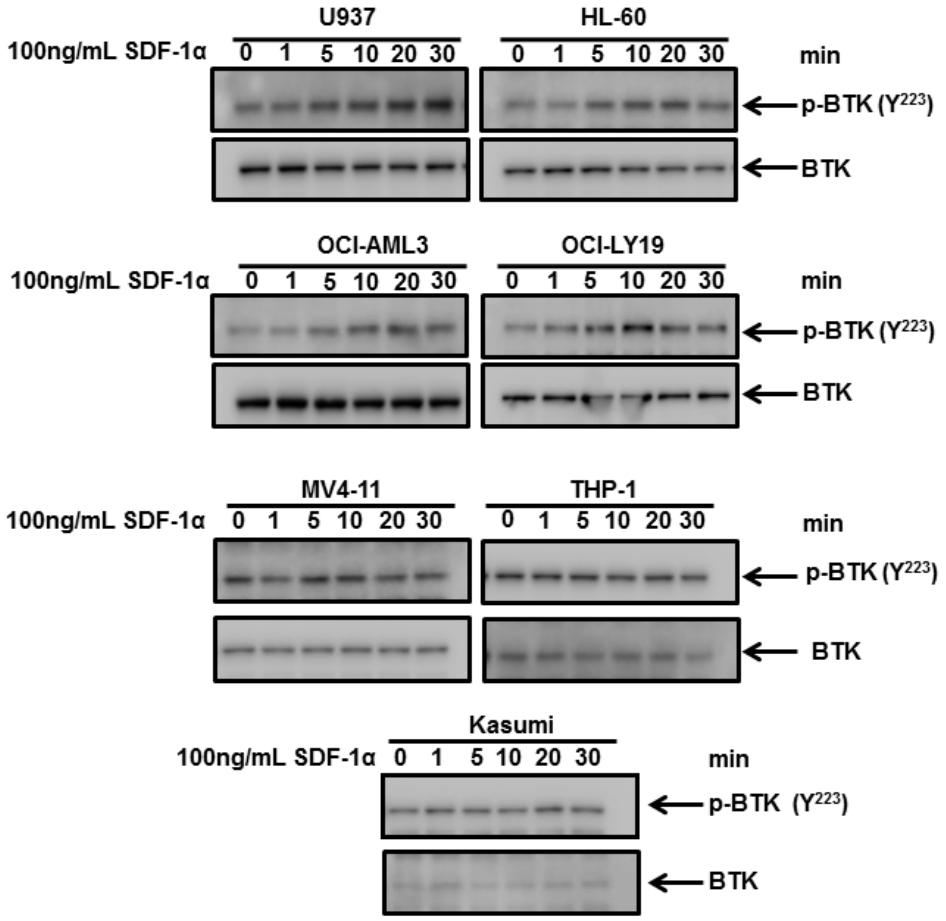

Figure 4.5 Activation of phosphorylated BTK in response to SDF-1α. Human leukaemic cell lines were stimulated with 100 ng/mL of SDF-1α in time course manner form 0, 1, 5, 10, 20, and 30 min. Phosphorylated BTK was probed for BTK activation. Western blot was performed in 4 dependent experiments, with this figure showing a representative blot.

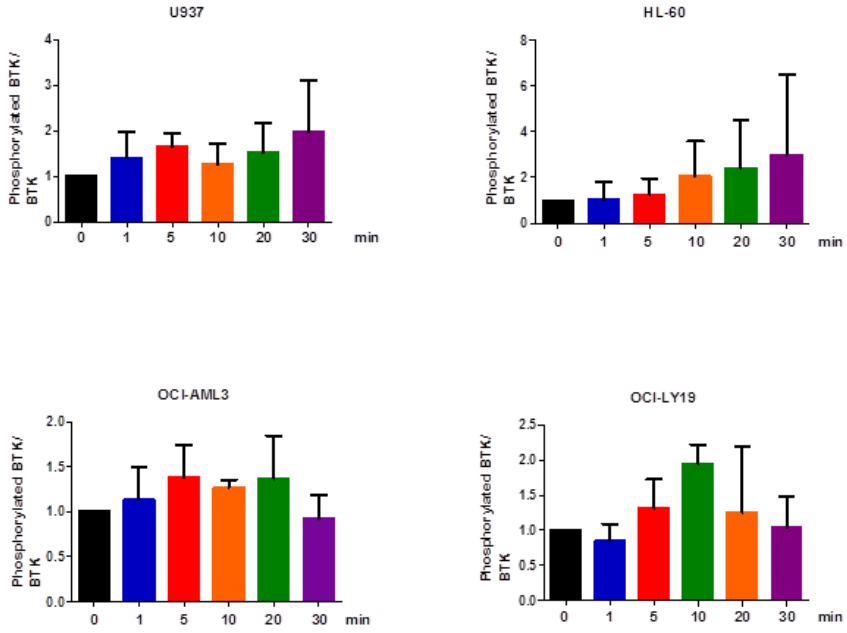

Figure 4.6 Densitometry of Western blot from figure 4.5 analysed from the same experiment.

Phosphorylated BTK band intensity was normalized with BTK and the value was calculated in relative to untreated cells. Data are analysed from four dependent repeat.

4.3 Discussion

The aim of this chapter was to identify whether BTK was activated as a downstream target of SDF-1α/CXCR4 signalling pathway in human leukaemia AML and CLL subtypes. We hypothesized that BTK activation was downstream of activated CXCR4 receptor in AML.

In order to prove the hypothesis that BTK is a downstream signalling protein of this pathway in AML and CLL, phosphorylation of BTK was investigated after 100 ng/mL SDF-1α treatment. In earlier results, p-BTK was examined after 10 min of 100 ng/mL SDF-1α treatment and the result showed similarity of p-BTK level in untreated cells and 100 ng/mL SDF-1α treated cells. Moreover, activation of p-ERK which is downstream of BTK is not obviously increased after 100 ng/mL SDF-1α treatment. In this experiment, PLCγ2 phosphorylation should be determined as a proximal target of BTK. Thus, we wondered whether p-BTK was not obviously activated because either CXCR4 was not expressed on our model cells, or p-BTK activation was not observed at precise time point.

The surface CXCR4 receptor was stained with CXCR4-PE antibody and the receptor density measured by FACS analyses. The results showed significant surface CXCR4 expression on human leukaemic cell lines that we used as models of AML and CLL. This is in agreement with other studies also showing CXCR4 expression on the cell surface of AML and CLL cell lines (Zaitseva et al., 2014, Burger et al., 1999). However, the receptor density on cell surface which is interpreted by mean fluorescence intensity was different for each cell line, thus CXCR4 expression is very much cell type-specific. Since CXCR4 is expressed on our models, BTK

phosphorylation should be detectable if we observe at the correct time point. Considering the cell treatment with time point aspect, there are two possible reasons that the elevation of p-BTK cannot be observed after 10 min treatment with 100 ng/mL SDF-1α. The first reason is the selected time point is too long to detect the activation which the signal transduction may have already be declined after 10 min. In general, signal transduction occurs very shortly after ligand binding, then the signal is transduced to cascade downstream signalling molecules and trigger subsequent effects in the cell response to receptor stimulation. The second reason is high basal level of p-BTK in untreated cells, may prevent our one time point clearly showing any tendency of activation. Therefore, cells were treated with 100 ng/mL SDF-1α in time course in order to detect activation of BTK, covering both earlier and later time points.

Extending our time points for analysis, showed conclusively, that SDF-1α-stimulated BTK activation in U937, HL-60, OCI-AML3, and OCI-LY19 while activation may not change in MV4-11, THP-1, and Kasumi-1. MV4-11 is a FLT3-ITD mutation-containing cell line, with p-BTK being highly expressed at steady state basal levels, therefore we possibly cannot observe p-BTK activation above the high basal levels already present (Pillinger et al., 2015). However, BTK should be involved in the SDF-1α (CXCL12)/CXCR4 pathway since pertussis toxin inhibits SDF-1α-induced p-BTK activation in MV4-11 cells (Zaitseva et al., 2014). Similarly, p-BTK does not change in THP-1 cells as well. As shown in other studies, BTK inhibition does not affect THP-1 cell survival, therefore, BTK may not play any role in this cell line (Rushworth et al., 2014). Nevertheless, BTK has been reportedly involved in another pathway including the Toll-like receptor 4 (TLR4)

pathway, where 1 μg LPS activates p-BTK after 5 min treatment in THP-1 cells (Jefferies et al., 2003). Kasumi-1 cells expresses low levels of both BTK and ERK comparing to the other cell lines. Interestingly, Kasumi-1 shows high expression of CXCR4 in the cell surface in another study (Zepeda-Moreno et al., 2012), while our findings indicated CXCR4 expression was lowest in Kasumi-1 cells among other cell types. Therefore, Kasumi-1 may not be a good system when testing chemokine responses. In addition, we have experienced issues whereby Kasumi-1 cells stop growing in culture, to give errant findings in other experiments too.

This chapter conclude that AML and CLL cell lines express CXCR4 receptor, and that BTK may be involved in signalling in the SDF-1α/CXCR4 signalling in AML and CLL cell lines.

Chapter V

The effect of $G\alpha_{12}$ and $G\alpha_{13}$ knockdown on SDF-1α/CXCR4 signalling in AML and CLL

5.1 Introduction

Lentiviruses are a group of viruses in *Retroviridae* family. The *Retrovirus* genus group of viruses can infect a wide range of host cells including proliferative cells and non-proliferative cells alike, including hematopoietic cells (Sakuma et al., 2012, Manjunath et al., 2009). Lentivirus technology is a transgene delivery tool that takes advantage of lentivirus properties, where the expression of the transgene is a very long-term expression system, due to the transgene being integrated into the transduced cell's genomic DNA after transfection. Since, lentivirus vectors are constructed and based upon HIV-1 virus, the safety issues surrounding the use of this vector in experimental protocols has to be of concern. By separating the viral genes encoding viral structure and protein machinery for integration, into several plasmids, and allowing the virus to infect host cells only once, the safety is improved. In addition, lentiviral vectors are also modified to increase the opportunity to infect wide range of host cells, making them more useful for cells that are able to be infected. In this study, we used third generation lentivirus delivery systems to infect $G\alpha_{12}$- and $G\alpha_{13}$-targeted shRNA into human leukaemia cell lines, in order to identify whether $G\alpha_{12}$ or $G\alpha_{13}$ proteins participate in the interaction of SDF-1α/CXCR4 and its signalling towards BTK.

CXCR4 is a seven transmembrane G-protein-coupled receptor (GPCR) that transduces the signal from SDF-1α through to G protein subunits and activates sequential downstream signalling pathway effects. In steady state, G proteins cooperate with CXCR4 receptor in the form of heterotrimeric multimers comprising of the α, and βγ subunits. When the G-protein α subunit is GDP-bound form, it is complexed with its

corresponding βγ dimer subunit and held in check. When the GPCR receptor is activated, GDP exchanges to the higher energy GTP and the Gα subunit becomes switched to an activated form through a conformational change that allows dissociation from its βγ subunit. The α subunit is no longer held in check, and is free to activate downstream processes.

In this chapter, we focus on Gα subunits which are divided into four main families, namely, $G\alpha_s$, $G\alpha_{i/o}$, $G\alpha_{q/11}$, and $G\alpha_{12/13}$, based on similarity of amino acid sequences (Hepler and Gilman, 1992, Simon et al., 1991). Different Gα subunit families contributes to distinct G-protein-coupled receptor (GPCR) actions and transduces the signal to different downstream effectors (Rubin, 2009). In general, CXCR4 receptor is thought to couple with $G\alpha_i$ family members, but it has been reported that CXCR4 may also transduce the SDF-1α signal to a different family of Gα subunits (Maghazachi, 1997, Rubin, 2009). In this study, we focus on the $G\alpha_{12}$ family which are comprised of $G\alpha_{12}$ and $G\alpha_{13}$, which are thought to modulate Rho monomeric G-protein, cytoskeletal remodeling and some tyrosine kinase-induced migrations. Moreover, $G\alpha_{12}$ is reported as a BTK TH/PH domain binding protein and $G\alpha_{13}$ contributes towards CXCR4 receptor and transduction of the signal to Rho in T cells and breast cancer (Jiang et al., 1998, Yagi et al., 2011, Tan et al., 2006). In acute leukaemia, CXCR4 transduces the signal from SDF-1α to $G\alpha_i$, with BTK reportedly involved in this pathway's control of migration (Zaitseva et al., 2014). Therefore, this chapter aims to identify in AML and CLL whether $G\alpha_{12}$ or $G\alpha_{13}$ family members cooperates with CXCR4 receptor and its activation of BTK.

5.2 Results

5.2.1 $G\alpha_{12}$ and $G\alpha_{13}$ expression in different cell lines

To understand the effect of $G\alpha_{12}$ family knockdown in AML and CLL, expression of these two Gα proteins were screened in different human leukaemia cell lines. The expression of G protein alpha subunit of the $G\alpha_{12}$ family was investigated on U937, HL-60, OCI-AML3, OCI-LY19, and HEK293T. As shown in Figure 5.1, all human leukeamic cell lines and HEK293T cells expressed $G\alpha_{12}$ and $G\alpha_{13}$ even though the expression level of these Gα proteins was different among each cell line. The difference between these two Gα units is not only the expression levels seen in each cell line, but also the relative abundance of $G\alpha_{12}$ and $G\alpha_{13}$ in each cell. The required amount of total protein measured is different for $G\alpha_{12}$ and $G\alpha_{13}$, where 10 μg was needed for $G\alpha_{12}$ detection, whilst $G\alpha_{13}$ needed use of approximately 20-40 μg of protein in order for it to be detected in these experiments. Therefore, $G\alpha_{12}$ protein is more plentiful than $G\alpha_{13}$ in our cellular models. The human monocyte cell line, U937, showed the highest expression of both $G\alpha_{12}$ and $G\alpha_{13}$ among these cells. On the other hand, $G\alpha_{12}$ and $G\alpha_{13}$ showed the lowest expression in HL-60 cells, especially $G\alpha_{13}$ which was only marginally detectable in this cell. The expression was similar in OCI-AML3, OCI-LY19, and HEK293T cells. Since these experiments were performed to choose a representative cell line for the $G\alpha_{12}$/$G\alpha_{13}$ knockdown experiment, we chose OCI-AML3 and OCI-LY19 cell lines are the best candidates among for such studies. Furthermore, both Gα proteins were detected in HEK293T cells, so this cell can also be used for the plasmid transfection in other experiments.

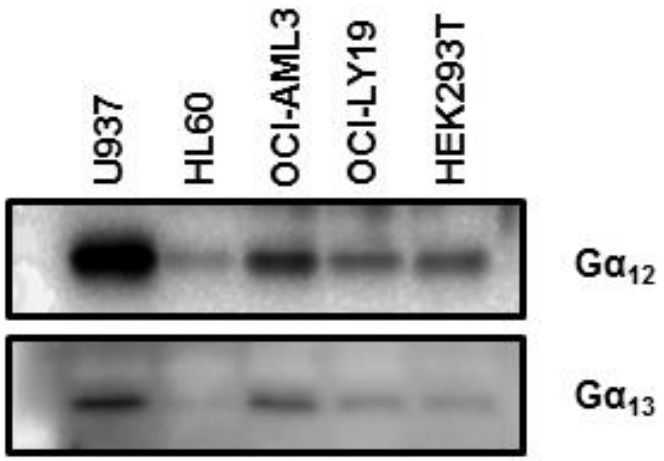

Figure 5.1 Expression of $G\alpha_{12}$ and $G\alpha_{13}$ in different cell lines.

Human leukaemic cells and HEK293T cell had protein extracted and analysed by Western blotting. Ten microgram protein was loaded for $G\alpha_{12}$ and 20 to 40 µg protein was required for $G\alpha_{13}$. Membranes were probed with $G\alpha_{12}$ (1:500) and $G\alpha_{13}$ (1:200) antibodies to observe basal expression of these two proteins.

5.2.2 $G\alpha_{12}$ and $G\alpha_{13}$ knockdown screening in HEK293T

HEK293T is a suitable model for mammalian cell transfection, so we screened for the knockdown efficiency of each $G\alpha_{12}$- and $G\alpha_{13}$-targeted shRNA plasmid on this cell, so as to evaluate the efficiency of each plasmid before shRNA transduction with lentivirus in the human leukaemia cells. Five plasmids for each $G\alpha_{12}$ and $G\alpha_{13}$ (including scramble as non-targeting control) were transfected into HEK293T separately according to the protocols outlined in the Materials and Methods chapter. The transfected HEK293T was incubated under cell culture conditions for 3 days before protein was extracted and Western blotting performed to investigate the knockdown efficiency of each of the shRNA plasmids. The results showed the $G\alpha_{12}$ knockdown efficiency was not apparently different among the five shRNA plasmids, with only E6 and E7 showing approximately 50% knockdown efficiency compared to the non-transfected control cells. The similarity for $G\alpha_{13}$-targeted shRNA plasmid was observed with all clones showing similar knockdown efficiency (see Figure 5.2). However, knockdown efficiency in HEK293T may differ from human leukaemic cells, therefore the shRNA plasmid clone E6 and clone C10 were chosen to make Lentivirus containing $G\alpha_{12}$- and $G\alpha_{13}$-targeted shRNAs, respectively to be used in OCI-AML3 and OCI-LY19 transduction experiments.

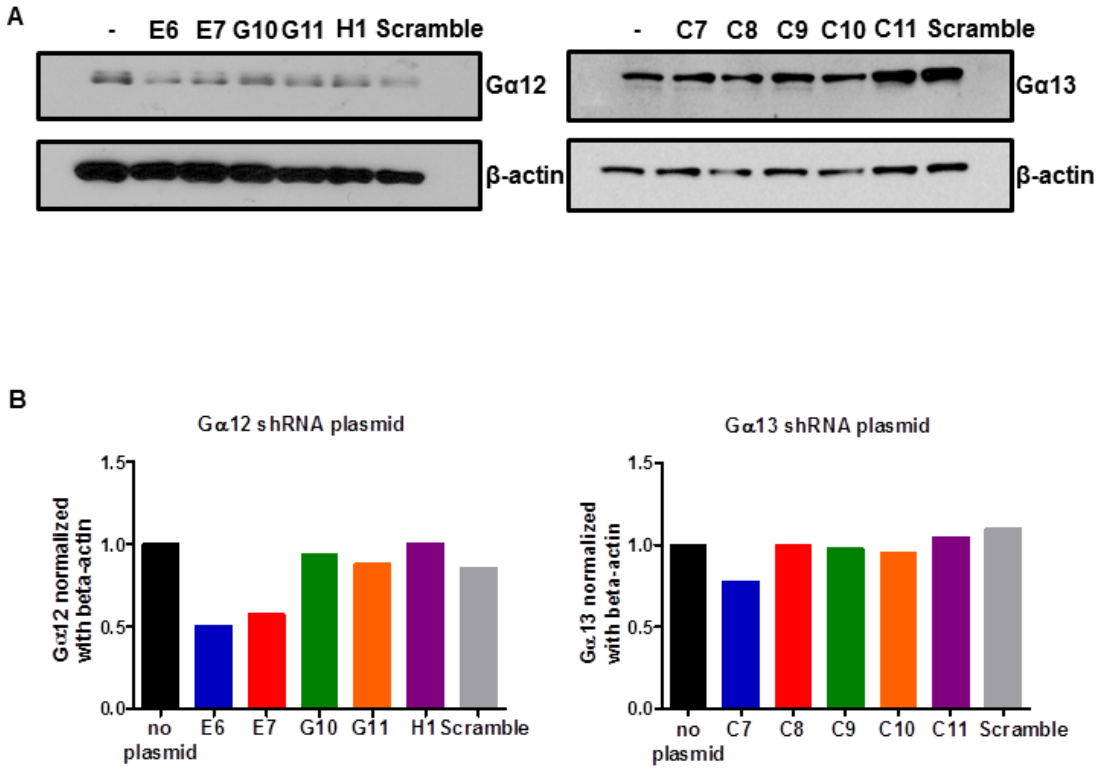

Figure 5.2 Knockdown efficiency of $G\alpha_{12}$ and $G\alpha_{13}$ targeted shRNA plasmids in HEK293T.

HEK293T was transfected with different $G\alpha_{12}$- or $G\alpha_{13}$-targeted shRNA plasmids. Protein lysate was prepared after 3 days of transfection. Western blotting shown in Figure A, with densitometry shown in Figure B. The bar graph showed $G\alpha_{12}$ or $G\alpha_{13}$ protein band intensity normalized to β-actin, plus the knockdown efficiency being compared to non-transfected (no plasmid) band densities.

5.2.3 $G\alpha_{12}$ and $G\alpha_{13}$ knockdown efficiency on OCI-AML3 and OCI-LY19

As we aim to investigate whether $G\alpha_{12}$ family G-proteins engage with the signal transduction from the CXCR4 receptor and its interaction with BTK on AML and CLL cells, $G\alpha_{12}$ or $G\alpha_{13}$ were knocked down as above and the functional assays were examined on the $G\alpha_{12}$ and $G\alpha_{13}$ knockdown cells. Since there are well known difficulties associated with efficient transfection or infection in hematopoietic cells, our lentivirus delivery system was used as a tool for delivering $G\alpha_{12}$- and $G\alpha_{13}$-targeted shRNA plasmids into human leukaemic cells. The selected shRNA plasmids from the previous experiment, which are E6 and C10, were transfected into HEK293T with the third generation lentivirus plasmid to produce $G\alpha_{12}$- or $G\alpha_{13}$-targeted shRNA contained lentivirus particles. OCI-AML3 and OCI-LY19 were transduced with these lentivirus plasmids containing appropriate shRNA sequences, as described in the Methods chapter. The transduced cells were selected by culturing for 6 days in the presence of 2-4 μg/mL puromycin as a selective pressure. The surviving cells were collected and their protein expression probed for $G\alpha_{12}$ or $G\alpha_{13}$ protein. As shown in Figure 5.3, the expression of both $G\alpha_{12}$ and $G\alpha_{13}$ from transduced cells after puromycin selection, is markedly lower than expression in wild-type and scrambled control cells, with knockdown efficiency being improved by the puromycin selection process, compared to the non-puromycin-selected population. Therefore, both $G\alpha_{12}$ and $G\alpha_{13}$ were successfully knocked down. $G\alpha_{13}$ shRNA knockdown efficiency is greater than $G\alpha_{12}$ shRNA-mediated knockdown as $G\alpha_{13}$ transfected cells were seen to be almost completely deplete the G-protein subunit. However, this result is consistent with previous experiments showing $G\alpha_{13}$ being less abundant

than $G\alpha_{12}$ in our cells, meaning that this protein may be easier to knockdown than $G\alpha_{12}$ protein in our AML and CLL cells. The transduced cells were reselected with 4 μg/mL puromycin for 6 days, then expression level of $G\alpha_{12}$ and $G\alpha_{13}$ were checked regularly, as shown in Figure 5.3B. The effect of $G\alpha_{12}$ or $G\alpha_{13}$ depletion was assessed in further experimentation.

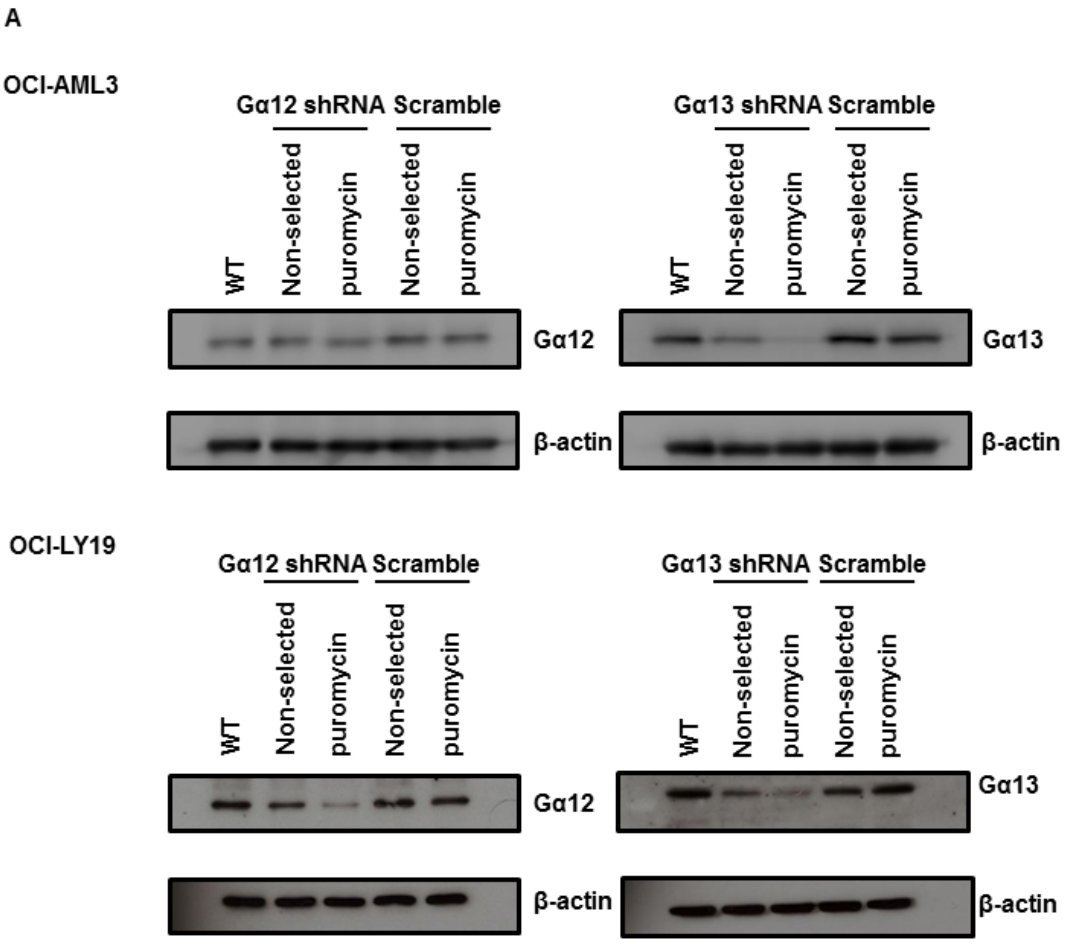

Figure 5.3 $G\alpha_{12}$- and $G\alpha_{13}$-targeted shRNA transduction into human leukaemic cell lines.

Lentiviruses containing $G\alpha_{12}$- or $G\alpha_{13}$-targeted shRNA were transduced into OCI-AML3 and OCI-LY19 by the spinoculum Method. The transduced cells were cultured under 2-4 μg/mL puromycin for 6 days. Thereafter, the surviving cells were examined for $G\alpha_{12}$ or $G\alpha_{13}$ knockdown efficiency (Figure A). The knockdown cells were further selected with puromycin culture, and the cell population checked regularly for knockdown of $G\alpha_{12}$ and $G\alpha_{13}$ protein expression (Figure B).

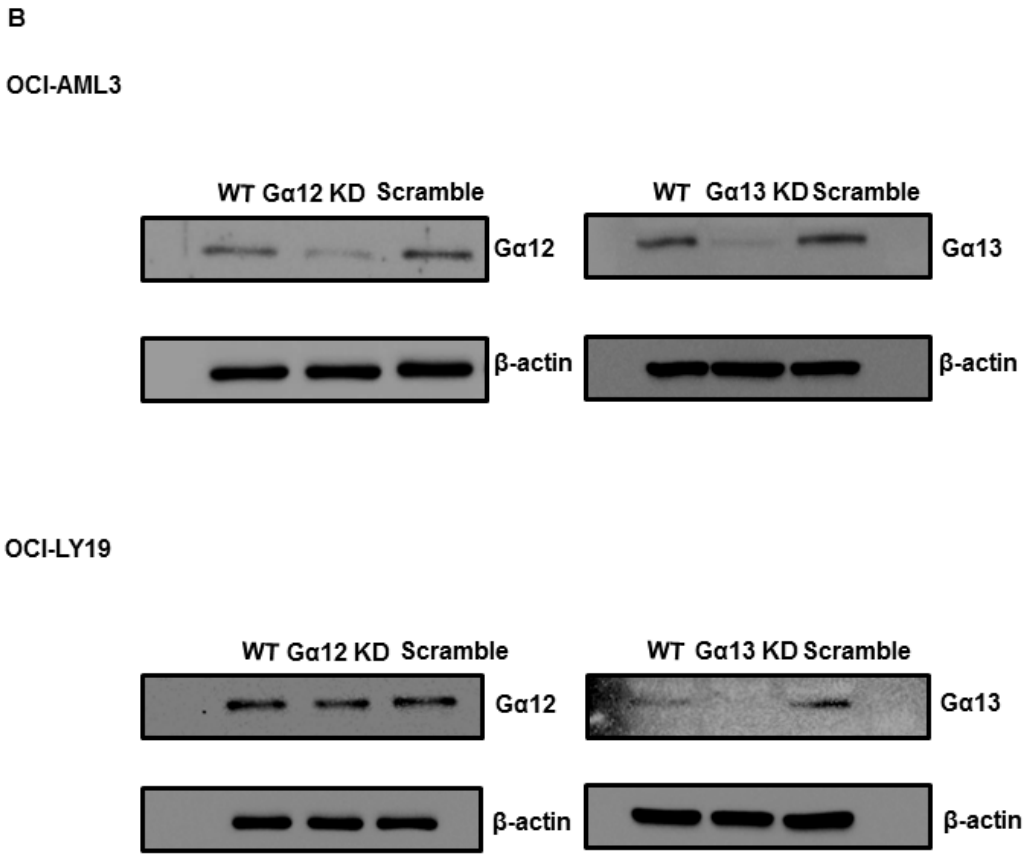

Figure 5.3 contd/. $G\alpha_{12}$- and $G\alpha_{13}$-targeted shRNA transduction into human leukaemic cell lines.

Lentiviruses containing $G\alpha_{12}$- or $G\alpha_{13}$-targeted shRNA were transduced into OCI-AML3 and OCI-LY19 by the spinoculum Method. The transduced cells were cultured under 2-4 µg/mL puromycin for 6 days. Thereafter, the surviving cells were examined for $G\alpha_{12}$ or $G\alpha_{13}$ knockdown efficiency (Figure A). The knockdown cells were further selected with puromycin culture, and the cell population checked regularly for knockdown of $G\alpha_{12}$ and $G\alpha_{13}$ protein expression (Figure B).

5.2.4 The effect of $G\alpha_{12}$ and $G\alpha_{13}$ on the SDF-1α/CXCR4 signalling pathway

To assess whether $G\alpha_{12}$ or $G\alpha_{13}$ played a role in the SDF-1α/CXCR4-mediated stimulation of BTK, we used the knockdown cells to judge any change in agonist stimulated cellular responses. BTK was phosphorylated after 100 ng/mL SDF-1α stimulation as shown in the previous chapter. As we hypothesize that $G\alpha_{12}$ or $G\alpha_{13}$ could participate with the CXCR4 receptor and transduced signal to activate BTK, therefore $G\alpha_{12}$ family knockdown cells were investigated for BTK activation by observing p-BTK and other phosphorylated proteins by Western blotting in SDF-1α/CXCR4-stimulated time courses. As shown in Figure 5.4, p-BTK was not elevated after 100 ng/mL SDF-1α treatment in the time courses in both OCI-AML3 and OCI-LY19. The phosphorylation of ERK 1/2 was also unchanged after SDF-1α/CXCR4 treatment in OCI-AML3 cells, while p-ERK was slightly changed in OCI-LY19. Given the disappointing stimulations that we expected and didn't observe, we tried to minimize the basal stimulatory levels seen in these cells under test. These cells were serum-starved in serum-free RPMI overnight before performing similar experiments. We suspected that serum-starvation may quiesce these cells and affect their basal expression of the phosphorylated kinases. The OCI-AML3 WT was used as a representative model to prove this. OCI-AML3 cells were plated overnight with different FBS concentrations, but our results showed that starvation did not have the desired effect on phosphorylation, since p-BTK and p-PLCγ2 (a kinase normally downstream of BTK activation) expression was high at 0 min under every FBS condition tested. Once again, our frustration with the p-BTK antisera led us to not have conclusive SDF-1α/CXCR4-stimualted BTK activation. Therefore, we used another

assay to test the interaction between the CXCR4 receptor and $G\alpha_{12}$, $G\alpha_{13}$, with BTK, to assess the effectiveness of $G\alpha_{12}$ and $G\alpha_{13}$ knockdown in these cells.

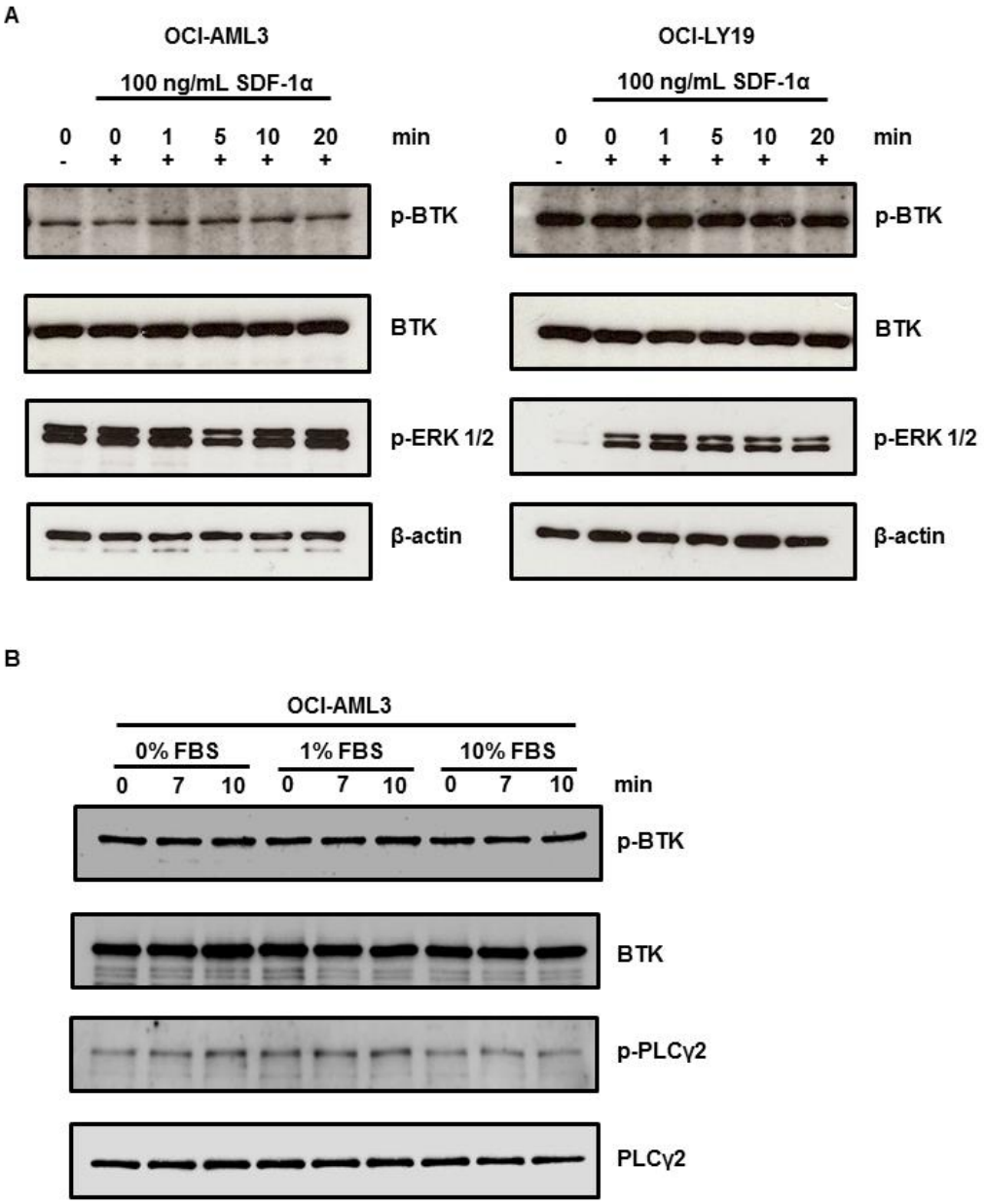

Figure 5.4 The effect of $G\alpha_{12}$ and $G\alpha_{13}$ knockdown on the SDF-1α/CXCR4 signalling pathway.

OCI-AML3 and OCI-LY19, wild-type (WT) cells were stimulated with 100 ng/mL SDF-1α in the indicated time course. Phosphorylated BTK and p-ERK1/2 were examined by Western blotting (Figure A). The effect of starvation on phosphorylated kinase expression was examined after 100 ng/mL SDF-1α treatment, as shown in Figure B.

5.2.4 $G\alpha_{12}$ and $G\alpha_{13}$ are not involved in AML and CLL survival after Ibrutinib treatment

Pharmaceutical BTK inhibition by ibrutinib has been reported to reduce survival and inhibit proliferation of primary AML, showing an effect on survival of some AML lines, U937 and FLT3-ITD AML cells (Zaitseva et al., 2014, Wu et al., 2016). As we aim to identify whether $G\alpha_{12}$ and $G\alpha_{13}$ interacts with BTK, BTK itself has been reported as an important signalling protein for AML cell survival, therefore we tested this hypothesis by treating the OCI-AML3 and OCI-LY19 with ibrutinib at different concentrations for up to three days and subsequent cell death was analysed by annexin-V/PI staining and FACS analyses. Overall, the percentage of cell death was not obviously different in $G\alpha_{12}$ and $G\alpha_{13}$ knockdown cells, compared to wild-type control cells of both OCI-AML3 and OCI-LY19, as shown in Figure 5.5. CLL cells showed slightly more sensitivity towards ibrutinib-induced death than AML cells. However, OCI-AML3 $G\alpha_{12}$ knockdown-mutant cells showed more ibrutinib-mediated cell death than wild-type or $G\alpha_{13}$ knockdown cells. Surprisingly, there was less than 50 percent of cells that died after 2.5% DMSO treatment which we used as a positive control for our cell death experiments. These graphs were calculated from two independent samples of OCI-LY19 while OCI-AML3 was performed once due to problems with cell contamination around the times of these experiments. What we can conclude from these series of experiments is that there is no dramatic ibrutinib-induced cell death in AML or CLL cells at any ibrutinib concentration, plus the effects of $G\alpha_{12}$ or $G\alpha_{13}$ protein family knockdown seems to not have any major effect on what minor cell survival changes that may be observable.

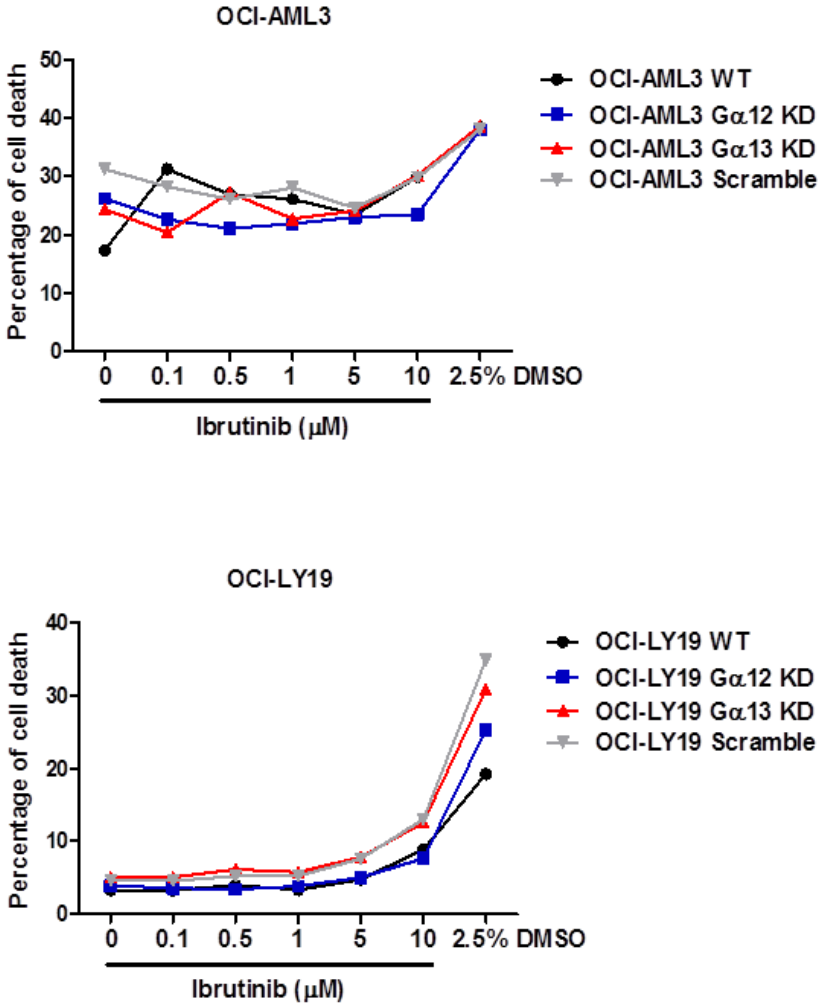

Figure 5.5 The effect of $G\alpha_{12}$ and $G\alpha_{13}$ on cell survival after ibrutinib treatment.

OCI-AML3 and OCI-LY19, both wild-type (WT), $G\alpha_{12}$ and $G\alpha_{13}$ family knockdown cells were treated with various concentration of ibrutinib (0.1, 0.5, 1, 5, and 10 μM) for 3 days. Ibrutinib-treated cells were then examined for cell death by annexin-V/PI staining and FACS analyses as described in the Materials and Methods chapter. The percentage of cell death was calculated by combining Annexin-V +ve/PI -ve, Annexin-V +ve/PI +ve, and Annexin V -ve/PI +ve cells. OCI-AML3 assessment from one experiment, with OCI-LY19 results averaged from two independent experiments.

5.2.5 Optimisation of the migration assay protocol

The CXCR4 is a G-protein-coupled receptor that controls cell migration toward SDF-1α. We aim to identify whether $G\alpha_{12}$ and $G\alpha_{13}$ coupled to the CXCR4 receptor. Therefore, migration assays were performed to investigate the effect of $G\alpha_{12}$ and $G\alpha_{13}$ knockdown on migration ability toward the SDF-1α chemokine. In the initial experiments, several protocols for the migration assays were not stated in Materials and Method chapter, due to there being very poor apparent migration in response to ligand and low signal-noise ratio; hence the need for optimisation of this assay to determine the most suitable protocol for our cell lines tested here.

First, we optimized cell number and amount of FBS in RPMI that befits this assay. CellTracker Green CMFDA Dye and fluorescence microscopy were used to optimize the measurement of migration. OCI-AML3 wild-type and OCI-LY19 wild-type cells (1×10^5, 2.5×10^5, and 5×10^5 cells/0.6 mL) were incubated with 10 μM CellTracker Green CMFDA Dye for 30 min, then cells were washed with media to remove excess dye and resuspended with either 1% FBS RPMI or serum-free RPMI. The indicated amount of OCI-AML3 and OCI-LY19 cells were seeded on 8 μm pore-diameter transwell inserts and placed in a 24-well plate containing 1% FBS RPMI or serum-free RPMI. Cells were allowed to migrate for 3 h under cell culture conditions then the migrated cells were counted under a fluorescent microscope. Results showed that 2.5×10^5 cells and assay performed with 1% FBS RPMI were the best conditions for a more successful migration assay, as shown in Figure 5.6A. However, OCI-LY19 migrated cells could not be counted due to there being too many cells remaining in the bottom of the chamber, migrating without any SDF-1α

treatment (data was not shown). This may be due to the smaller cell size for CLL cells than AML cells, thereby allowing CLL cells to diffuse through the pores rather than it be a more active migratory process. For this reason, the effect of $G\alpha_{12}$ and $G\alpha_{13}$ knockdown was examined only on the OCI-AML3 cells.

Since we struggled with reproducibility after migration assay were performed (n = 2) showing different results as seen in Figure 5.7A, we developed a secondary protocol. In this next protocol, the cell density, cell staining, and the incubation time were the same as previously measured, but the migratory cells were detected instead by a microplate reader rather than counting them under a fluorescence microscope. The results revealed that untreated and 100 ng/mL SDF-1α treatment conditions were not apparently different in the amount of migrated cells observed, even though cells obviously migrated towards the 100 ng/mL SDF-1α stimulus compared to untreated cells (as measured when the bottom chamber was observed under light microscopy before migrated cells were sampled, and measured by fluorescence microplate reader) as shown in Figure 5.7B. In this case, we think the microplate reader is not a sufficiently good detection system for this migration assay, similar to counting cells by fluorescence microscope, where the signal strength isn't strong enough to give sufficient signal-noise ratio to enable adequate quantification.

Lastly, OCI-AML3 wild-type cells were used for the migration assay optimisation. OCI-AML3 cells were resuspended with 1% FBS at 2.5 x 10^5 cells (0.6 mL) density then seeded into a 8 μm transwell insert and placed on a 24-well culture plate containing 1% FBS RPMI (untreated control) or

various concentrations of SDF-1α (100 ng/mL, 200 ng/mL, and 400 ng/mL) in 1% FBS RPMI. 10% FBS RPMI treatment was used as a migration positive control stimulus. Cells were allowed to migrate toward SDF-1α for 3 h and 4 h under cell culture conditions. Migrated cells were counted under a light microscope with trypan blue staining. Results revealed that 200 ng/mL SDF-1α was the optimal concentration to induce migration of OCI-AML3 cells when they were incubated with chemokine for 4 h (Figure 5.6B). Therefore, 200 ng/mL SDF-1α-induced cell migration and 4 h incubation time are good conditions for this migration assay. This protocol was applied to the remaining migration assay experiments, as outlined in the Materials and Methods chapter.

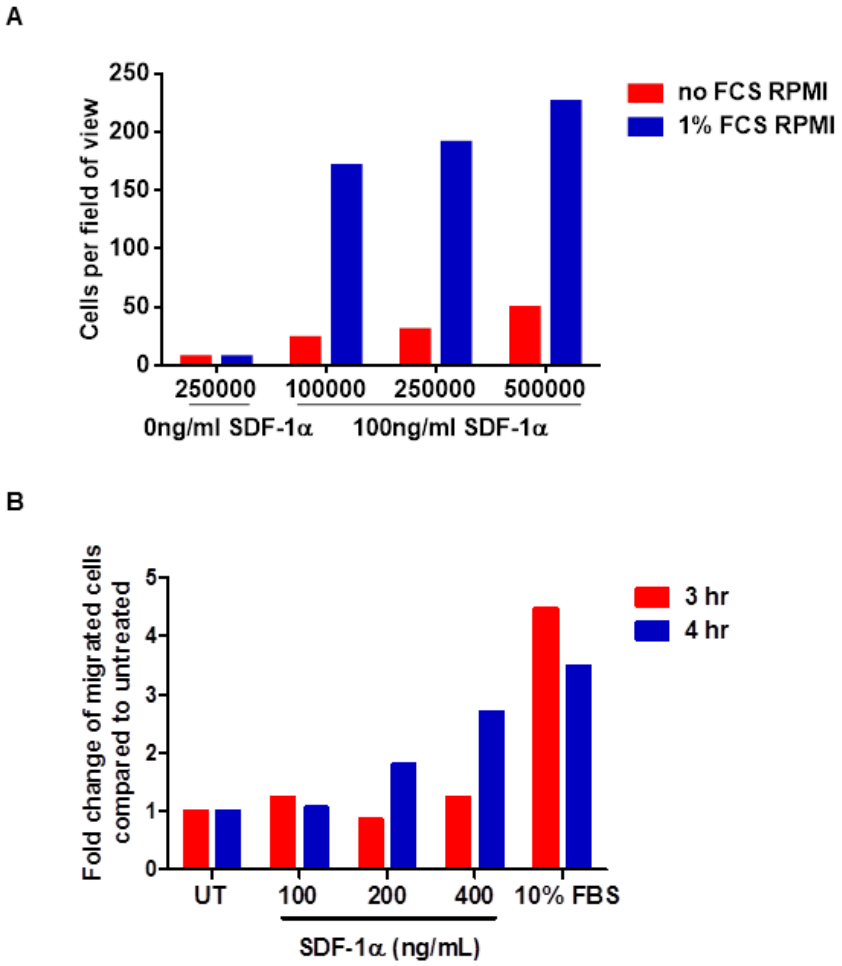

Figure 5.6 Migration assay optimization with OCI-AML3 wild-type cells.

Different cell densities of OCI-AML3 cells as indicated were seeded onto 8 µm transwell inserts to determine optimal cell number and FBS concentration for a migration assay. Figure A, CellTracker Green CMFDA Dye was used to stain cells, with migrated cells counted by fluorescence microscopy after 3 h incubation with 100 ng/mL SDF-1α in the bottom chamber (RPMI ± 1% FBS). Figure B, various concentration of SDF-1α and incubation times as indicated are shown in Figure B, with migrated cells being counted with trypan blue exclusion staining.

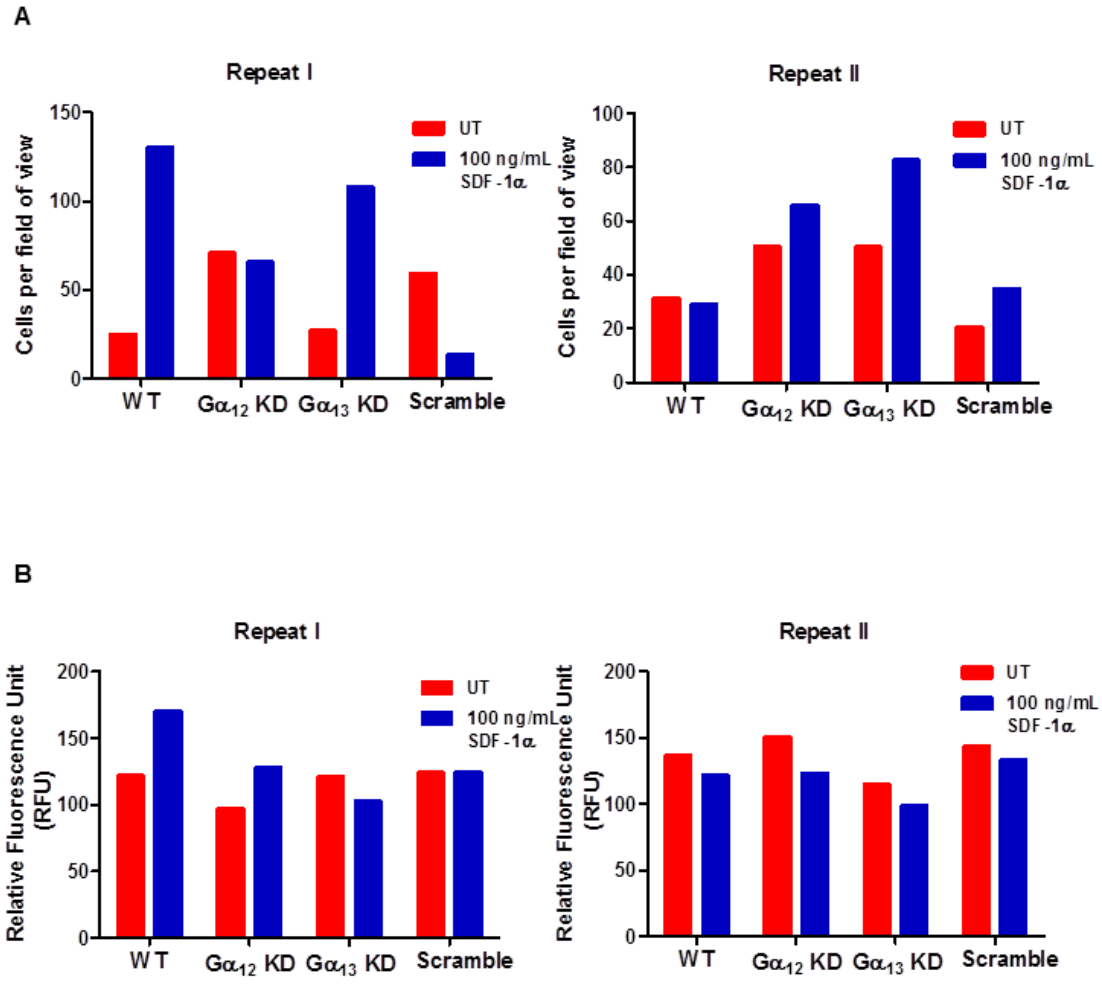

Figure 5.7 The effect of $G\alpha_{12}$ and $G\alpha_{13}$ knockdown on migration toward SDF-1α.

OCI-AML3 wild-type and $G\alpha_{12}$ or $G\alpha_{13}$ subtype knockdown cells were incubated with CellTracker Green CMFDA Dye for 30 min and allowed to migrate towards 100 ng/mL SDF-1α for 3 h. Migrated cells were counted by fluorescence microscopy (A) or the fluorescence intensity measured at 492/517 nm excitation/emission spectra (B). These experiments represent the average of two independent experiments for each method tested.

5.2.6 $G\alpha_{12}$ and $G\alpha_{13}$ are important for OCI-AML3 migration towards SDF-1α via its CXCR4 receptor.

Since $G\alpha_i$ has been already been identified by another research group to engage with the CXCR4 receptor in leukaemia cells, it has been reported that other families of Gα have the potential to be an effector molecule of this receptor (Tan et al., 2006, Zaitseva et al., 2014). Therefore, we aimed to identify whether $G\alpha_{12}$ and $G\alpha_{13}$ transduce signalling through CXCR4 in OCI-AML3 cells, with the migration assay being used as a functional assay to prove this hypothesis. OCI-AML3 wild-type cells and $G\alpha_{12}$ and $G\alpha_{13}$ knockdown cells were permitted to migrate towards 200 ng/ml of SDF-1α for 4 h as described. The migrated cells being counted in triplicate. As shown in Figure 5.8, the fold change of migrated cells from each G-protein knockdown cell were compared to wild-type (WT) cells. SDF-1α stimulation was apparent in each of the wild-type, $G\alpha_{12}$- $G\alpha_{13}$-knockdown cells ($P < 0.01$ (**), $n = 8$). The $G\alpha_{12}$ and $G\alpha_{13}$ knockdown appeared to suppress this agonist CXCR4-mediated migration. However, although there was inhibition in the $G\alpha_{12}$ knockdown cells, with the inhibition seen being statistically significant ($P < 0.05$ (*), $n = 8$), the inhibition of SDF-1α-stimulated migration in $G\alpha_{13}$ knockdown cells was equally statistically significant ($P < 0.05$ (*), $n = 8$)(see Figure 5.8). Migratory ability was seen when 10% FBS was the stimulus ($P < 0.05$ (*)). Interestingly, all three cell variants were unaffected by $G\alpha_{12}$ or $G\alpha_{13}$ knockdown when migrating towards the 10% FBS stimulus, unlike when migrating towards a SDF-1α stimulus, which is impeded by G-protein knockdown. Therefore, $G\alpha_{12}$ and $G\alpha_{13}$ can both be seen to be CXCR4-linked, with both partially controlling migration towards SDF-1α in OCI-AML3 cells.

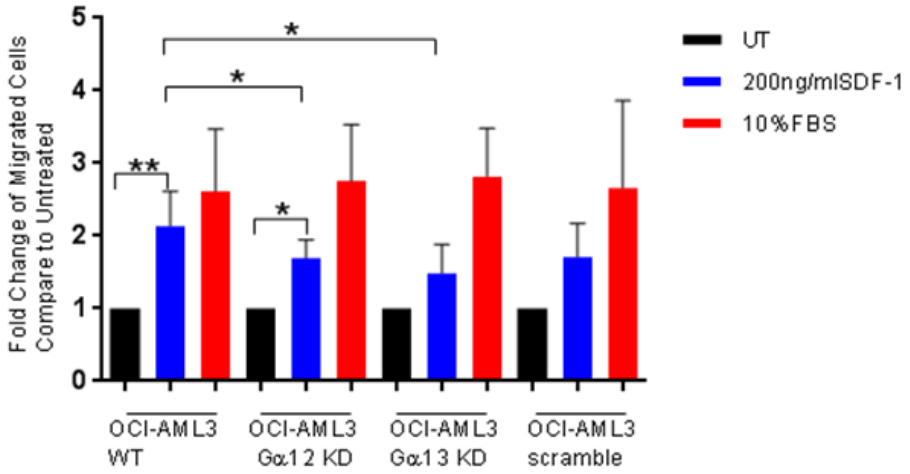

Figure 5.8 The effect of $G\alpha_{12}$ and $G\alpha_{13}$ knockdown on chemotaxis towards 200 ng/mL SDF-1α.

OCI-AML3 wild-type (WT) and $G\alpha_{12}$ or $G\alpha_{13}$ knockdown cells were incubated in a transwell migration chamber in the presence of 200 ng/mL SDF-1α or 10% FBS (positive control) present in the bottom chamber. Cells were incubated for 4 h then migrated cells were counted by trypan blue exclusion staining. These data represent the mean ± SD fold stimulation from 8 independent repeat experiments (n = 8). Student's T-test was used as a determination of the statistical significance between wild-type and each knockdown (KD) cell ($P < 0.05$ (*); $P < 0.01$ (**)).

5.2.7 The effect on migration of $G\alpha_{12}$ subtype knockdown after ibrutinib treatment

We aimed to identify whether BTK is downstream of $G\alpha_{12}$ and $G\alpha_{13}$ in the signal transduction capability of the CXCR4 receptor. Therefore, migration towards SDF-1α was investigated after BTK inhibition by ibrutinib treatment. As shown in Figure 5.9A, p-BTK was successfully inhibited by ibrutinib from 100 nM to 10 μM after 2 h inhibitor treatment. Wild-type OCI-AML3 cells and $G\alpha_{12}$ and $G\alpha_{13}$ knockdown cells were treated with the indicated concentrations of ibrutinib from previous Western blotting experiments (2 h preteated) before incubation with 200 ng/mL SDF-1α for a further 4 h. Migrated cells were counted by trypan blue staining. The results showed the amount of migrated cells did not significantly differ comparing untreated wild-type OCI-AML3 cells to $G\alpha_{12}$ or $G\alpha_{13}$ knockdown cells. Cell migration slightly reduced in $G\alpha_{12}$ knockdown and scrambled control transduced cells when cells were treated with ibrutinib, on the other hand, migrated cells showed an increased in $G\alpha_{13}$ knockdown cells even p-BTK was also inhibited by ibrutinib. These experiments were not conclusive as the effect of ibrutinib on migration (as seen previously in this chapter) is not consistent or significant – thus we are unable to conclude of any involvement of BTK in the migration of OCI-AML3 cells induced by SDF-1α.

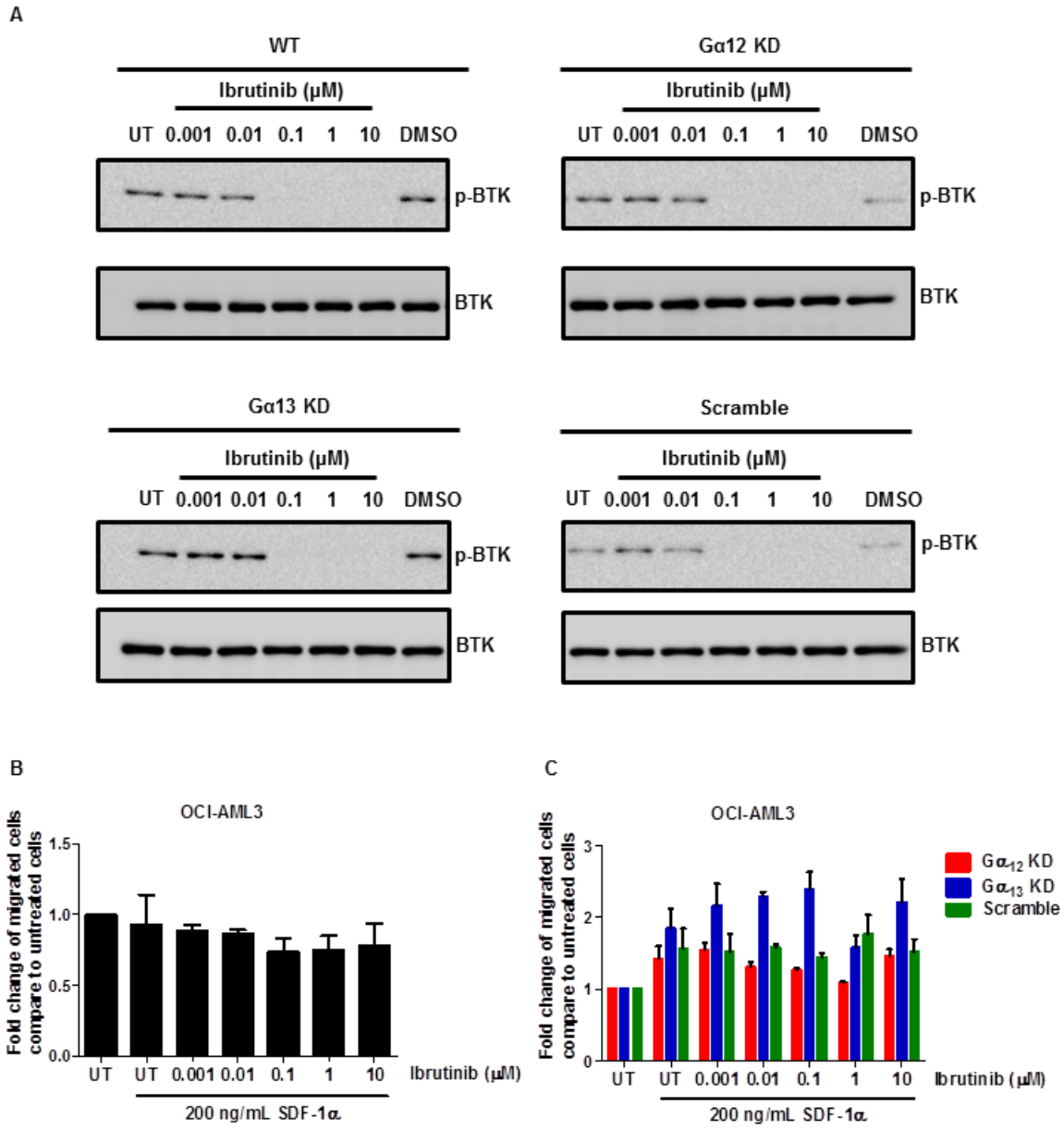

Figure 5.9 The effect of BTK inhibition on migration toward 200 ng/mL SDF-1α in $G\alpha_{12}$ and $G\alpha_{13}$ knockdown cells.

OCI-AML3 wild-type (WT) and $G\alpha_{12}$ or $G\alpha_{13}$ knockdown cells were treated for 2 h with 1 nM - 10 μM ibrutinib then incubated with 200 ng/mL SDF-1α for a further 4 h. Phosphorylation of BTK after ibrutinib treatment (A), or SDF-1α-induced migration (B) is shown (means ± SEM, n = 2).

5.2.8 The effect on cytokine production of $G\alpha_{12}$ family knockdown cells after ibrutinib treatment

To examine the effect of BTK inhibition on cytokine expression in $G\alpha_{12/13}$ family suppressed cells, OCI-AML3 wild-type, $G\alpha_{12}/G\alpha_{13}$ knockdown, and scramble control cells were seeded at 2.5 x 10^5 or 5 x 10^5 cells/0.6 mL density. Cells were treated with different concentrations of Ibrutinib for 2 h then incubated with 200ng/mL SDF-1α for a further 4 h. Cellular RNA was extracted and mRNA converted to cDNA, before qPCR was performed to investigate the mRNA expression of several cytokines. This experiment was performed three times with slightly differing methodology. Data from each experiment was plot into wild type and knockdown cells separately. Overall, there was no obvious difference between untreated and treated cells in either wild-type or $G\alpha_{12}$ and $G\alpha_{13}$ knockdown cells, apart from IL-8 (Figure 5.10A & F) and IL-12A (Figure 5.10D). As shown in Figure 5.10E and F, cells were treated with 20 ng/mL TNF-α stimulus to act as a control, however, we could not detect the expected increase in cytokine expression that normally occurs after TNF-α treatment. Therefore, these experiments were not conclusive and are probably more indicative of the high basal activities of signalling and mRNA production that are often associated with these type of leukemia cancer cells. Further optimisation work is needed to improve the preconditioning of these cells to allow more reproducible and reliable signalling findings.

A

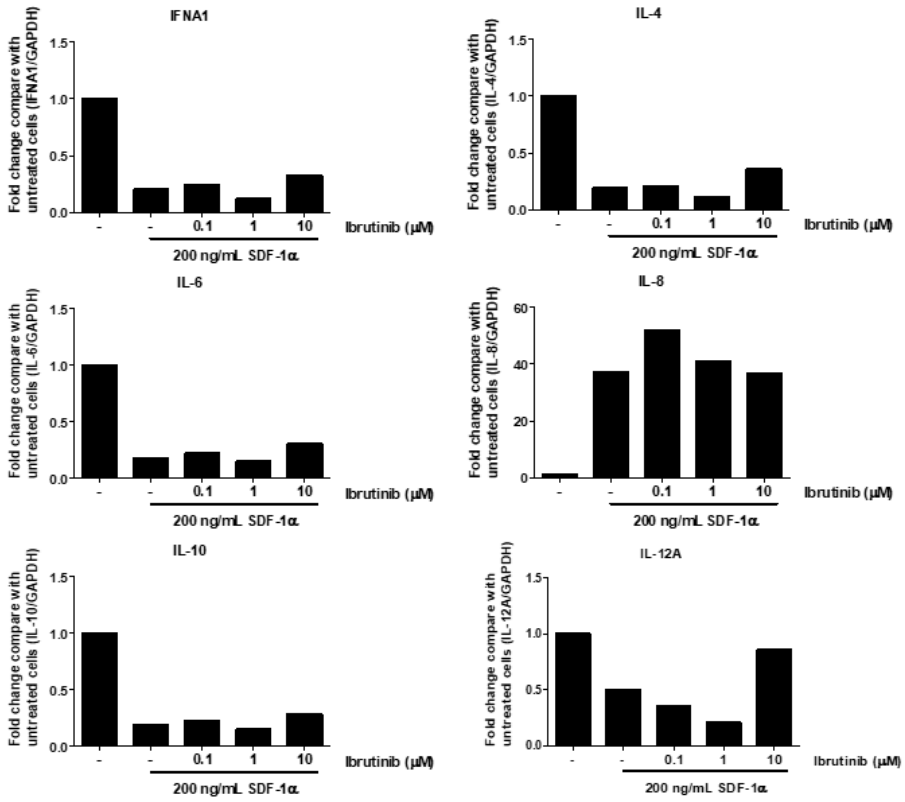

Figure 5.10 The effect of $G\alpha_{12}$ and $G\alpha_{13}$ on SDF-1α induced cytokines production in ibrutinib treated cells.

OCI-AML3 WT and $G\alpha_{12}$ family knockdown were treated with various concentration of ibrutinib (0.1, 1, and 10 μM) for 2 hr then continually incubated with 200 ng/mL SDF-1α for 4 hr. The cytokines expression was examined by qPCR. Figure A-F represent different experiment which slightly different in each. Figure A-B, WT (A) and Knockdown (B) cells were treated with three concentrations of Ibrutinib. Figure C-D, WT (C) and knockdown (D) cells were treated with 1 μM Ibrutinib and H_2O was used for vehicle control. Figure E-F, WT (E) and knockdown (F) cells were treated with the same condition with experiment in figure C and D and TNF-α treated cells were used as positive control.

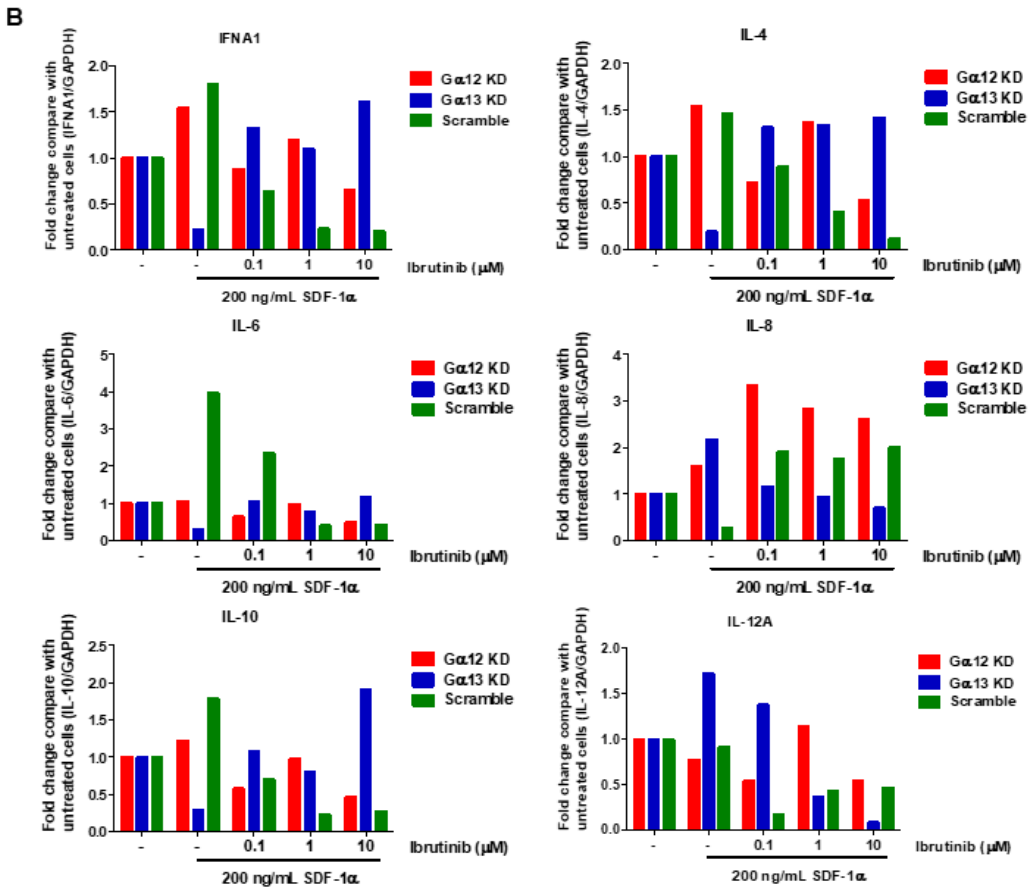

Figure 5.10 contd/ The effect of $G\alpha_{12}$ and $G\alpha_{13}$ on SDF-1α induced cytokines production in ibrutinib treated cells.

OCI-AML3 WT and $G\alpha_{12}$ family knockdown were treated with various concentration of ibrutinib (0.1, 1, and 10 μM) for 2 hr then continually incubated with 200 ng/mL SDF-1α for 4 hr. The cytokines expression was examined by qPCR. Figure A-F represent different experiment which slightly different in each. Figure A-B, WT (A) and Knockdown (B) cells were treated with three concentrations of Ibrutinib. Figure C-D, WT (C) and knockdown (D) cells were treated with 1 μM Ibrutinib and H_2O was used for vehicle control. Figure E-F, WT (E) and knockdown (F) cells were treated with the same condition with experiment in figure C and D and TNF-α treated cells were used as positive control.

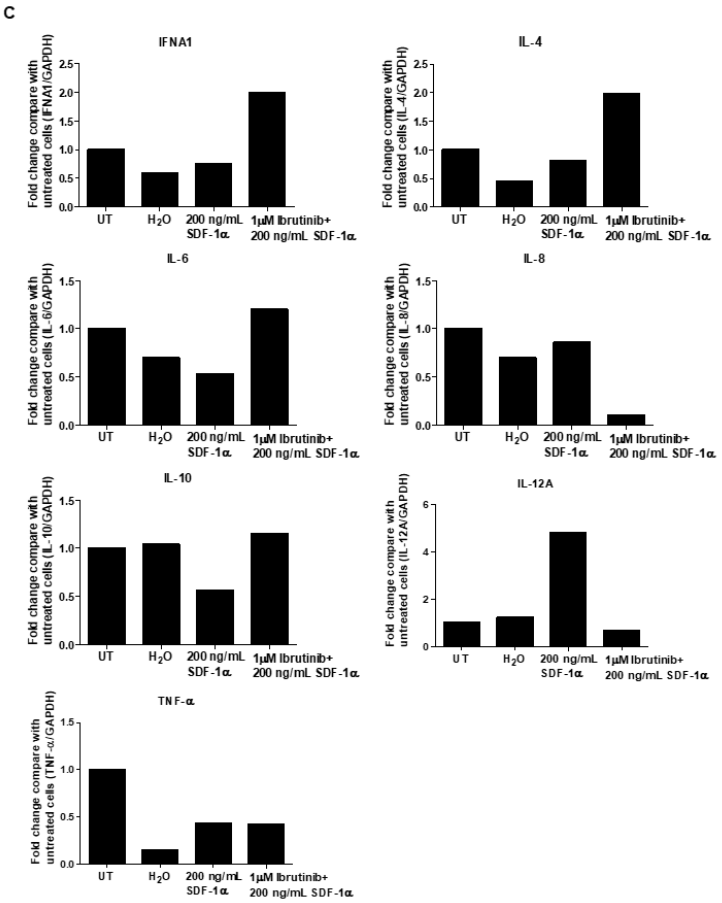

Figure 5.10 contd/ The effect of $G\alpha_{12}$ and $G\alpha_{13}$ on SDF-1α induced cytokines production in ibrutinib treated cells

OCI-AML3 WT and $G\alpha_{12}$ family knockdown were treated with various concentration of ibrutinib (0.1, 1, and 10 μM) for 2 hr then continually incubated with 200 ng/mL SDF-1α for 4 hr. The cytokines expression was examined by qPCR. Figure A-F represent different experiment which slightly different in each. Figure A-B, WT (A) and Knockdown (B) cells were treated with three concentrations of Ibrutinib. Figure C-D, WT (C) and knockdown (D) cells were treated with 1 μM Ibrutinib and H_2O was used for vehicle control. Figure E-F, WT (E) and knockdown (F) cells were treated with the same condition with experiment in figure C and D and TNF-α treated cells were used as positive control.

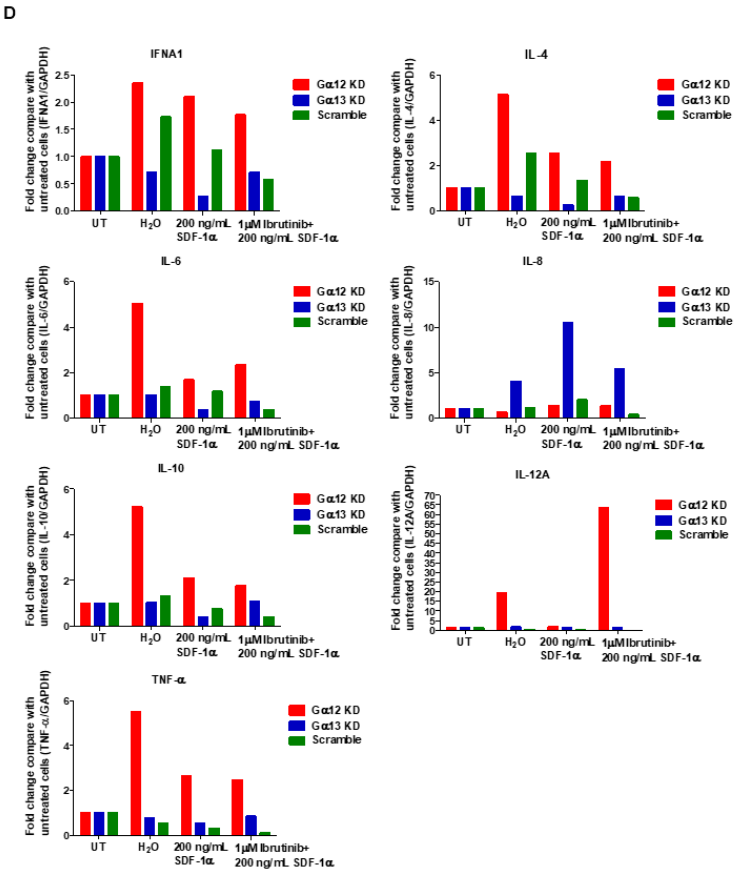

Figure 5.10 contd/ The effect of $G\alpha_{12}$ and $G\alpha_{13}$ on SDF-1α induced cytokines production in ibrutinib treated cells.

OCI-AML3 WT and $G\alpha_{12}$ family knockdown were treated with various concentration of ibrutinib (0.1, 1, and 10 μM) for 2 hr then continually incubated with 200 ng/mL SDF-1α for 4 hr. The cytokines expression was examined by qPCR. Figure A-F represent different experiment which slightly different in each. Figure A-B, WT (A) and Knockdown (B) cells were treated with three concentrations of Ibrutinib. Figure C-D, WT (C) and knockdown (D) cells were treated with 1 μM Ibrutinib and H_2O was used for vehicle control. Figure E-F, WT (E) and knockdown (F) cells were treated with the same condition with experiment in figure C and D and TNF-α treated cells were used as positive control.

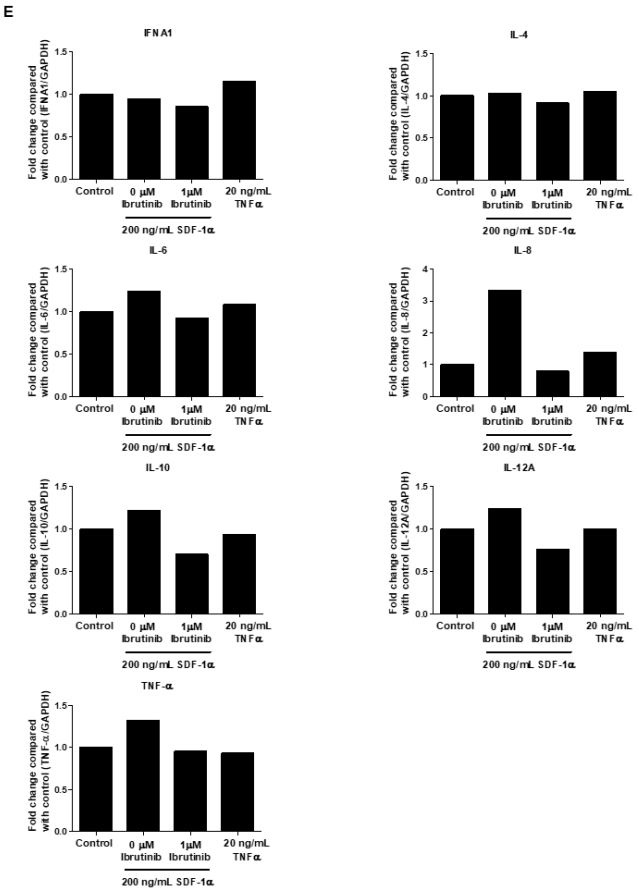

Figure 5.10 contd/ The effect of $G\alpha_{12}$ and $G\alpha_{13}$ on SDF-1α induced cytokines production in ibrutinib treated cells

OCI-AML3 WT and $G\alpha_{12}$ family knockdown were treated with various concentration of ibrutinib (0.1, 1, and 10 μM) for 2 hr then continually incubated with 200 ng/mL SDF-1α for 4 hr. The cytokines expression was examined by qPCR. Figure A-F represent different experiment which slightly different in each. Figure A-B, WT (A) and Knockdown (B) cells were treated with three concentrations of Ibrutinib. Figure C-D, WT (C) and knockdown (D) cells were treated with 1 μM Ibrutinib and H_2O was used for vehicle control. Figure E-F, WT (E) and knockdown (F) cells were treated with the same condition with experiment in figure C and D and TNF-α treated cells were used as positive control.

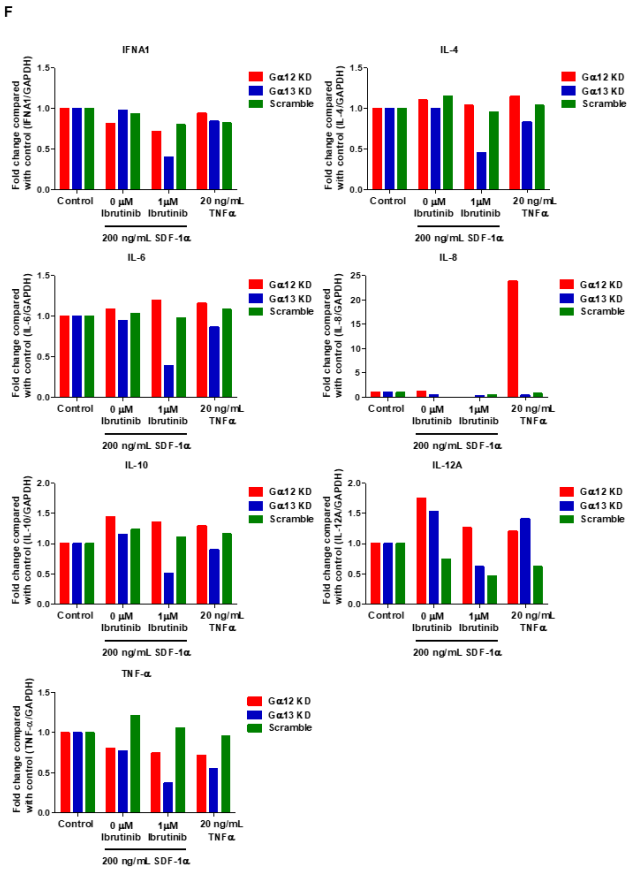

Figure 5.10 contd/ The effect of $G\alpha_{12}$ and $G\alpha_{13}$ on SDF-1α induced cytokines production in ibrutinib treated cells.

OCI-AML3 WT and $G\alpha_{12}$ family knockdown were treated with various concentration of ibrutinib (0.1, 1, and 10 μM) for 2 hr then continually incubated with 200 ng/mL SDF-1α for 4 hr. The cytokines expression was examined by qPCR. Figure A-F represent different experiment which slightly different in each. Figure A-B, WT (A) and Knockdown (B) cells were treated with three concentrations of Ibrutinib. Figure C-D, WT (C) and knockdown (D) cells were treated with 1 μM Ibrutinib and H_2O was used for vehicle control. Figure E-F, WT (E) and knockdown (F) cells were treated with the same condition with experiment in figure C and D and TNF-α treated cells were used as positive control.

5.3 Discussion

The main objective of this study was identifying whether $G\alpha_{12}$ and $G\alpha_{13}$ linked with the CXCR4 receptor in AML and CLL leukaemia subtypes. The OCI-AML3 and OCI-LY19 were transfected with lentivirus containing $G\alpha_{12}$ or $G\alpha_{13}$ targeted shRNAs then the effect of $G\alpha_{12}$ or $G\alpha_{13}$ knockdown was investigated to answer this research question.

The basal expression of these two Gα proteins in $G\alpha_{12/13}$ subtype was examined in various cell lines, including U937, HL-60, OCI-AML3, OCI-LY19, and HEK293T. The differences in expression levels was observed in each cell line with the highest expression being found in U937 whilst HL-60 showing the lowest expression of $G\alpha_{12}$ and $G\alpha_{13}$ among cells tested. Interesting, we found the relative expression of $G\alpha_{12}$ and $G\alpha_{13}$ was obviously different which can imply that these two proteins in the $G\alpha_{12}$ family have different abundance in each cell line for an unknown physiological reason. These experimental findings are supported by the studies of others (Tan et al., 2006).

Lentivirus-based shRNA transfection was used to suppress $G\alpha_{12}$ and $G\alpha_{13}$ mRNA expression in OCI-AML3 and OCI-LY19. Experiments were performed to screen knockdown efficiency of $G\alpha_{12}$ and $G\alpha_{13}$ targeted shRNA in HEK293T cells. Results revealed similar knockdown efficiency for each of the shRNA plasmids tested with only some of them showing approximately 50% knockdown for $G\alpha_{12}$ but less than 50% for $G\alpha_{13}$. The E6 and C10 shRNA plasmids which target $G\alpha_{12}$ and $G\alpha_{13}$ respectively were chosen to make lentivirus-containing shRNA plasmid in packaging HEK293T cells, then transduced into OCI-AML3 and OCI-LY19. After the

puromycin selection step, results revealed that the knockdown efficiency in leukaemia cell lines was better than HEK293T cells, especially $G\alpha_{13}$-targeted shRNA since only cells containing the integrated shRNA plasmid can survive and were enriched under the puromycin selection.

The effects of $G\alpha_{12}$ and $G\alpha_{13}$ knockdown were investigated in OCI-AML3 and OCI-LY19. We hypothesized that BTK is the downstream effector that receives a signal from $G\alpha_{12}$ or $G\alpha_{13}$ after CXCR4 receptor is stimulated. Therefore, BTK and ERK1/2 activation were examined after CXCR4 receptor signalling pathway stimulation by SDF-1α. The phosphorylation of BTK and ERK1/2 were not elevated after 100 ng/mL SDF-1α treatment which showed that p-BTK was activated in SDF-1α treated OCI-AML3 from the previous chapter. As OCI-AML3 and OCI-LY19 were serum-starved overnight before performing experiment, thus the starvation step may affect cell stress and induced a higher basal background of phosphorylated protein. To investigate this suspected influence, OCI-AML3 (chosen as a representative cell) were incubated overnight with serum-free RPMI, 1% FBS RPMI, and 10% FBS RPMI, then BTK and PLCγ2 phosphorylation observed after 100 ng/mL SDF-1α treatment. The result from Figure 5.4B revealed that starvation did not provoke a change in the basal levels of p-BTK and p-PLCγ2 since expression level of these two phosphorylated protein was not obviously different in each FBS concentration – the protein phosphorylation at 0 min from starved cells were as high as cells that were plated overnight in 10% FBS RPMI. Therefore, the high basal levels of these phosphorylated proteins may be generated by the cell itself and not an external factor. According to this experiment, we cannot interpret the effect of $G\alpha_{12}$ or $G\alpha_{13}$ suppression by

studying BTK activation, so we require other assays to investigate the relationship of the SDF-1α/CXCR4 pathway, $G\alpha_{12}$ subtypes and BTK in AML and CLL leukaemia subtypes.

The involvement of BTK has been reported on cell survival, so wild-type and $G\alpha_{12}$ or $G\alpha_{13}$ knockdown cells were examined for cell death responses after exposure to various concentrations of BTK inhibitor ibrutinib. Surprisingly, the percentage of dead cells was less than 50% after ibrutinib treatment fully for 72 h. However, OCI-AML3 seemed more sensitive to ibrutinib than OCI-LY19 cells since less than 20 percent of death cells was observed after ibrutinib treatment while OCI-AML3 showed higher percent of death cells at the same concentration of ibrutinib. Therefore, $G\alpha_{12}$ and $G\alpha_{13}$ may not interact with BTK or they may interact with BTK but the interaction is not correlating or involving the cell survival response.

The SDF-1α/CXCR4 signalling pathway controls cell motility and $G\alpha_i$ is reported to couple this receptor. However, it is possible that more than one family of Gα protein may participate in a G-protein-coupled receptors signalling (Rubin, 2009). Therefore, we aimed to identify $G\alpha_{12}$ family members apart from $G\alpha_i$ proteins that have already been reported from several research groups. In order to examine the effect of $G\alpha_{12}$ or $G\alpha_{13}$ knockdown on migration toward SDF-1α, the migration assay was optimized for the reliable result when we faced problems about detection, system limitations and reproducibility. Fluorescence dye was used as a first method when cells were stained with CellTracker Green CMFDA dye and migrated cells were counted under a fluorescence microscope.

Interestingly, OCI-LY19 migrated without SDF-1α induction. Even this cell line expresses CXCR4 receptor but this phenomenon may be caused by the cell type size characteristic as 8 μm transwell inserts appear too big for this cell line. However, we can set up the optimal cell number for migration assay of OCI-AML3 but unfortunately, we could not get reproducible data when the actual migration assay was performed. Fluorescence intensity was used as a second method to detect migrated cells. Results fluctuated between untreated and SDF-1α-treated in wild-type and $G\alpha_{12}$ knockdown cells, and there were differences between untreated and SDF-1α treated cells in $G\alpha_{13}$ knockdown and scramble control cells, as results were not correlated between the cells found at the bottom of the transwell chamber being observed under light microscopy or fluorescence microscopy measurements. There are some possible explanations that can explain these anomalous result. Firstly, there is a limitation of this measurement method that cannot detect fluorescence intensity when it was emitted from a small amount of cells because migrated cells were aliquoted into a small volume from 24-well plate to 96-well plate for measurement. Secondly, this detection method may be too variable from sample to sample so that data is not consistent enough to analyse reproducibly or accurately. We took advantage of the fact that we could observe cells under a microscope were actually seen to migrate toward SDF-1α, so trypan blue cell counting was used as the third method to measure cell migration. According to our results, OCI-AML3 showed a defect in migration toward SDF-1α when both $G\alpha_{12}$ or $G\alpha_{13}$ was knocked down compare to wild-type cells. However, $G\alpha_{12}$ knockdown should have relatively more effect to inhibiting migration than $G\alpha_{13}$ knockdown due to $G\alpha_{13}$ protein being nearly fully suppressed in knockdown cells, but $G\alpha_{12}$ protein knockdown is much less dramatic, but

there is still considerable inhibition of migration in these $G\alpha_{12}$ knockdown cells. Therefore, this result implies that $G\alpha_{12}$ or $G\alpha_{13}$ both participate with the CXCR4 receptor to transduce its signal from its ligand to regulate cell motility. As migration did not completely reduce in either $G\alpha_{12}$ or $G\alpha_{13}$ suppressed cells, there probably is another protein that helps carry this signal to downstream effectors. This other protein could be Gαi which has already identified from other studies, or it is possible that other unknown pathways can control cell migration in these cell too (Tan et al., 2006, Zaitseva et al., 2014).

This study we question that $G\alpha_{12}$ or $G\alpha_{13}$ also couples with CXCR4 and transduce the signal from CXCR4 receptor and induce BTK activation after SDF-1α stimulation. The coupling of $G\alpha_{12}$/$G\alpha_{13}$ with CXCR4 receptor we already identified from the previous experiments. Therefore, BTK was pharmacologically inhibited with ibrutinib and migration assay performed to examine whether BTK inhibition affects migration in wild-type or $G\alpha_{12}$ or $G\alpha_{13}$ OCI-AML3 cells. The p-BTK was successfully inhibited but the migration assay results were not convincing. These experiments were performed in wild-type OCI-AML3 and knockdown cells, where incubation with ibrutinib for 2 h then washing before SDF-1α treatment means that the washing steps between the two treatments may affect the cell migration such that the amount of cells at the beginning of the assay may not accurately relate to the migrated cells found at the end of experiment. In addition, p-BTK in OCI-AML3 cells has being high without any treatment as shown in previous experiment. This is an ongoing difficulty to get better signalling information out of AML cells which naturally have very high

basal activities in many biochemical processes, making these cells highly active and highly drug-resistant.

To consider the effect of $G\alpha_{12}$ subtype knockdown and BTK inhibition on cytokine expression, wild-type OCI-AML3 and $G\alpha_{12}/G\alpha_{13}$ knockdown cells were treated with ibrutinib for 2 h and then continually incubated with 200 ng/mL SDF-1α for 4 h, but instead of migration, the expression of cytokines was examined by qPCR. Wild-type and $G\alpha_{12}$ subtype knockdown cells were treated with DMSO diluted ibrutinib but DMSO seems has an effect on cytokines mRNA expression as the amount of DMSO was higher than 2%, which is not good for cells stability. Therefore water was used as a diluent to minimize the effect of DMSO. The TNF-α was used as a positive control at 20ng/mL which should cause considerable induction of some cytokines particularly TNF-α itself (often a 20-50 fold increase is expected). However, there was not much difference in cytokine expression between untreated and treated cells even in the positive control. Therefore, we cannot conclude the interaction between $G\alpha_{12/13}$ subtypes and BTK, as this experimental approach needed further optimisation to gain more reliable and reproducible results.

In summary, we can conclude that $G\alpha_{12}$ or $G\alpha_{13}$ subunits are coupled to the CXCR4 receptor to transduce its SDF-1α signal, and that both G-protein subunits are involved in controlling AML cell migration processes. However, more needs to be done to gain more reliable results with these troublesome cells and better understand these signalling pathway in AML.

Chapter VI

General Discussion

General Discussion and Conclusions

This study comprises two main objectives in order to understand the role of BTK in different aspects of leukaemia. The first objective is investigation of BTK and p-BTK in the nucleus and cytoplasm of human leukaemia AML and CLL subtypes. The second objective is identification of whether $G\alpha_{12}$ and $G\alpha_{13}$ couple with CXCR4 receptor and transduce signals to activate BTK and cellular response via BTK in AML and CLL leukaemia subtypes.

Acute myeloid leukaemia and chronic lymphocytic leukaemia have a high incidence in the elderly. The standard treatment strategy of AML is to introduce the patient with high dosage of cytarabine and an anthracycline, usually daunorubicin. This treatment shows favourable outcomes for younger AML diagnosed patients while patients older than 65 suffer from high cytotoxicity side effects. Therefore, a new therapeutic strategy is needed to increase the favourable outcome for this group of patients. Ibrutinib is a BTK inhibitor used to treat CLL leukaemia and shows a good outcome for older patient. Interestingly, several studies reveal the influence of BTK in the pathophysiology of AML. Therefore, BTK may be a protein kinase with a vital role in AML as well as CLL and BTK can also be a potentially candidate drug target for AML treatment. Indeed, the potential of BTK to be a drug target for AML has been previously reported. The FLT3-ITD, mutation present in high percentages of relapsed AML patients, shows sensitivity to ibrutinib treatment in AML cell lines. Understanding the role of BTK in AML could provide relapsed AML patients with a new therapeutic strategy, the use of BTK inhibitors.

BTK is a non-receptor tyrosine kinase, which allows flexibility in cellular localization. Indeed, BTK is found in the cytoplasm, nucleus and plasma membrane. BTK phosphorylation may regulate compartmentalization as it is thought to allow translocation to different cell compartment to regulate function. This mechanism is not fully understood. BTK expression (BTK) and phosphorylation (p-BTK) was investigated, we looked at the cytoplasm and nuclear localization of BTK in AML and CLL cell lines to characterize changes in activation and expression levels in the cellular fractions. Additionally, we wanted to identify BTK binding partners and the role of BTK in nucleus. After optimizing the protocol to analyze the levels of BTK expression and phosphorylation, we found that BTK is not only expressed, but also activated by phosphorylation in both the cytoplasm and nucleus, of AML and CLL cell lines at basal levels. This finding is relevant to consolidate BTK as a target in AML. However, we need further experiments to understand the function of BTK and to explain the important of the nuclear localization and its function in nucleus. There are proposed models of BTK nuclear translocation and identification of putative BTK binding proteins, including transcription factor TFII-I, STAT5A, and Bright, however, the direct role of BTK in nucleus has not been established (Mohamed et al., 2000, Gustafsson et al., 2012, Novina et al., 1999, Mahajan et al., 2001, Rajaiya et al., 2005).

BTK serves as a linker molecule that can be activated from several pathways and control diverse responses. The SDF-1α/CXCR4 axis also activates BTK and its downstream protein in B cells and B cell malignancy (de Gorter et al., 2007, de Rooij et al., 2012, Chang et al., 2013, Ponader et al., 2012, Hendriks et al., 2014). The CXCR4 is G protein-coupled-

receptor which the pertussis toxin sensitive $G\alpha_i$ subunit has been reported to link with in most cells including AML (Zaitseva et al., 2014). SDF-1α/CXCR4 plays a role in cell migration and metastasis in response to SDF-1α binding. In leukaemia and other cancers, CXCR4 and its ligand, SDF-1α, are main participants in the microenvironment which provides supportive survival signal and protects cancer cells from drug-induced apoptosis which leads to disease relapse. In addition, the SDF-1α/CXCR4 pathway is not completely understood and the regulation may be cell type specific (Bruhl et al., 2003). The second aspect of this thesis, we were interested in SDF-1α/CXCR4 pathway in AML, particularly, the Gα subunit of the G-protein coupled receptor and its relationship with BTK. We targeted the $G\alpha_{12}$ or $G\alpha_{13}$ to study the SDF-1α induced cellular response in AML and CLL leukaemia subtypes. However, other Gα subtypes can also be coupled with CXCR4 leading to the same cellular activity through distinct downstream cascades, as shown in Jurkat T cells (Tan et al., 2006). We have hypothesized that $G\alpha_{12}$ subtypes receives signalling from CXCR4 receptor and activates BTK, leading to regulation of migration, gene expression, and cell survival in response to SDF-1α in in AML and CLL.

In order to understand the conveyance of signalling from CXCR4 to BTK after SDF-1α binding and to identify $G\alpha_{12}$ subtypes that link to this receptor, human leukaemic cell lines were analyzed for expression levels of CXCR4 receptor. The result revealed that all cell lines used in this study express CXCR4 receptor. Moreover, BTK is phosphorylated after SDF-1α treatment in U937, HL-60, OCI-AML3, and OCI-LY19. Other studies also show BTK activation after SDF-1α treatment in different cell lines (Zaitseva

et al., 2014, de Gorter et al., 2007, Bam et al., 2013). The expression of $G\alpha_{12}$ and $G\alpha_{13}$ was examined in AML cell line, CLL cell line, and HEK293T where $G\alpha_{12}$ showed higher protein expression than $G\alpha_{13}$ while the abundance of these Gα subunits was vice versa in Jurkat T cells which mean the abundancy of Gα protein is cell type specific (Tan et al., 2006). The difference in basal expression level between $G\alpha_{12}$ and $G\alpha_{13}$ has been also reported previously (Strathmann and Simon, 1991). In this study, we aim to fulfill the knowledge of SDF-1α/CXCR4 signalling pathway in human leukaemia, particularly the involvement of Gα subunit and downstream signalling. Even though CXCR4 links with Gαi but other Gα subtypes also has been reported to link with this receptor (Rubin, 2009, Tan et al., 2006, Maghazachi, 1997, Zaitseva et al., 2014). In addition to Gαi, we aim to identify the $G\alpha_{12}$ subtypes whether $G\alpha_{12}$ or $G\alpha_{13}$ which belong to this family has a responsibility to transduce signal from CXCR4 upon SDF-1α binding to activate downstream cascade in AML. $G\alpha_{12}$ and $G\alpha_{13}$ targeted shRNA were transduced into OCI-AML3 and OCI-LY19 to suppress $G\alpha_{12}$ and $G\alpha_{13}$ protein expression. The effect of $G\alpha_{12}$ subtypes reduction was examined by migration assay, both OCI-AML3 wild-type (WT) and OCI-AML3 $G\alpha_{12}$ subtypes knockdown were allowed migration in response to SDF-1α. Since OCI-LY19 migrated in absence of SDF-1α, OCI-LY19 was excluded from this study and the effect of $G\alpha_{12}$ subtypes knockdown and other experiments were performed in OCI-AML3 only. The ability of SDF-1α to induce cell migration was investigated in $G\alpha_{12}$ and $G\alpha_{13}$ suppressed OCI-AML3 and the result reveals that cell migration was significantly reduced after $G\alpha_{12}$ or $G\alpha_{13}$ knockdown compared to wild-type (WT) and scramble transfected cells. In addition, migration was rescued in the presence of 10% FBS. This data suggests that either $G\alpha_{12}$ or $G\alpha_{13}$

participates in SDF-1α/CXCR4 signalling pathway. Interestingly, this result supports our hypothesis that more than one Gα subtype is involved in migration since the migration ability of knockdown cells did not completely reduce. Moreover, it is possible that SDF-1α binds not only to CXCR4 but CXCR7 too. In addition, CXCR7 was reported its expresses on AML can control cell migration (Melo et al., 2014, Kim et al., 2015).

Since BTK has been reported several times as a regulator of cell migration in response to SDF-1α binding (Bam et al., 2013, de Gorter et al., 2007, de Rooij et al., 2012, Zaitseva et al., 2014), our data suggests BTK is a downstream molecule of either $G\alpha_{12}$ or $G\alpha_{13}$ in SDF-1α/CXCR4 signalling pathway for AML. To assess role of BTK in this pathway, we measured the pharmacological effect of the BTK specific inhibitor, ibrutinib, in the inhibition of BTK in $G\alpha_{12}$ and $G\alpha_{13}$ knockdown and wild-type (WT) cells by measuring downstream phosphorylation, cell survival, migration, and cytokine production. BTK is involved in cell survival and SDF-1α/CXCR4 signalling provides survival support to cells in the bone marrow microenvironment, thus we hypothesize that $G\alpha_{12}$ or $G\alpha_{13}$ convey signalling to a downstream cascade to control cell survival mediated by BTK. To test this hypothesis, OCI-AML3 and OCI-LY19 both wild-type (WT) and $G\alpha_{12}$ and $G\alpha_{13}$ knockdown were exposed to increasing concentrations of ibrutinib for 3 days and cell death was examined by flow cytometry using annexin V/PI staining for cell death. We found that BTK inhibition did not affect cell survival in wild-type and knockdown cells, in addition $G\alpha_{12}$ and $G\alpha_{13}$ knockdown does not have an effect on cell survival in OCI-AML3 and OCI-LY19 (Figure 5.5). Although some studies show BTK inhibition effect cell survival (Ponader et al., 2012, Nimmagadda et

al., 2017), our results suggests that no changes occur. However, there is study demonstrating only U937 sensitivity to Ibrutinib among four other cell lines, therefore, it is possible that BTK may not be involved in survival of OCI-AML3 and OCI-LY19 (Rushworth et al., 2014). The role of BTK in cell migration in response to SDF-1α binding is also proposed for other cell lines (Zaitseva et al., 2014, Ponader et al., 2012).

In this study, we also aimed to investigate the role of BTK in migration in $G\alpha_{12/13}$-linked CXCR4 receptor toward SDF-1α in AML. Unfortunately, we cannot conclude the importance of BTK in $G\alpha_{12/13}$-linked CXCR4 receptor in response to SDF-1α in AML cell lines from this study because the result is not reliable enough for interpretation. Focusing on OCI-AML3 wild-type (WT), fold change of migrated cells neither obviously increased nor decreased after SDF-1α and ibrutinib treatment even though knockdown cells showed slight changes in contrast with previous experiments where OCI-AML3 obviously migrated toward SDF-1α. It is possible that BTK can control migration and cooperate with $G\alpha_{12}$ and $G\alpha_{13}$ but we are limited to the assays used. It is possible that further optimization is required.

Besides cell motility, SDF-1α/CXCR4 signalling also controls gene expression, especially genes involved in cell survival. We hypothesized that expression of genes that regulate cell growth will increase in response to SDF-1α/CXCR4 signalling in OCI-AML3 wild-type (WT) and $G\alpha_{12}$ or $G\alpha_{13}$ knockdown and these genes may under BTK regulation. In this study, cytokine encoded genes were chosen to investigate participation of BTK in gene expression after SDF-1α treatment. Result shows mRNA levels of cytokines were variable, therefore, we could not identify significant

changes. Because this experiment is very promising and optimization can be quite challenging, we suggest further optimization for accurate results. Notably, our positive control, TNF-α, expression remains unchanged when we expect massive upregulation of gene expression after SDF-1α treatment. We consider the inconclusive data because of experimental condition. Since, SDF-1α/CXCR4 controls cytokine encoded gene expression via NF-κB and BTK has been reported as an upstream regulator of NF-κB (Scupoli et al., 2008, Hendriks et al., 2014).

In summary, this work reveals two significant findings. Phosphorylated BTK was found in nucleus, which suggests it is actively regulating proteins after nuclear translocation. In addition, CXCR4 can transduce signalling to $G\alpha_{12}$ subtypes upon SDF-1α treatment and it is possibly controlling stimulation of cell motility. Overall, our data supports previously published data that BTK has an important function in AML and it could be a targeted for AML therapy. However, we cannot confidently prove the involvement of BTK in this pathway in AML leukaemia subtype. According to the results from this study, we proposed the summarize schematic of SDF-1α/CXCR4 signalling pathway in OCI-AML3 as shown in figure 6.1.

Perspectives on Future Work

This study aims to understand role of BTK in nucleus and identify participation of BTK in SDF-1α/CXCR4 signalling pathway. Even though, this study reveals two main findings that BTK may have important functions in the nucleus and $G\alpha_{12}$ subtypes and involved in signal transduction in SDF-1α/CXCR4 pathway. However, we still cannot explore the role of BTK in the nucleus and the importance of BTK in SDF-

1α/CXCR4 signal transduction. To completely understand role of BTK in nucleus, the nuclear localization and putative BTK binding partners should be investigated. BTK expression and phosphorylation will be examined in BTK wild-type (WT) and domain mutant and the putative BTK binding protein can be pull down compare between wild-type and domain mutant in both cytoplasmic and nuclear fraction.

In order to complete the understanding of SDF-1α/CXCR4 axis and involvement of BTK in this pathway, the migration assay and cytokine production after ibrutinib treatment have to be optimized. In addition, the experiment should be performed with more AML cell line as well as patient sample in order to understand role of BTK in clinical situation.

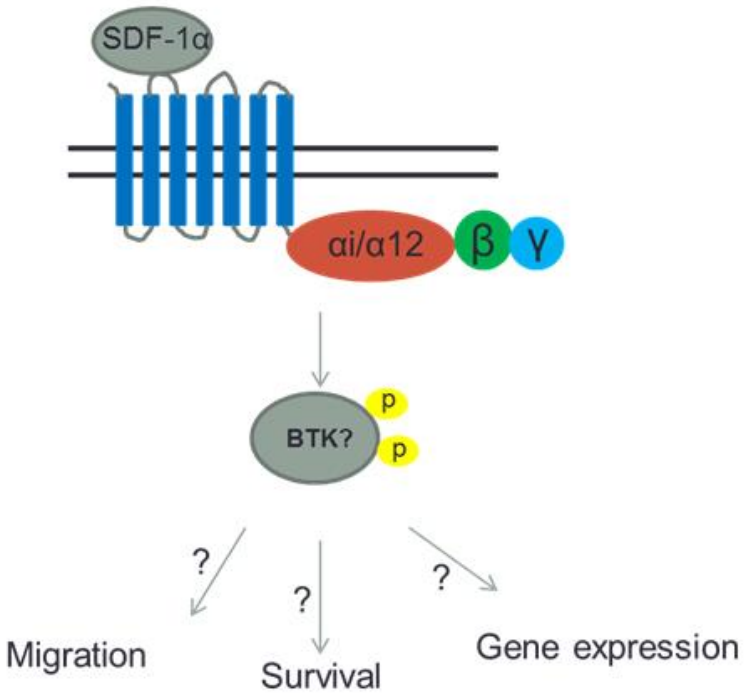

Figure 6.1 Summary schematic of SDF-1α/CXCR4 signalling pathway in OCI-AML3.

Results were concluded and proposed as a model of SDF-1α/CXCR4 signal transduction in OCI-AML3. Once ligand binding, the signal is transduced from receptor to downstream molecule through Gαi or $G\alpha_{12}$ subclass. Then Gα subunit activates other proteins which BTK may be one of $G\alpha_{12}$ subclass target and control migration, survival, or gene expression in response to SDF-1α. However, the participation of BTK in this pathway is still unclear and need further experiment to prove this hypothesis.

References

ARBER, D. A., ORAZI, A., HASSERJIAN, R., THIELE, J., BOROWITZ, M. J., LE BEAU, M. M., BLOOMFIELD, C. D., CAZZOLA, M. & VARDIMAN, J. W. 2016. The 2016 revision to the World Health Organization classification of myeloid neoplasms and acute leukemia. *Blood,* 127**,** 2391-405.

ASOU, H., TASHIRO, S., HAMAMOTO, K., OTSUJI, A., KITA, K. & KAMADA, N. 1991. Establishment of a human acute myeloid leukemia cell line (Kasumi-1) with 8;21 chromosome translocation. *Blood,* 77**,** 2031-6.

BACCARANI, M., CASTAGNETTI, F., GUGLIOTTA, G., PALANDRI, F. & ROSTI, G. 2014. Treatment recommendations for chronic myeloid leukemia. *Mediterr J Hematol Infect Dis,* 6**,** e2014005.

BAM, R., LING, W., KHAN, S., PENNISI, A., VENKATESHAIAH, S. U., LI, X., VAN RHEE, F., USMANI, S., BARLOGIE, B., SHAUGHNESSY, J., EPSTEIN, J. & YACCOBY, S. 2013. Role of Bruton's tyrosine kinase in myeloma cell migration and induction of bone disease. *Am J Hematol,* 88**,** 463-71.

BENNETT, J. M., CATOVSKY, D., DANIEL, M. T., FLANDRIN, G., GALTON, D. A., GRALNICK, H. R. & SULTAN, C. 1976. Proposals for the classification of the acute leukaemias. French-American-British (FAB) co-operative group. *Br J Haematol,* 33**,** 451-8.

BINET, J. L., AUQUIER, A., DIGHIERO, G., CHASTANG, C., PIGUET, H., GOASGUEN, J., VAUGIER, G., POTRON, G., COLONA, P., OBERLING, F., THOMAS, M., TCHERNIA, G., JACQUILLAT, C., BOIVIN, P., LESTY, C., DUAULT, M. T., MONCONDUIT, M., BELABBES, S. & GREMY, F. 1981. A new prognostic classification of chronic lymphocytic leukemia derived from a multivariate survival analysis. *Cancer,* 48**,** 198-206.

BIRNIE, G. D. 1988. The HL60 cell line: a model system for studying human myeloid cell differentiation. *Br J Cancer Suppl,* 9**,** 41-5.

BLESCH, A. 2004. Lentiviral and MLV based retroviral vectors for ex vivo and in vivo gene transfer. *Methods,* 33**,** 164-72.

BRUHL, H., COHEN, C. D., LINDER, S., KRETZLER, M., SCHLONDORFF, D. & MACK, M. 2003. Post-translational and cell type-specific regulation of CXCR4 expression by cytokines. *Eur J Immunol,* 33**,** 3028-37.

BURGER, J. A., BURGER, M. & KIPPS, T. J. 1999. Chronic lymphocytic leukemia B cells express functional CXCR4 chemokine receptors that mediate spontaneous migration beneath bone marrow stromal cells. *Blood,* 94**,** 3658-67.

BURGER, J. A. & KIPPS, T. J. 2006. CXCR4: a key receptor in the crosstalk between tumor cells and their microenvironment. *Blood,* 107**,** 1761-7.

CHANG, B. Y., FRANCESCO, M., DE ROOIJ, M. F., MAGADALA, P., STEGGERDA, S. M., HUANG, M. M., KUIL, A., HERMAN, S. E., CHANG, S., PALS, S. T., WILSON, W., WIESTNER, A., SPAARGAREN, M., BUGGY, J. J. & ELIAS, L. 2013. Egress of CD19(+)CD5(+) cells into peripheral blood following treatment with the Bruton tyrosine kinase inhibitor ibrutinib in mantle cell lymphoma patients. *Blood,* 122**,** 2412-24.

CHAPLIN, D. D. 2010. Overview of the immune response. *J Allergy Clin Immunol,* 125**,** S3-23.

CHEN, J., ODENIKE, O. & ROWLEY, J. D. 2010. Leukaemogenesis: more than mutant genes. *Nat Rev Cancer,* 10**,** 23-36.

CHEN, S. S., CHANG, B. Y., CHANG, S., TONG, T., HAM, S., SHERRY, B., BURGER, J. A., RAI, K. R. & CHIORAZZI, N. 2016. BTK inhibition results in impaired CXCR4 chemokine receptor surface expression, signaling and function in chronic lymphocytic leukemia. *Leukemia,* 30**,** 833-43.

CORTES, J. E., TALPAZ, M. & KANTARJIAN, H. 1996. Chronic myelogenous leukemia: a review. *Am J Med,* 100**,** 555-70.

DE GORTER, D. J., BEULING, E. A., KERSSEBOOM, R., MIDDENDORP, S., VAN GILS, J. M., HENDRIKS, R. W., PALS, S. T. & SPAARGAREN, M. 2007. Bruton's tyrosine kinase and phospholipase Cgamma2 mediate chemokine-controlled B cell migration and homing. *Immunity,* 26**,** 93-104.

DE KOUCHKOVSKY, I. & ABDUL-HAY, M. 2016. 'Acute myeloid leukemia: a comprehensive review and 2016 update'. *Blood Cancer J,* 6**,** e441.

DE ROOIJ, M. F., KUIL, A., GEEST, C. R., ELDERING, E., CHANG, B. Y., BUGGY, J. J., PALS, S. T. & SPAARGAREN, M. 2012. The clinically active BTK inhibitor PCI-32765 targets B-cell receptor- and chemokine-controlled adhesion and migration in chronic lymphocytic leukemia. *Blood,* 119**,** 2590-4.

DOHNER, H., ESTEY, E. H., AMADORI, S., APPELBAUM, F. R., BUCHNER, T., BURNETT, A. K., DOMBRET, H., FENAUX, P., GRIMWADE, D., LARSON, R. A., LO-COCO, F., NAOE, T., NIEDERWIESER, D., OSSENKOPPELE, G. J., SANZ, M. A., SIERRA, J., TALLMAN, M. S., LOWENBERG, B., BLOOMFIELD, C. D. & EUROPEAN, L. 2010. Diagnosis and management of acute myeloid leukemia in adults: recommendations from an international expert panel, on behalf of the European LeukemiaNet. *Blood,* 115**,** 453-74.

DOHNER, H., WEISDORF, D. J. & BLOOMFIELD, C. D. 2015. Acute Myeloid Leukemia. *N Engl J Med,* 373**,** 1136-52.

DOMBRET, H. 2011. Gene mutation and AML pathogenesis. *Blood,* 118**,** 5366-7.

DORSAM, R. T. & GUTKIND, J. S. 2007. G-protein-coupled receptors and cancer. *Nat Rev Cancer,* 7**,** 79-94.

ESTEY, E. 2016. Acute myeloid leukemia: 2016 Update on risk-stratification and management. *Am J Hematol,* 91**,** 824-46.

FENG, Y., BRODER, C. C., KENNEDY, P. E. & BERGER, E. A. 1996. HIV-1 entry cofactor: functional cDNA cloning of a seven-transmembrane, G protein-coupled receptor. *Science,* 272**,** 872-7.

GRIBBEN, J. G. 2010. How I treat CLL up front. *Blood,* 115**,** 187-97.

GUSTAFSSON, M. O., HUSSAIN, A., MOHAMMAD, D. K., MOHAMED, A. J., NGUYEN, V., METALNIKOV, P., COLWILL, K., PAWSON, T., SMITH, C. I. & NORE, B. F. 2012. Regulation of nucleocytoplasmic shuttling of Bruton's tyrosine kinase (Btk) through a novel SH3-dependent interaction with ankyrin repeat domain 54 (ANKRD54). *Mol Cell Biol,* 32**,** 2440-53.

GUSTAFSSON, M. O., MOHAMMAD, D. K., YLOSMAKI, E., CHOI, H., SHRESTHA, S., WANG, Q., NORE, B. F., SAKSELA, K. & SMITH, C. I. 2017. ANKRD54 preferentially selects Bruton's Tyrosine Kinase (BTK) from a Human Src-Homology 3 (SH3) domain library. *PLoS One,* 12**,** e0174909.

HALLEK, M. 2017. Chronic lymphocytic leukemia: 2017 update on diagnosis, risk stratification, and treatment. *Am J Hematol,* 92**,** 946-965.

HALLEK, M., SHANAFELT, T. D. & EICHHORST, B. 2018. Chronic lymphocytic leukaemia. *Lancet*.

HENDRIKS, R. W., YUVARAJ, S. & KIL, L. P. 2014. Targeting Bruton's tyrosine kinase in B cell malignancies. *Nat Rev Cancer,* 14**,** 219-32.

HEPLER, J. R. & GILMAN, A. G. 1992. G proteins. *Trends Biochem Sci,* 17**,** 383-7.

HERMAN, S. E., GORDON, A. L., HERTLEIN, E., RAMANUNNI, A., ZHANG, X., JAGLOWSKI, S., FLYNN, J., JONES, J., BLUM, K. A., BUGGY, J. J., HAMDY, A., JOHNSON, A. J. & BYRD, J. C. 2011. Bruton tyrosine kinase represents a promising therapeutic target for treatment of chronic lymphocytic leukemia and is effectively targeted by PCI-32765. *Blood,* 117**,** 6287-96.

HERMAN, S. E., GORDON, A. L., WAGNER, A. J., HEEREMA, N. A., ZHAO, W., FLYNN, J. M., JONES, J., ANDRITSOS, L., PURI, K. D., LANNUTTI, B. J., GIESE, N. A., ZHANG, X., WEI, L., BYRD, J. C. & JOHNSON, A. J. 2010. Phosphatidylinositol 3-kinase-delta inhibitor CAL-101 shows promising preclinical activity in chronic lymphocytic leukemia by antagonizing intrinsic and extrinsic cellular survival signals. *Blood,* 116**,** 2078-88.

HIBBS, M. L. & DUNN, A. R. 1997. Lyn, a src-like tyrosine kinase. *Int J Biochem Cell Biol,* 29**,** 397-400.

HIRANO, M., KIKUCHI, Y., NISITANI, S., YAMAGUCHI, A., SATOH, A., ITO, T., IBA, H. & TAKATSU, K. 2004. Bruton's tyrosine kinase (Btk) enhances transcriptional co-activation activity of BAM11, a Btk-associated molecule of a subunit of SWI/SNF complexes. *Int Immunol,* 16**,** 747-57.

JABBOUR, E. & KANTARJIAN, H. 2016. Chronic myeloid leukemia: 2016 update on diagnosis, therapy, and monitoring. *Am J Hematol,* 91**,** 252-65.

JABBOUR, E. & KANTARJIAN, H. 2018. Chronic myeloid leukemia: 2018 update on diagnosis, therapy and monitoring. *Am J Hematol,* 93**,** 442-459.

JABBOUR, E., THOMAS, D., CORTES, J., KANTARJIAN, H. M. & O'BRIEN, S. 2010. Central nervous system prophylaxis in adults with acute lymphoblastic leukemia: current and emerging therapies. *Cancer,* 116**,** 2290-300.

JAMROZIAK, K., PULA, B. & WALEWSKI, J. 2017. Current Treatment of Chronic Lymphocytic Leukemia. *Curr Treat Options Oncol,* 18**,** 5.

JEFFERIES, C. A., DOYLE, S., BRUNNER, C., DUNNE, A., BRINT, E., WIETEK, C., WALCH, E., WIRTH, T. & O'NEILL, L. A. 2003. Bruton's tyrosine kinase is a Toll/interleukin-1 receptor domain-binding protein that participates in nuclear factor kappaB activation by Toll-like receptor 4. *J Biol Chem,* 278**,** 26258-64.

JIANG, Y., MA, W., WAN, Y., KOZASA, T., HATTORI, S. & HUANG, X. Y. 1998. The G protein G alpha12 stimulates Bruton's tyrosine kinase and a rasGAP through a conserved PH/BM domain. *Nature,* 395**,** 808-13.

KAMP, M. E., LIU, Y. & KORTHOLT, A. 2016. Function and Regulation of Heterotrimeric G Proteins during Chemotaxis. *Int J Mol Sci,* 17.

KHAN, W. N., SIDERAS, P., ROSEN, F. S. & ALT, F. W. 1995. The role of Bruton's tyrosine kinase in B-cell development and function in mice and man. *Ann N Y Acad Sci,* 764**,** 27-38.

KIKUCHI, Y., HIRANO, M., SETO, M. & TAKATSU, K. 2000. Identification and characterization of a molecule, BAM11, that associates with the pleckstrin homology domain of mouse Btk. *Int Immunol,* 12**,** 1397-408.

KIM, H. Y., LEE, S. Y., KIM, D. Y., MOON, J. Y., CHOI, Y. S., SONG, I. C., LEE, H. J., YUN, H. J., KIM, S. & JO, D. Y. 2015. Expression and functional roles of the chemokine receptor CXCR7 in acute myeloid leukemia cells. *Blood Res,* 50**,** 218-26.

KIM, V. N., MITROPHANOUS, K., KINGSMAN, S. M. & KINGSMAN, A. J. 1998. Minimal requirement for a lentivirus vector based on human immunodeficiency virus type 1. *J Virol,* 72**,** 811-6.

KOBILKA, B. K. 2007. G protein coupled receptor structure and activation. *Biochim Biophys Acta,* 1768**,** 794-807.

KUMAR, C. C. 2011. Genetic abnormalities and challenges in the treatment of acute myeloid leukemia. *Genes Cancer,* 2**,** 95-107.
KUROSAKI, T. 2002. Regulation of B-cell signal transduction by adaptor proteins. *Nat Rev Immunol,* 2**,** 354-63.
LINDVALL, J. M., BLOMBERG, K. E., VALIAHO, J., VARGAS, L., HEINONEN, J. E., BERGLOF, A., MOHAMED, A. J., NORE, B. F., VIHINEN, M. & SMITH, C. I. 2005. Bruton's tyrosine kinase: cell biology, sequence conservation, mutation spectrum, siRNA modifications, and expression profiling. *Immunol Rev,* 203**,** 200-15.
MAGHAZACHI, A. A. 1997. Role of the heterotrimeric G proteins in stromal-derived factor-1alpha-induced natural killer cell chemotaxis and calcium mobilization. *Biochem Biophys Res Commun,* 236**,** 270-4.
MAHAJAN, S., VASSILEV, A., SUN, N., OZER, Z., MAO, C. & UCKUN, F. M. 2001. Transcription factor STAT5A is a substrate of Bruton's tyrosine kinase in B cells. *J Biol Chem,* 276**,** 31216-28.
MANJUNATH, N., WU, H., SUBRAMANYA, S. & SHANKAR, P. 2009. Lentiviral delivery of short hairpin RNAs. *Adv Drug Deliv Rev,* 61**,** 732-45.
MANO, H. 1999. Tec family of protein-tyrosine kinases: an overview of their structure and function. *Cytokine Growth Factor Rev,* 10**,** 267-80.
MARTENS, J. H. & STUNNENBERG, H. G. 2010. The molecular signature of oncofusion proteins in acute myeloid leukemia. *FEBS Lett,* 584**,** 2662-9.
MATUTES, E., MORILLA, R., OWUSU-ANKOMAH, K., HOULIHAN, A. & CATOVSKY, D. 1994a. The immunophenotype of splenic lymphoma with villous lymphocytes and its relevance to the differential diagnosis with other B-cell disorders. *Blood,* 83**,** 1558-62.
MATUTES, E., OWUSU-ANKOMAH, K., MORILLA, R., GARCIA MARCO, J., HOULIHAN, A., QUE, T. H. & CATOVSKY, D. 1994b. The immunological profile of B-cell disorders and proposal of a scoring system for the diagnosis of CLL. *Leukemia,* 8**,** 1640-5.
MELO, R. C. C., LONGHINI, A. L., BIGARELLA, C. L., BARATTI, M. O., TRAINA, F., FAVARO, P., DE MELO CAMPOS, P. & SAAD, S. T. 2014. CXCR7 is highly expressed in acute lymphoblastic leukemia and potentiates CXCR4 response to CXCL12. *PLoS One,* 9**,** e85926.
MOFFAT, J., GRUENEBERG, D. A., YANG, X., KIM, S. Y., KLOEPFER, A. M., HINKLE, G., PIQANI, B., EISENHAURE, T. M., LUO, B., GRENIER, J. K., CARPENTER, A. E., FOO, S. Y., STEWART, S. A., STOCKWELL, B. R., HACOHEN, N., HAHN, W. C., LANDER, E. S., SABATINI, D. M. & ROOT, D. E. 2006. A lentiviral RNAi library for human and mouse genes applied to an arrayed viral high-content screen. *Cell,* 124**,** 1283-98.
MOHAMED, A. J., VARGAS, L., NORE, B. F., BACKESJO, C. M., CHRISTENSSON, B. & SMITH, C. I. 2000. Nucleocytoplasmic shuttling of Bruton's tyrosine kinase. *J Biol Chem,* 275**,** 40614-9.
NAGASAWA, T. 2014. CXC chemokine ligand 12 (CXCL12) and its receptor CXCR4. *J Mol Med (Berl),* 92**,** 433-9.
NAGASAWA, T., HIROTA, S., TACHIBANA, K., TAKAKURA, N., NISHIKAWA, S., KITAMURA, Y., YOSHIDA, N., KIKUTANI, H. & KISHIMOTO, T. 1996. Defects of B-cell lymphopoiesis and bone-marrow myelopoiesis in mice lacking the CXC chemokine PBSF/SDF-1. *Nature,* 382**,** 635-8.
NEVES, S. R., RAM, P. T. & IYENGAR, R. 2002. G protein pathways. *Science,* 296**,** 1636-9.
NIMMAGADDA, S. C., FREY, S., EDELMANN, B., HELLMICH, C., ZAITSEVA, L., KONIG, G. M., KOSTENIS, E., BOWLES, K. M. & FISCHER, T. 2017. Bruton's tyrosine kinase and RAC1 promote cell survival in MLL-rearranged acute myeloid leukemia. *Leukemia*.

NORE, B. F., VARGAS, L., MOHAMED, A. J., BRANDEN, L. J., BACKESJO, C. M., ISLAM, T. C., MATTSSON, P. T., HULTENBY, K., CHRISTENSSON, B. & SMITH, C. I. 2000. Redistribution of Bruton's tyrosine kinase by activation of phosphatidylinositol 3-kinase and Rho-family GTPases. *Eur J Immunol,* 30**,** 145-54.

NOVINA, C. D., KUMAR, S., BAJPAI, U., CHERIYATH, V., ZHANG, K., PILLAI, S., WORTIS, H. H. & ROY, A. L. 1999. Regulation of nuclear localization and transcriptional activity of TFII-I by Bruton's tyrosine kinase. *Mol Cell Biol,* 19**,** 5014-24.

O'ROURKE, L. M., TOOZE, R., TURNER, M., SANDOVAL, D. M., CARTER, R. H., TYBULEWICZ, V. L. & FEARON, D. T. 1998. CD19 as a membrane-anchored adaptor protein of B lymphocytes: costimulation of lipid and protein kinases by recruitment of Vav. *Immunity,* 8**,** 635-45.

ORTOLANO, S., HWANG, I. Y., HAN, S. B. & KEHRL, J. H. 2006. Roles for phosphoinositide 3-kinases, Bruton's tyrosine kinase, and Jun kinases in B lymphocyte chemotaxis and homing. *Eur J Immunol,* 36**,** 1285-95.

PAL SINGH, S., DAMMEIJER, F. & HENDRIKS, R. W. 2018. Role of Bruton's tyrosine kinase in B cells and malignancies. *Mol Cancer,* 17**,** 57.

PILLINGER, G., ABDUL-AZIZ, A., ZAITSEVA, L., LAWES, M., MACEWAN, D. J., BOWLES, K. M. & RUSHWORTH, S. A. 2015. Targeting BTK for the treatment of FLT3-ITD mutated acute myeloid leukemia. *Sci Rep,* 5**,** 12949.

PONADER, S., CHEN, S. S., BUGGY, J. J., BALAKRISHNAN, K., GANDHI, V., WIERDA, W. G., KEATING, M. J., O'BRIEN, S., CHIORAZZI, N. & BURGER, J. A. 2012. The Bruton tyrosine kinase inhibitor PCI-32765 thwarts chronic lymphocytic leukemia cell survival and tissue homing in vitro and in vivo. *Blood,* 119**,** 1182-9.

QUENTMEIER, H., MARTELLI, M. P., DIRKS, W. G., BOLLI, N., LISO, A., MACLEOD, R. A., NICOLETTI, I., MANNUCCI, R., PUCCIARINI, A., BIGERNA, B., MARTELLI, M. F., MECUCCI, C., DREXLER, H. G. & FALINI, B. 2005. Cell line OCI/AML3 bears exon-12 NPM gene mutation-A and cytoplasmic expression of nucleophosmin. *Leukemia,* 19**,** 1760-7.

RAI, K. R. & JAIN, P. 2016. Chronic lymphocytic leukemia (CLL)-Then and now. *Am J Hematol,* 91**,** 330-40.

RAI, K. R., SAWITSKY, A., CRONKITE, E. P., CHANANA, A. D., LEVY, R. N. & PASTERNACK, B. S. 1975. Clinical staging of chronic lymphocytic leukemia. *Blood,* 46**,** 219-34.

RAJAIYA, J., HATFIELD, M., NIXON, J. C., RAWLINGS, D. J. & WEBB, C. F. 2005. Bruton's tyrosine kinase regulates immunoglobulin promoter activation in association with the transcription factor Bright. *Mol Cell Biol,* 25**,** 2073-84.

RUBIN, J. B. 2009. Chemokine signaling in cancer: one hump or two? *Semin Cancer Biol,* 19**,** 116-22.

RUSHWORTH, S. A., MURRAY, M. Y., ZAITSEVA, L., BOWLES, K. M. & MACEWAN, D. J. 2014. Identification of Bruton's tyrosine kinase as a therapeutic target in acute myeloid leukemia. *Blood,* 123**,** 1229-38.

SAITO, K., SCHARENBERG, A. M. & KINET, J. P. 2001. Interaction between the Btk PH domain and phosphatidylinositol-3,4,5-trisphosphate directly regulates Btk. *J Biol Chem,* 276**,** 16201-6.

SAKUMA, T., BARRY, M. A. & IKEDA, Y. 2012. Lentiviral vectors: basic to translational. *Biochem J,* 443**,** 603-18.

SAULTZ, J. N. & GARZON, R. 2016. Acute Myeloid Leukemia: A Concise Review. *J Clin Med,* 5.

SCUPOLI, M. T., DONADELLI, M., CIOFFI, F., ROSSI, M., PERBELLINI, O., MALPELI, G., CORBIOLI, S., VINANTE, F., KRAMPERA, M., PALMIERI, M., SCARPA, A., ARIOLA, C., FOA, R. & PIZZOLO, G. 2008. Bone marrow stromal cells and the upregulation

of interleukin-8 production in human T-cell acute lymphoblastic leukemia through the CXCL12/CXCR4 axis and the NF-kappaB and JNK/AP-1 pathways. *Haematologica,* 93**,** 524-32.

SHAHJAHANI, M., MOHAMMADIASL, J., NOROOZI, F., SEGHATOLESLAMI, M., SHAHRABI, S., SABA, F. & SAKI, N. 2015. Molecular basis of chronic lymphocytic leukemia diagnosis and prognosis. *Cell Oncol (Dordr),* 38**,** 93-109.

SHI, C. S. & KEHRL, J. H. 2001. PYK2 links G(q)alpha and G(13)alpha signaling to NF-kappa B activation. *J Biol Chem,* 276**,** 31845-50.

SHIROZU, M., NAKANO, T., INAZAWA, J., TASHIRO, K., TADA, H., SHINOHARA, T. & HONJO, T. 1995. Structure and chromosomal localization of the human stromal cell-derived factor 1 (SDF1) gene. *Genomics,* 28**,** 495-500.

SHORT, N. J. & RAVANDI, F. 2016. Acute Myeloid Leukemia: Past, Present, and Prospects for the Future. *Clin Lymphoma Myeloma Leuk,* 16 Suppl**,** S25-9.

SIDEROVSKI, D. P. & WILLARD, F. S. 2005. The GAPs, GEFs, and GDIs of heterotrimeric G-protein alpha subunits. *Int J Biol Sci,* 1**,** 51-66.

SIEGEL, R. L., MILLER, K. D. & JEMAL, A. 2017. Cancer Statistics, 2017. *CA Cancer J Clin,* 67**,** 7-30.

SIMON, M. I., STRATHMANN, M. P. & GAUTAM, N. 1991. Diversity of G proteins in signal transduction. *Science,* 252**,** 802-8.

SLAGER, S. L., BENAVENTE, Y., BLAIR, A., VERMEULEN, R., CERHAN, J. R., COSTANTINI, A. S., MONNEREAU, A., NIETERS, A., CLAVEL, J., CALL, T. G., MAYNADIE, M., LAN, Q., CLARKE, C. A., LIGHTFOOT, T., NORMAN, A. D., SAMPSON, J. N., CASABONNE, D., COCCO, P. & DE SANJOSE, S. 2014. Medical history, lifestyle, family history, and occupational risk factors for chronic lymphocytic leukemia/small lymphocytic lymphoma: the InterLymph Non-Hodgkin Lymphoma Subtypes Project. *J Natl Cancer Inst Monogr,* 2014**,** 41-51.

STRATHMANN, M. P. & SIMON, M. I. 1991. G alpha 12 and G alpha 13 subunits define a fourth class of G protein alpha subunits. *Proc Natl Acad Sci U S A,* 88**,** 5582-6.

SUN, Y., CHEN, B. R. & DESHPANDE, A. 2018. Epigenetic Regulators in the Development, Maintenance, and Therapeutic Targeting of Acute Myeloid Leukemia. *Front Oncol,* 8**,** 41.

SUNDSTROM, C. & NILSSON, K. 1976. Establishment and characterization of a human histiocytic lymphoma cell line (U-937). *Int J Cancer,* 17**,** 565-77.

TAN, W., MARTIN, D. & GUTKIND, J. S. 2006. The Galpha13-Rho signaling axis is required for SDF-1-induced migration through CXCR4. *J Biol Chem,* 281**,** 39542-9.

TASHIRO, K., TADA, H., HEILKER, R., SHIROZU, M., NAKANO, T. & HONJO, T. 1993. Signal sequence trap: a cloning strategy for secreted proteins and type I membrane proteins. *Science,* 261**,** 600-3.

TEICHER, B. A. & FRICKER, S. P. 2010. CXCL12 (SDF-1)/CXCR4 pathway in cancer. *Clin Cancer Res,* 16**,** 2927-31.

TERWILLIGER, T. & ABDUL-HAY, M. 2017. Acute lymphoblastic leukemia: a comprehensive review and 2017 update. *Blood Cancer J,* 7**,** e577.

TORRECILLA, J., RODRIGUEZ-GASCON, A., SOLINIS, M. A. & DEL POZO-RODRIGUEZ, A. 2014. Lipid nanoparticles as carriers for RNAi against viral infections: current status and future perspectives. *Biomed Res Int,* 2014**,** 161794.

TRENTIN, L., FRASSON, M., DONELLA-DEANA, A., FREZZATO, F., PAGANO, M. A., TIBALDI, E., GATTAZZO, C., ZAMBELLO, R., SEMENZATO, G. & BRUNATI, A. M. 2008. Geldanamycin-induced Lyn dissociation from aberrant Hsp90-stabilized cytosolic complex is an early event in apoptotic mechanisms in B-chronic lymphocytic leukemia. *Blood,* 112**,** 4665-74.

TSUCHIYA, S., YAMABE, M., YAMAGUCHI, Y., KOBAYASHI, Y., KONNO, T. & TADA, K. 1980. Establishment and characterization of a human acute monocytic leukemia cell line (THP-1). *Int J Cancer,* 26**,** 171-6.

VARNAI, P., BONDEVA, T., TAMAS, P., TOTH, B., BUDAY, L., HUNYADY, L. & BALLA, T. 2005. Selective cellular effects of overexpressed pleckstrin-homology domains that recognize PtdIns(3,4,5)P3 suggest their interaction with protein binding partners. *J Cell Sci,* 118**,** 4879-88.

VIHINEN, M., MATTSSON, P. T. & SMITH, C. I. 2000. Bruton tyrosine kinase (BTK) in X-linked agammaglobulinemia (XLA). *Front Biosci,* 5**,** D917-28.

WEBB, C. F., YAMASHITA, Y., AYERS, N., EVETTS, S., PAULIN, Y., CONLEY, M. E. & SMITH, E. A. 2000. The transcription factor Bright associates with Bruton's tyrosine kinase, the defective protein in immunodeficiency disease. *J Immunol,* 165**,** 6956-65.

WIZNEROWICZ, M. & TRONO, D. 2005. Harnessing HIV for therapy, basic research and biotechnology. *Trends Biotechnol,* 23**,** 42-7.

WOLACH, O., AMITAI, I. & DEANGELO, D. J. 2017. Current challenges and opportunities in treating adult patients with Philadelphia-negative acute lymphoblastic leukaemia. *Br J Haematol,* 179**,** 705-723.

WOYACH, J. A., JOHNSON, A. J. & BYRD, J. C. 2012. The B-cell receptor signaling pathway as a therapeutic target in CLL. *Blood,* 120**,** 1175-84.

WU, H., HU, C., WANG, A., WEISBERG, E. L., WANG, W., CHEN, C., ZHAO, Z., YU, K., LIU, J., WU, J., NONAMI, A., WANG, L., WANG, B., STONE, R. M., LIU, S., GRIFFIN, J. D., LIU, J. & LIU, Q. 2016. Ibrutinib selectively targets FLT3-ITD in mutant FLT3-positive AML. *Leukemia,* 30**,** 754-7.

YAGI, H., TAN, W., DILLENBURG-PILLA, P., ARMANDO, S., AMORNPHIMOLTHAM, P., SIMAAN, M., WEIGERT, R., MOLINOLO, A. A., BOUVIER, M. & GUTKIND, J. S. 2011. A synthetic biology approach reveals a CXCR4-G13-Rho signaling axis driving transendothelial migration of metastatic breast cancer cells. *Sci Signal,* 4**,** ra60.

ZAITSEVA, L., MURRAY, M. Y., SHAFAT, M. S., LAWES, M. J., MACEWAN, D. J., BOWLES, K. M. & RUSHWORTH, S. A. 2014. Ibrutinib inhibits SDF1/CXCR4 mediated migration in AML. *Oncotarget,* 5**,** 9930-8.

ZEPEDA-MORENO, A., SAFFRICH, R., WALENDA, T., HOANG, V. T., WUCHTER, P., SANCHEZ-ENRIQUEZ, S., CORONA-RIVERA, A., WAGNER, W. & HO, A. D. 2012. Modeling SDF-1-induced mobilization in leukemia cell lines. *Exp Hematol,* 40**,** 666-74.

Appendix

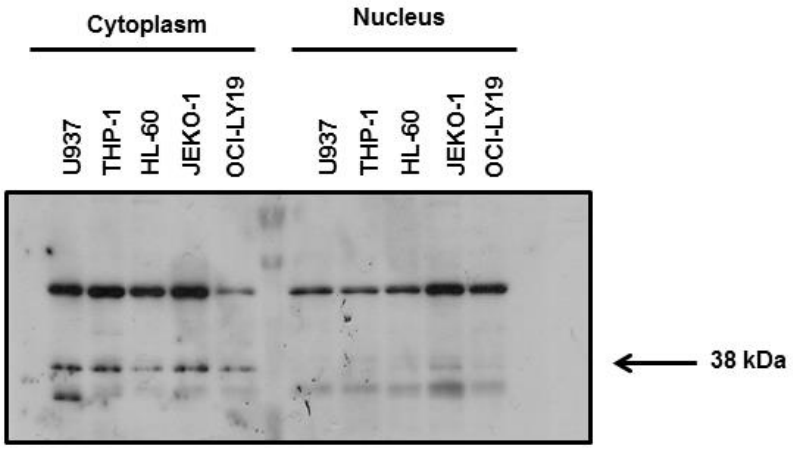

Figure A1 TATA binding protein antibody.

Human leukaemic cells are fractionated and cytoplasmic and nuclear protein were prepared as describe in Materials and Methods. The TATA binding protein (TBP) was used as a nuclear marker to examine protein purity. The arrow indicates TBP expected size which is not major band in this blot (38 kDa).

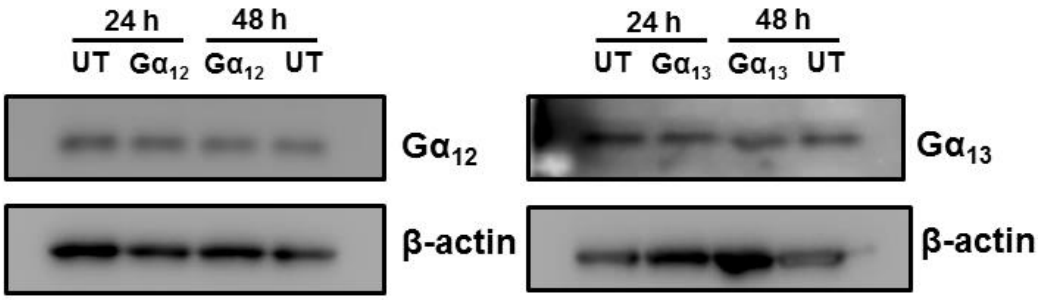

Figure A2 $G\alpha_{12}$- and $G\alpha_{13}$- targeted siRNA transfection in HEK293T by using TransIT-mRNA transfection kit.

Human embryonic kidney (HEK293T) was transfected with $G\alpha_{12}$- or $G\alpha_{13}$-targeted siRNA and incubated for 2 days. The transfected cells were performed protein extraction and Western blot as describe in the Materials and Methods section.

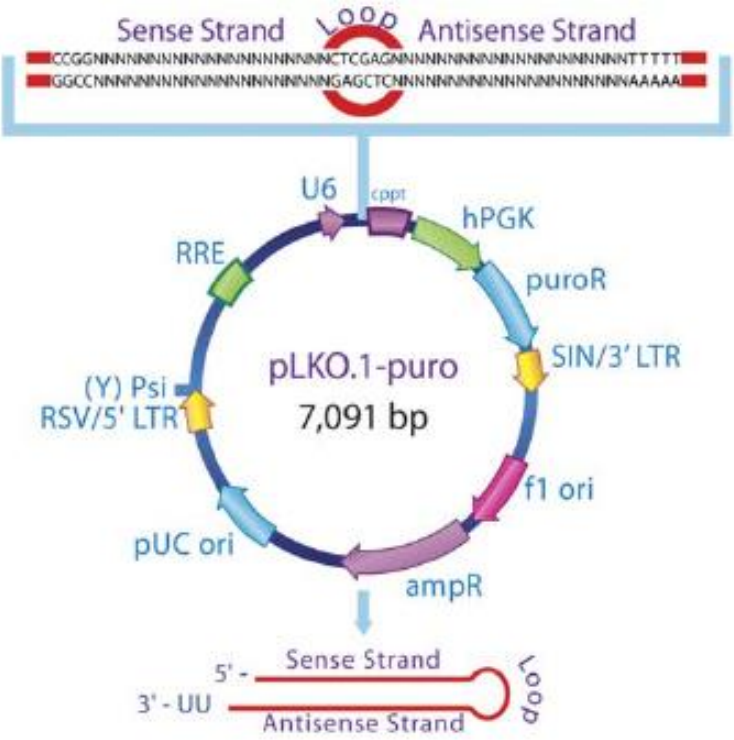

Figure A3 pLKO.1 plasmid for shRNA (Moffat et al., 2006).

This figure represents the plasmid construct of $G\alpha_{12}$- and $G\alpha_{13}$- targeted shRNA plasmid that we used in this study. This figure is adapted from Moffat et al (Moffat et al., 2006) DOI: 10.1016/j.cell.2006.01.040

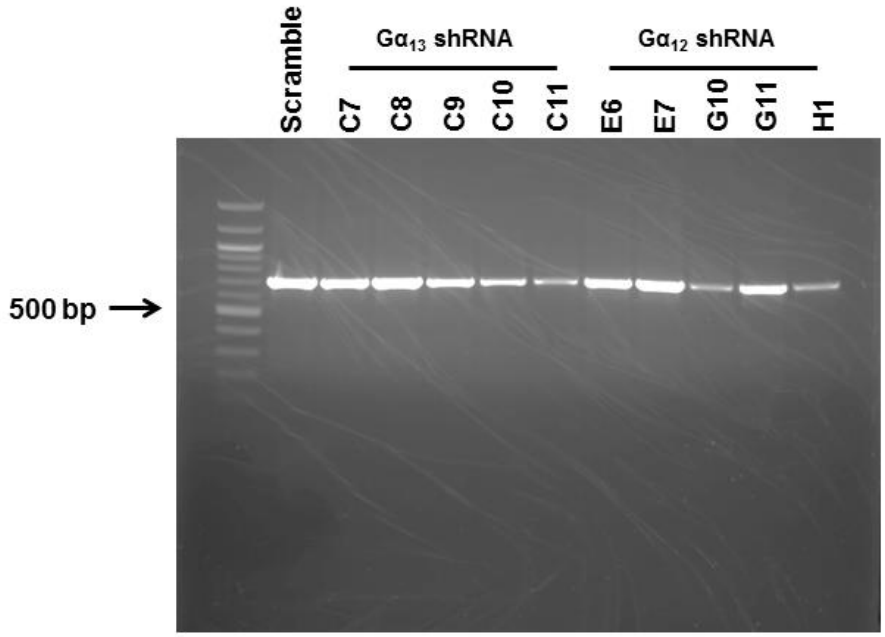

Figure A4 $G\alpha_{12}$- and $G\alpha_{13}$- targeted short hairpin RNA plasmid screening.

The $G\alpha_{12}$- and $G\alpha_{13}$- targeted shRNA were perform plasmid DNA extraction as describe in Materials and Methods. Plasmids were screened the present of puromycin resistance gene by primers in Table 1.

Gene	hPGK Forward	Puromycin Reverse	Product size (bp)	Tm
Puromycin resistance	GTGTTCCGCATTCTGCAAGC	CCGGAATTCTCAGGCACCGGG	607	56

Table A1 Primer for short hairpin screening.

This table shows the primers used for puromycin resistance gene amplification.